Sedimentological facies models and correlation of the Kobbe Formation in the Goliat Field compared with outcrops at Sørkapp-Land, Spitsbergen

Master of Science Thesis in Petroleum Geology

By

Bo Haugan

07.08.12

Department of Earth Science, University of Bergen, and

Department of Arctic Geology, University Centre in Svalbard

Abstract

Detailed sedimentological and sequence stratigraphical analysis of the Kobbe Formation in the Hammerfest Basin, Barents Sea, and the Karentoppen Member, Spitsbergen, contributes to an increased understanding of depositional processes and sand body geometry. Outcrop studies on the Karentoppen Member and core studies on the reservoir section in the Goliat Field is conducted to better define thicknesses, lateral continuity, and vertical stacking patterns of the sandstone bodies in the Anisian-Ladinian, mid-Triassic facies.

Refined facies analyses of the Kobbe Formation reveals a proximal deltaic environment dominantly consisting of an estuarine, tidal-fluvial channel environment. The Karentoppen Member reveals a more distal facies development dominantly consistent of a delta front, shallow marine environment with amalgamated distributary channels as a characteristic feature. Based on this study, a westerly source is consistent with previous study.

The two study areas are compared based on the results collected from outcrop studies and core logging and the end product is the analogy between the these studies.

Acknowledgements

First of all I would like to thank my supervisor Professor Snorre Olaussen for the master thesis, discussions, help conducting fieldwork and core logging as well as being supportive through the whole writing process.

I would like to thank co-supervisor Professor William Helland-Hansen for all the help with formalities surrounding the thesis.

I would also like to thank Eni Norge who made this project possible by financial support, which was used to conduct fieldwork and core logging on Svalbard and in Stavanger. A special thank you goes to Geir Dalen who assisted fieldwork on Svalbard and helped with everything in connection with Eni Norge.

A thank you goes to UNIS for a study desk and the help with logistics during fieldwork and other adventures.

I would also like to thank my fellow master student Bjarte Rismyhr for insightful help and good discussion during the whole writing process. Thanks to all my other fellow students from UiB and UiO for valuable discussion during lunches and coffee breaks.

Finally I would like to thank my family for great patience and support throughout the whole process.

Bo Haugan

Oslo, 07.08.2012

Table of Contents

1. Geological framework

Regional setting of the Barents Sea and Svalbard

The Barents Sea is located between the Norwegian-Greenland Sea in the west and Novaya Zemlya in the east, and between the northern Norwegian and Russian coastlines in the south to the Arctic Ocean in the north (Figure 1). The North Sea, off southwestern mainland Norway, and the Barents Sea were once part of a much larger epicontinental sea, prior to the NE Atlantic Ocean in early Cenozoic time (Faleide & Tsikalas et al. 2008).

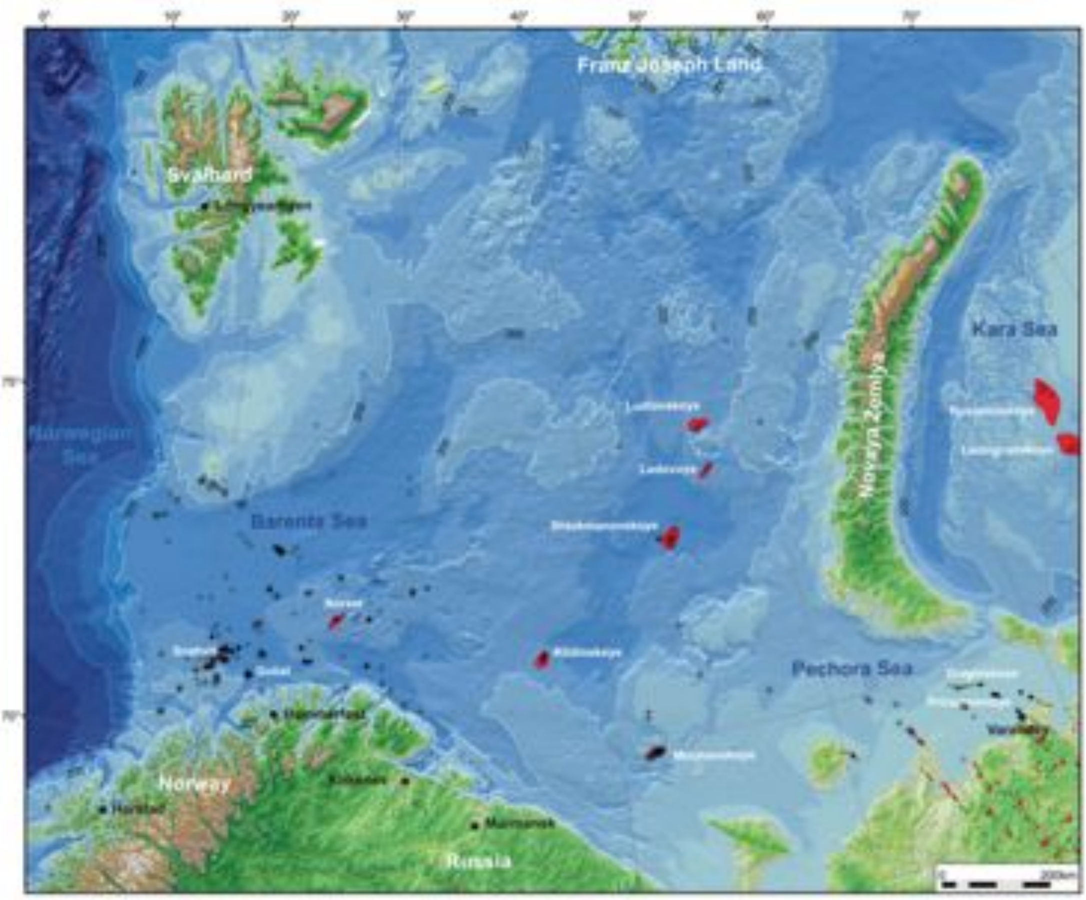

Figure 1 - Bathymetry map of the greater Barents Sea. Depth contours in meters (Henriksen et al. 2011)

Major tectonic events have played a role on the formation and deposition on the Barents shelf and the conjugate continental margins off Greenland and Norway, e.g. the Precambrian Grenvillian, the Ordovician-Silurian Caledonides, and Palaeogene west

Spitsbergen orogenies (Dallmann et al. 1999). Structural elements of the Barents Sea are presented in (Figure 2). Palaeocontinental evolution of the present Arctic and Norwegian-Greenland Seas is evident from changes in tectonic regime and palaeoclimatic indicators on Svalbard (Steel & Worsley, 1984).

The Svalbard archipelago is an uplifted part of the Barents shelf and contains a diverse and complex geological history (Figure 1). The archipelago is defined between 74°N to 81°N latitude and 10°E to 35°E longitude and comprises of an almost complete stratigraphic rock succession ranging in age from Precambrium to Oligocene. The lithology of Svalbard comprises of igneous, metamorphic and sedimentary rocks.

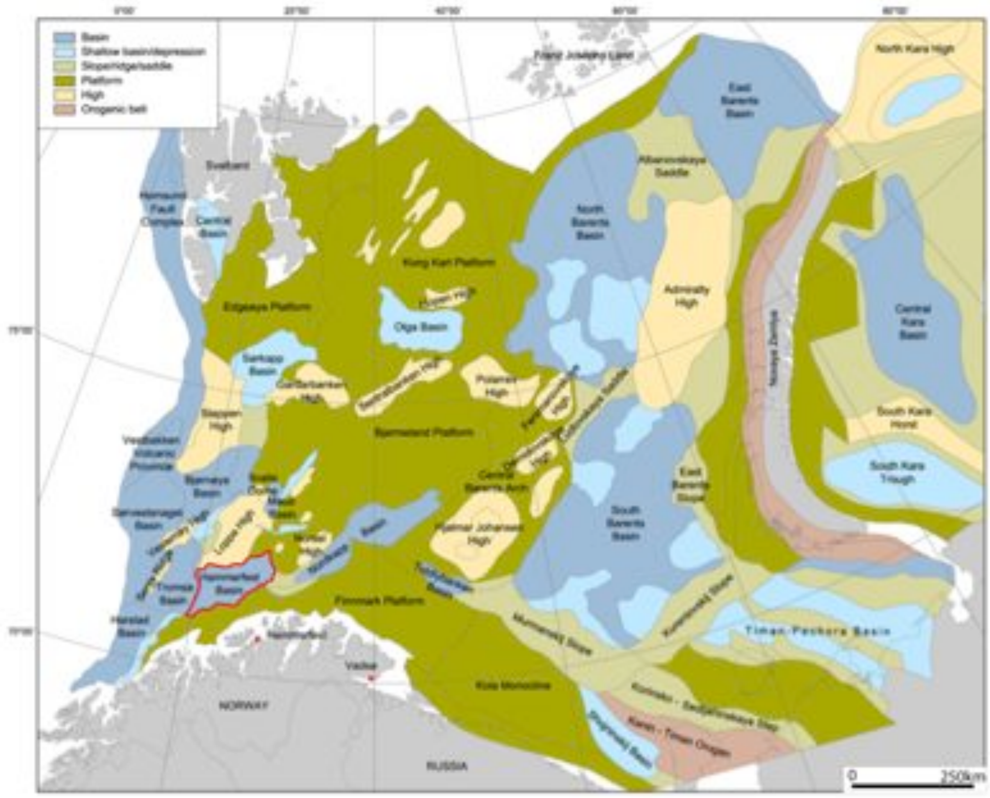

Figure 2 – Structural elements of the Barents Sea. The Hammerfest basin is marked in red. Modified from (Henriksen et al. 2011)

The tectonic framework of Svalbard is dominated by lineaments oriented N-S and NW-SE, where the most important of these are the Lomfjorden/Agardhbukta, Billefjorden, Inner Hornsund and Palaeo-Hornsund fault zones (Steel & Worsley, 1984).

The following chapter will briefly highlight the geological history of Svalbard as well as the greater Barents Sea with focus on the Triassic period A chronostratigraphic summary is presented in (Figure 3) below.

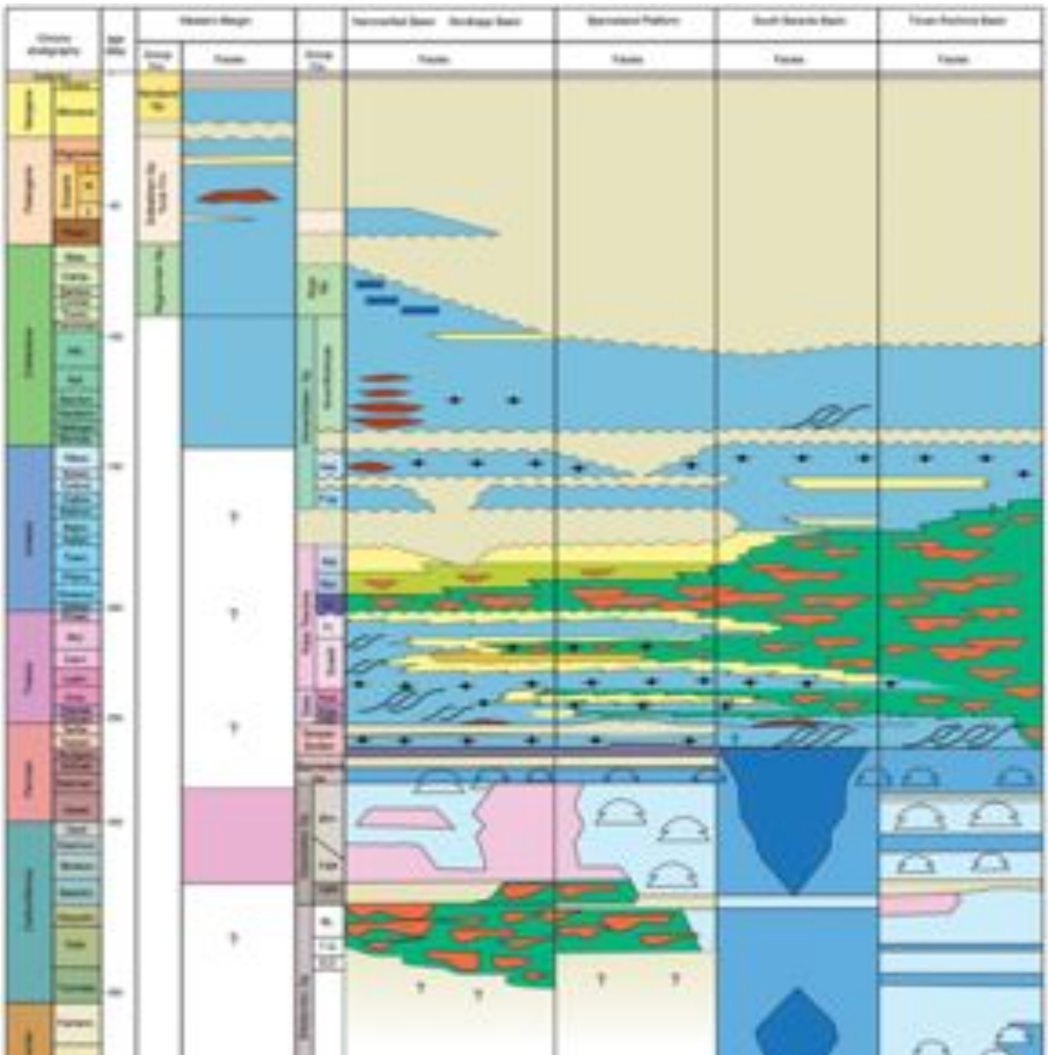

Figure 3 - Chronostratigraphy and facies summary of the greater Barents Sea. The indicated lithostratigraphy applies to the Norwegian section and is based on Worsley et al. (1988), Dallmann et al. (1999) and Larssen et al. (2005). Figure from Henriksen et al. (2011)

Pre-Caledonian (Basement)

As most literature available on geological history of the Barents Sea has main emphasis on post-Caledonian periods, only the Pre-Caledonian successions on Svalbard will be reviewed here.

The pre-Caledonian rocks on Svalbard are often referred to as *Hecla Hoek* and range from Precambrian – Lower Palaeozoic, comprising of sedimentary, metasedimentary and igneous rocks (Worsley 2008). The relationship between Svalbard and Northern Norway during the Caledonian movements in Silurian is suggested to comprise of three structural provinces, where Svalbard´s basement rocks were brought together during the main orogenic phase (Harland 1997; Worsley 2008). The most important Caledonian tectonic event on Svalbard, Ny-Friesland orogenic phase is now referred to as the equivalent to the Scandian orogeny phase of the Caledonides (Harland 1997; Dallmann et al. 1999). The entire succession has a maximum aggregate thickness of 20km, is commonly divided into 20 different lithostratigrahical groups, and generally categorized into three terranes (Worsley 2008).

Late Silurian – Devonian

The result of the orogenic phase, is a thick, kilometre long succession of post-orogenic sediments often referred to as *the Old Red*, from late Silurian to Early Devonian age (Worsley 2008). The name Old Red derives from the red coloured sediments, suggested to be deposited in southern arid zones, south of the equator. These deposits were essentially confined to a major graben on northern Spitsbergen (Worsley 2008). A transition from red to grey sediments marks the movement/transition from the southern arid zones to the equatorial tropics (Steel & Worsley 1984; Worsley 2008).

The Devonian succession comprises of the coarse-grained fluvial deposits of the Red Bay group, which are further overlain by the clastic fluvial red-beds of Andrée Land group. Ordovician to Devonian tectonic development in the Barents Sea exhibited NW-trending highs and depressions with generation of deep Devonian basins. However, Ordovician to Devonian strata has not been encountered in the Norwegian part of the Barents Sea (Fossum et al. 2001; O´Leary et al. 2004). Towards the end of Devonian, development of fault-bounded basins commences on Svalbard and Bjørnøya (e.g. Steel & Worsley 1984; Nøttvedt et al. 1993ab; Gudlaugsson et al. 1998).

Carboniferous – Early Permian

The Billefjorden Group is deposited during early Carboniferous into late Carboniferous, and comprises of delta plain, fluvial and lacustrine deposits (Worsley, 2008; Gjelberg and Steel, 1981). Coal mining in the Russian settlement Pyramiden on Spitsbergen occurred within the Billefjorden Group, and was of commercial quantities. The humid deposits of Billefjorden Group are overlain by shallow marine-shelf carbonates of sabkha environments within the Gipsdalen Group (Worsley, 2008; Gjelberg and Steel, 1981).

Both the Barents Sea and Svalbard experienced further rifting, where this tectonic phase is related to the initiation of the Atlantic rift system between Norway and Greenland (Henriksen et al. 2011). Several sedimentary basins were possibly initiated at this time, e.g. Tromsø, Bjørnøya, Nordkapp, Fingerdjupet, Maud and possibly Hammerfest (Gudlaugsson et al. 1998; Henriksen et al. 2011). The result is continental source rock development, as seen in many basins e.g. Svalbard, Finnmark basin, East Greenland and Sverdrup Basin (Henriksen et al. 2011).

The Late Carboniferous exhibited regional subsidence in the central and eastern parts of the Barents Sea, with development of a regional sag basin covering the entire Barents Shelf (Gudlaugsson et al. 1998). The continued northward movement of Laurasia influenced the deposits due to climatic conditions and increasing latitude. The transition from the tropical continental deposits of the Billefjorden Group into the arid Gipsdalen Group may reflect these changes. The evaporites of the Gipsdalen Group is divided between Late Carboniferous and Early Permian.

Late Permian – Early Triassic

The transition from the evaporitic Gipsdalen Group into the siliciclastic deposits of the Tempelfjorden Group marks a significant change in depositional environments (Steel and Worsley 1984). This lithological transition is due to the development of a marine seaway between Norway and Greenland, causing a change in oceanic circulation (Stemmerik et al. 1999; Worsley 2008; Henriksen et al. 2011). Cold-water spiculites within the Tempelfjorden Group displays this transition overlying the warmer water carbonates (Worsley 2008). The Permian spiculites are extremely hard and display a prominent and easily identifiable seismic facies e.g. Ørn Formation in the Barents Sea. The transition from Late Permian to Early Triassic boundary exhibits a regional unconformity, where subaerial exposure on Svalbard has been documented (Mørk et al.

1999a). Within these periods, the transition from silica-rich shales to non-siliceous shales also corresponds to the Late Permian mass extinction.
Tectonically, the Triassic was a quite period in the western Barents Sea including Svalbard, except for local fault tectonics. Although subsidence of large magnitude was active in the northern and southern Barents Sea basins, forming significant depocenters (Riis et al. 2008).

Early Triassic – Middle Triassic

In general, the early to middle Triassic comprises of silisiclastic deposits sourced from the Uralides in the east, though dominantly sourced from the west on Spitsbergen, creating the Sassendalen Group (Figure 4) (Riis et al. 2008; Steel and Worsley 1984).
Marine shales and delta front to shoreface sandstones dominate the Sassendalen Group within Early and Middle Triassic (Steel and Worsley 1984). The organic rich shales within the Bravaisberget (west) and Botneheia (east) Formations in the Sassendalen Group on Svalbard are time-equivalent to the source rock of the Steinkobbe Formation in the Barents Sea (Figure 5) (Riis et al. 2008). The Bravaisberget and Botneheia Formations have been described in detail by many workers, e.g. Krajewski et al. (2007) and Worsley (2008), and are often used to display the general shallow shelf development of the Middle Triassic depositional system on Svalbard (Figure 4). These formations are time-equivalent to the Steinkobbe and Kobbe Formations in the Barents Sea. The Karentoppen Member on Svalbard is a key locality within the Bravaisberget Formation showing conglomerates, herringbone cross-bedded sandstones infilling large channel

Figure 4 - Type section of the Bravaisberget Formation at Bravaisberget seen from Van Keulenfjorden, Spitsbergen (Krajewski et al. 2007)

structures and a general sediment transport to the E-SE. The Karentoppen Member will be thoroughly reviewed in the fieldwork chapter.
The abrupt change form the underlying sandy siltstones of the Klappmyss Formation in the Barents Sea to the organic-rich claystone of the Kobbe Formation may represent a major transgressive boundary (Riis et al. 2008). Many workers believe that this is a major transgressive episode across the Arctic in early Anisian (Mørk et al. 1989; Riis et al. 2008).

The present Triassic lithostratigraphy in the southwestern Barents Sea was defined by Worsley (1988) and later revised by Mørk et al. (1999) in Figure 5 below. There has been no exploration activity by the oil industry in the northern Barents Sea, though data acquisition and data interpretations have been completed by the Norwegian Petroleum Directorate (Riis et al. 2008).

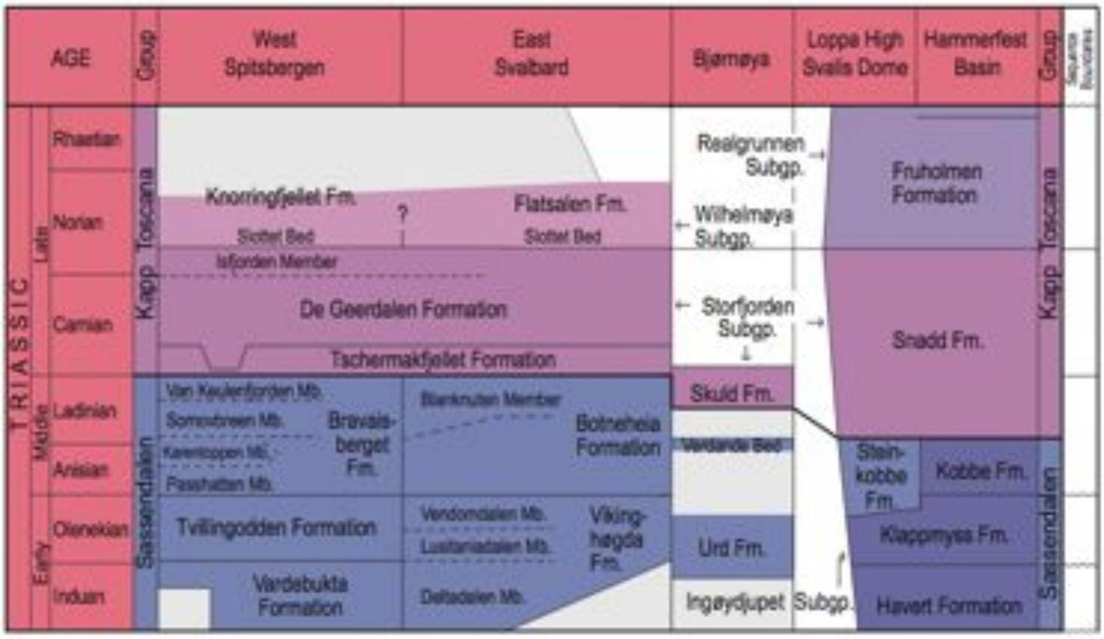

Figure 5 - Overview of the Triassic lithostratigraphy of Svalbard and the Barents Sea, simplified from Mørk et al. (1999), The positions of major Boreal Triassic sequence boundaries are based on Egorov & Mørk (2000). Figure modified by Riis et al. (2008)

Late Triassic – Middle Jurassic

The Kapp Toscana Group, overlying the Sassendalen Group, within the Late Triassic to Middle Jurassic exhibits an overall progradational nature (Steel and Worsley 1984; Riis et al. 2008). The Kapp Toscana Group is bounded by the transgressive event in Early

Carnian (Snadd Formation) and an unconformity/condensed section in Middle Jurassic (Fuglen Formation) (Henriksen et al. 2011). The westward progradation from the Uralides continued as the main source in the southern Barents Sea was coming from the south and east (Riis et al. 2008; Mørk 1999). The western Barents changed character during this period from a marine shelf with a central deep trough (Anisian), to a paralic platform (late Carnian). Therefore, the De Geerdalen Formation on Svalbard is proposed as the time-equivalent to the Snadd Formation in the Barents Sea (Figure 5) (Riis et al. 2008).

The Late Triassic to Middle Jurassic comprises of the main reservoir successions in the western Barents Sea within the Norwegian sector and includes the Fruholmen, Tubåen, Nordmela and Stø Formations (Realgrunnen subgroup) (Henriksen et al. 2011).

Late Jurassic – Late Cretaceous

As the latter section revealed a period of low tectonic activity, this period shows increased tectonic activity culminating in the Early Cretaceous, which is still the present day configuration of highs and basins (Gabrielsen et al. 1990; Henriksen et al. 2011). The Hammerfest Basin endured rifting and subsided relative to the Loppa High and Finnmark Platform (Henriksen et al. 2011). Uplift of the northwestern Barents Sea and present day Svalbard was active during Early Cretaceous in relation to the development of the early Arctic basin and is a predecessor of the transtensional movements in the western margins of the archipelago (Steel and Worsley 1985; Glørstad-Clark et al. 2010). Following these tectonic activities, an igneous province in Franz Josef Land was evident (Doré 1991; Worsley 2008; Glørstad-Clark et al. 2010).

The black shales of the Agardhfjellet Formation were deposited during the Late Jurassic all across Spitsbergen and are located within the Adventdalen Group (Dypvik et al. 1991; Worsley 2008). During the main rifting, progradation of the fluvial and deltaic system of the Helvetiafjellet Formation took place on Svalbard (Gjelberg and Steel 1995; Henriksen et al. 2011). These deposits mark a major stratigraphic boundary within the Hauterivian/Barremian periods. The Late Jurassic Agardhfjellet Formation time-equivalent in the Barents Sea is the black shales of the Hekkingen Formation. Upper Jurassic shales are considered excellent source rocks for petroleum in the western parts of the Barents Shelf, with organic contents up to 20% (Worsley et al. 2008).

The transition between the Late Jurassic and Late Cretaceous exhibits a highly condensed succession on Svalbard, showing periods of non-deposition and erosion

(Steel and Worsley 1984). The uplift and erosion of the northwestern areas continued throughout the Late Cretaceous exposing present day basement rocks, Devonian- and Upper Palaeozoic rocks (Worsley 2008). All of Upper Cretaceous is eroded away and marks a major stratigraphic break between Cretaceous and Cenozoic successions.

Cenozoic

The opening of the Norwegian-Greenland Sea continued in the Cenozoic and eventually formed a passive margin in Oligocene (Figure 6) (Nøttvedt et al. 1988; Faleide et al. 1996; Ryseth et al. 2003; Henriksen et al. 2011). The western margin along Svalbard experienced tectonic compression, leading to the formation of the western fold-and-thrust belt on Svalbard, though prior to the opening of the Norwegian-Greenland Sea (Steel et al. 1985; Worsley 2008). After the tectonic organization took place in early Oligocene, Greenland moved in a westward direction (Faleide and Tsikalas et al. 2008).

As a result of the western fold-and-thrust belt on Svalbard, sedimentary successions were deposited in a foreland basin, also referred to as the Central Tertiary basin, generating the Van Mijenfjorden Group (Harland 1997). The Van Mijenfjorden Group is divided into seven formations and comprises of continental to marine sediments deposited in transgressional and regressional cycles.
The Cenozoic strata in the southwestern areas of the Barents Sea is present over large areas, though not as widespread as the underlying Cretaceous strata, where Palaeocene-Early Eocene marine mudrocks rest unconformably on Cretaceous in the Hammerfest basin (Gabrielsen et al. 1990; Faleide et al. 1993; Henriksen

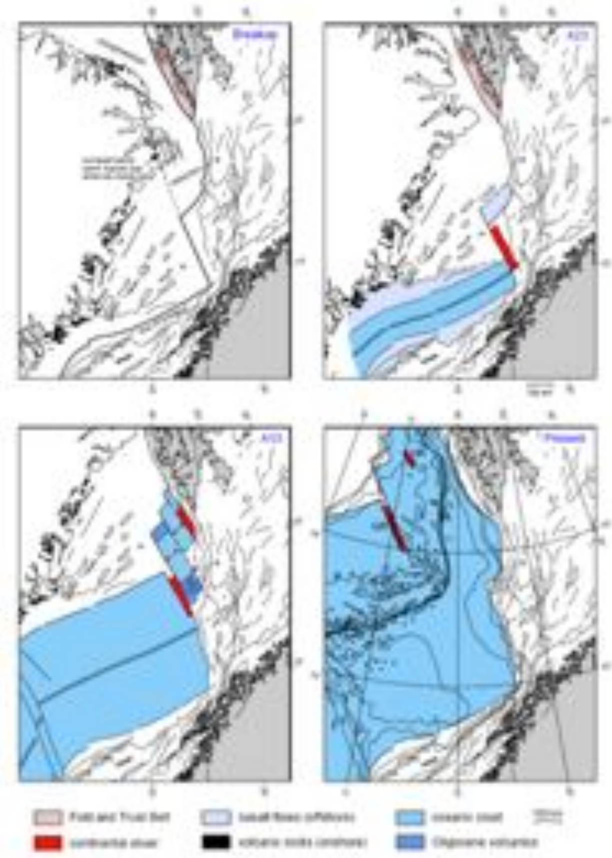

Figure 6 - Cenozoic plate tectonic evolution of the Norwegian-Greenland Sea. (GR: Greenland Ridge, HR: Hovgård Ridge, VVP: Vestbakken Volcanic Basin) Note the Fold-and-thrust belt highlighted in pink (Faleide and Tsikalas et al. 2008)

et al. 2011). However, at the surrounding platform areas, e.g. Finnmark, Bjarmeland and parts of the Loppa High, the Cenozoic strata is absent below Quaternary, which may be due to uplift, subsequent glacial erosion, subsidence and re-deposition of eroded material (Vorren et al. 1991; Eidvin et al. 1993; Richardsen et al. 1993; Faleide et al. 1996; Henriksen et al. 2011).

2. Fieldwork

Figure 7 – Overview map of Svalbard zooming in on study area in red box. (Map modified from Svalbardkartet; Norsk Polarinstitutt 2011)

Field area

The Mesozoic Karentoppen Member is located on southwestern Spitsbergen, which is the largest of the seven islands constituting the Svalbard archipelago (Figure 7). The field camp was located on a plateau of basement rocks a few hundred meters below the outcrops of the Karentoppen Member (ca. 650m a.s.l.). Fieldwork was carried out in mid-august 2011 together with professor Snorre Olaussen (UNIS) and reservoir geologist Geir Dalen (Eni Norge A/S). As the field area is situated in a remote area on Spitsbergen, a helicopter was used as transport to and from the location. During fieldwork, the weather conditions were fairly stable, however the camp area was quite wind prone throughout the week.

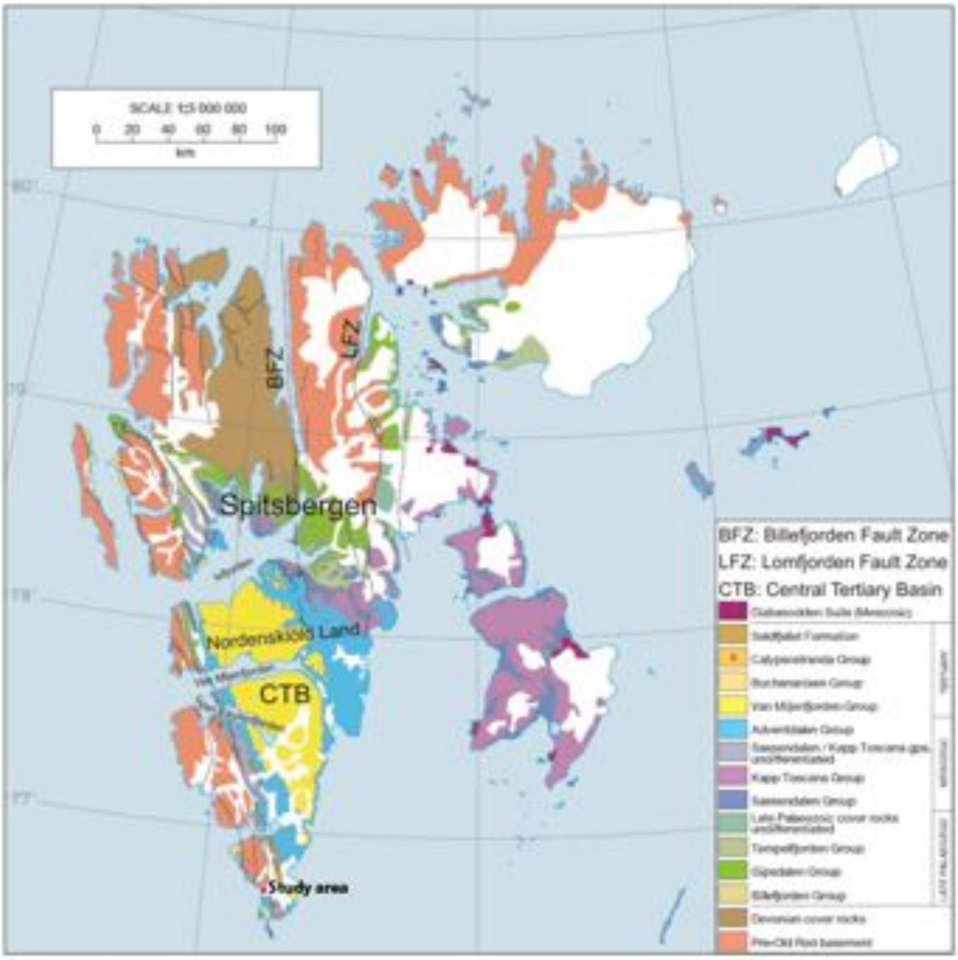

Figure 8 - Geological map of Svalbard. Note the Sassendalen Group (dark purple) which is of main interest and the highlighted study area (modified by Gjelberg 2011 from Dallmann et al. 1999)

Purpose of study

Purpose of the study was to investigate if the proximal facies of the Middle Triassic Karentoppen Member is a suitable analogue to the Kobbe Formation in the Goliat Field. Logged and cored section in the Goliat Field should be compared with outcrop studies. A good outcrop analogue could improve the reservoir characterisation of the main reservoir unit in the Goliat Field. As for the Karentoppen Member, the upper part of the Kobbe Formation in the Goliat Field is reported as a proximal facies development (Mørk et al. 1982 and NPD fact pages). This is in contrast to lateral time equivalent exposures on Spitsbergen or nearby exploration wells in the Hammerfest Basin and thereby, the Karentoppen Member at Karentoppen, Sørkapp, Spitsbergen seems to be a suitable candidate. Sedimentological and sequence stratigraphic analyses is used as aid to define correlative surfaces between outcrops on Spitsbergen and cores from the Goliat Field. The geological map of Svalbard from Dallmann et al. (1999) is presented in Figure 8. Mørk et al. (1982) reported a deltaic environment, e.g. distributary and delta front depositional environments at Karentoppen, as illustrated in Figure 9 and the member can therefore be an analogue to the reservoir unit in the Goliat Field. The fieldwork conducted in 2011 confirms the overall proximal facies of the units.

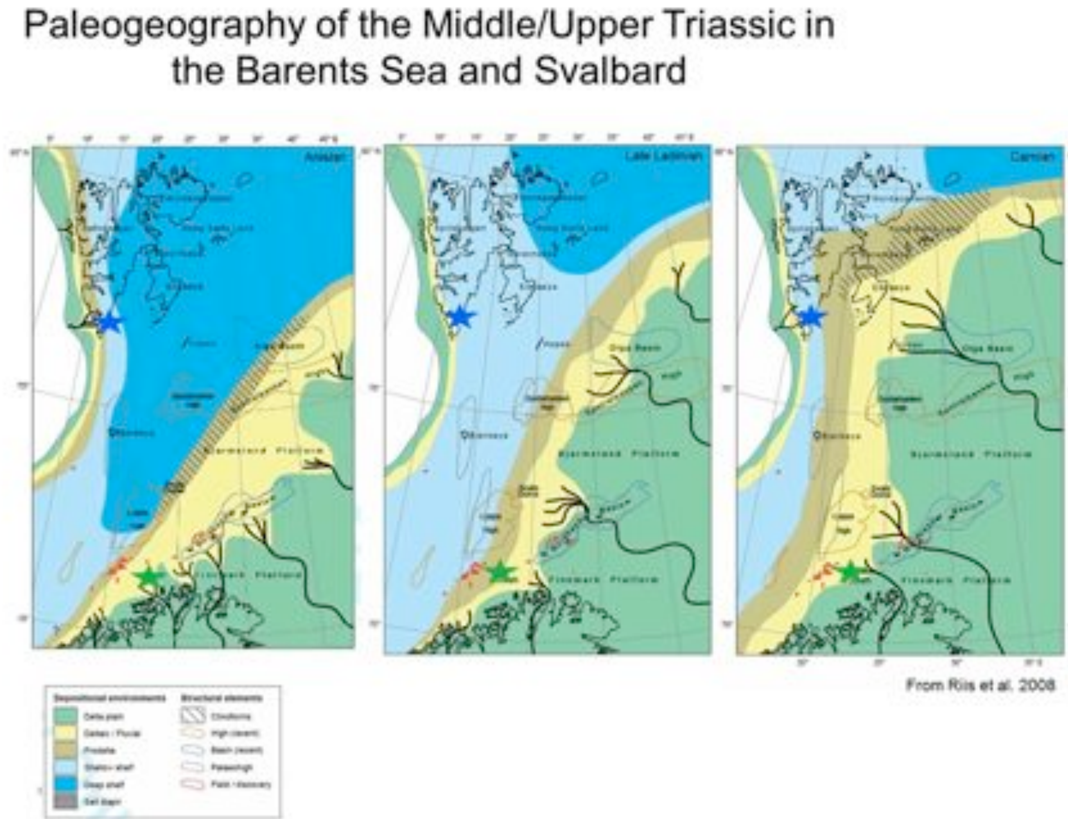

Figure 9 - Major westward prograding system in the Middle/Upper Triassic. Outcrops at Karentoppen (blue star) support a minor westward prograding system. Relatively proximal facies is developed in Anisian-Ladinian at Karentoppen and the Goliat Field (green star) (Modified from Riis et al. 2008)

The location of Goliat and Karentoppen are superimposed on Figure 9, modified from Riis et al. (2008), which shows the proposed palaeography of the Middle Upper Triassic in the Barents Sea and Svalbard. The outcrops studied together with core logging will be used to better define thickness, lateral continuity and vertical stacking pattern of the sand bodies (reservoir bodies) in a Middle Triassic facies.

Previous work

The Karentoppen Member is part of the Bravaisberget Formation within the Sassendalen Group in Early Triassic (Mørk et al. 1999) (Figure 10). The outcropping Karentoppen Member is situated on the western side of the Central Tertiary Basin (CTB) and this part of Spitsbergen might have been previously buried too more than 4 km depth (Faleide et al. 2008) (given normal temperature gradients e.g. 30-35°C pr. km).

Figure 10 - Overview of the studied outcrop, Karentoppen Member. Note the scale to the right in photo.

The exposure occurs as well quartz cemented sandstone and brittle shale, however both sedimentary and biogenic structures are well preserved.
The stratigraphic schemes used in this study is based Previous work on the Triassic and Lower Jurassic successions was conducted by Mørk et al. (1982), who also established the currently used stratigraphic definition (Mørk et al. 1999). Buchan et al. (1965) had the basis for the present scheme, which combined unpublished mapping units used by Norwegian Polar Institute (NPI) geologists and their own fieldwork. In the next few decades, work carried out on Triassic and Lower Jurassic rocks on southern Spitsbergen were conducted by Birkenmajer (1977), Worsley and Mørk (1978), Mørk et al. (1982).

Methods

The results presented in this master thesis were acquired by sedimentlogical l logging of the outcrops at Karentoppen, SW Spitsbergen (Figure 10). The main observed features are large- and small-scale sedimentological structures, bed thicknesses, key boundaries, texture and colour. These features were logged by hand on millimetre paper in 1:20 scale. Both large- and small-scale palaeocurrent measurements were conducted by use of a geological compass.

3. Facies associations – Fieldwork

Introduction

In order to present the sedimentary rock succession in the most appropriate way, a division into lithofacies and facies associations is done. The individual lithofacies are divided on the basis of sedimentary texture, sedimentary structures, colour and degree of bioturbation. Assemblages of lithofacies are comprised and constitute the subsequent division into facies associations. The lithofacies are listed in Table 1 below. A definition of facies associations is provided by Collinson (1969, p.207): "Groups of facies genetically related to one another and which have some environmental significance". Every facies association represents a bounded entity and differs from the other facies associations by alterations in the formational and depositional processes.
A few of the facies associations are not individually interpreted on the basis of sedimentary structures or grain size. Interpretations are therefore based on the surrounding facies associations and the formational mechanisms. Geometrical architecture and palaeoflow measurements are also included in the facies associations. On the basis of the interpreted facies associations, palaeogeographic reconstructions and facies models are constructed. A brief description of the facies associations together with the proposed depositional environment is presented in Table 2.

Table 1 – Lithofacies divided on the basis of grain size, descriptions and interpretations

Lithofacies	Grain size	Description	Interpretation
F1	**Claystone** (See Fig. 11 from logged outcrop, and Fig. 27,30,31,41,44,47 from Goliat wells)	**Black/dark grey flaky shale. Possible glauconite mineral**	**Deposits from suspension in a calm environment**
F2	**Clay-/siltstone and very fine grained sandstone** (See Fig. 12 from logged outcrop, and Fig.	**Dark grey, soft shale with intermittent beds of sandstone. Small scale ripples and intense bioturbation.**	**Deposits settled from suspension with rapid deposition of very fine sandstone through storm ventilation.**

	27,30,31,41,44,47,50 from Goliat wells)		
F3	**Very fine- to fine grained sandstone** (See Fig. 12,20 from logged outcrop, and Fig. 28,40,41,44,50 from Goliat wells)	**Phosphate/siderite nodules in horizontal bands, bioturbation and small scale ripples**	**Deposition from oscillation and combined flow in a relatively shallow marine environment**
F4	**Very fine- to fine grained sandstone** (See Fig. 12,15,16,20 from logged outcrop, and Fig. 28,40,42,48,49,50 from Goliat wells)	**Small scale current- and wave induced structures**	**Deposition from oscillation and combined flow**
F5	**Very fine- to fine grained sandstone** (See Fig. 15,16 from logged outcrop, and Fig. 28,35,42,43,48 from Goliat wells)	**Larger scale trough cross-stratification. Possible tidal-features.**	**Deposition from migration of dunes (distributary channels)**
F6	**Fine grained sandstone** (See Fig. 15,16 from logged outcrop, and Fig. 29,49 from Goliat wells)	**Confined massive sandstone with plane parallel lamination**	**Deposition from high velocity oscillation and unidirectional flow**
F7	**Fine grained sandstone** (See Fig. 15,16 from logged outcrop, and Fig. 29,35,48 from Goliat wells)	**Larger scale tabular cross-stratification with tangential foresets**	**Deposition from migration of dunes (distributary channels)**
F8	**Fine grained**	**Massive and**	**Rapid deposition within**

	sandstone (See Fig. 15,16,21 from logged outcrop, and Fig. 42 from Goliat wells)	**structureless sandstone. Bed thickness up to 2m.**	**distributary channels**
F9	**Fine to medium grained sandstone** (See Fig. 21 from logged outcrop, and Fig. 29,35,36,42,43,48 from Goliat wells)	**Trough cross-stratification with coarse-grained foresets and plane parallel lamination. Possible tidal-features.**	**Rapid deposition from migration of dunes**
F10	**Fine to coarse grained sandstone** (See Fig. 21 from logged outcrop, and Fig. 36,43,48 from Goliat wells)	**Reverse graded sandstone beds with trough cross-stratification and coarse grained foresets**	**Deposition from mouth bar progradation**

Table 2 - Five facies associations (FA1-FA5) with depositional environment

Facies associations:	**Depositional environment:**
FA1 – (F1-F2)	Offshore transition (prodelta)
FA2 – (F2-F4)	Distal to proximal delta front environment
FA3 – (F4-F8)	Lower delta plain; amalgamated distributary channels
FA4 – (F3-F4)	Shallow marine shelf sediments
FA5 – (F8-F10)	Proximal delta front

Facies association 1 (FA1) – Offshore transition (Prodelta)

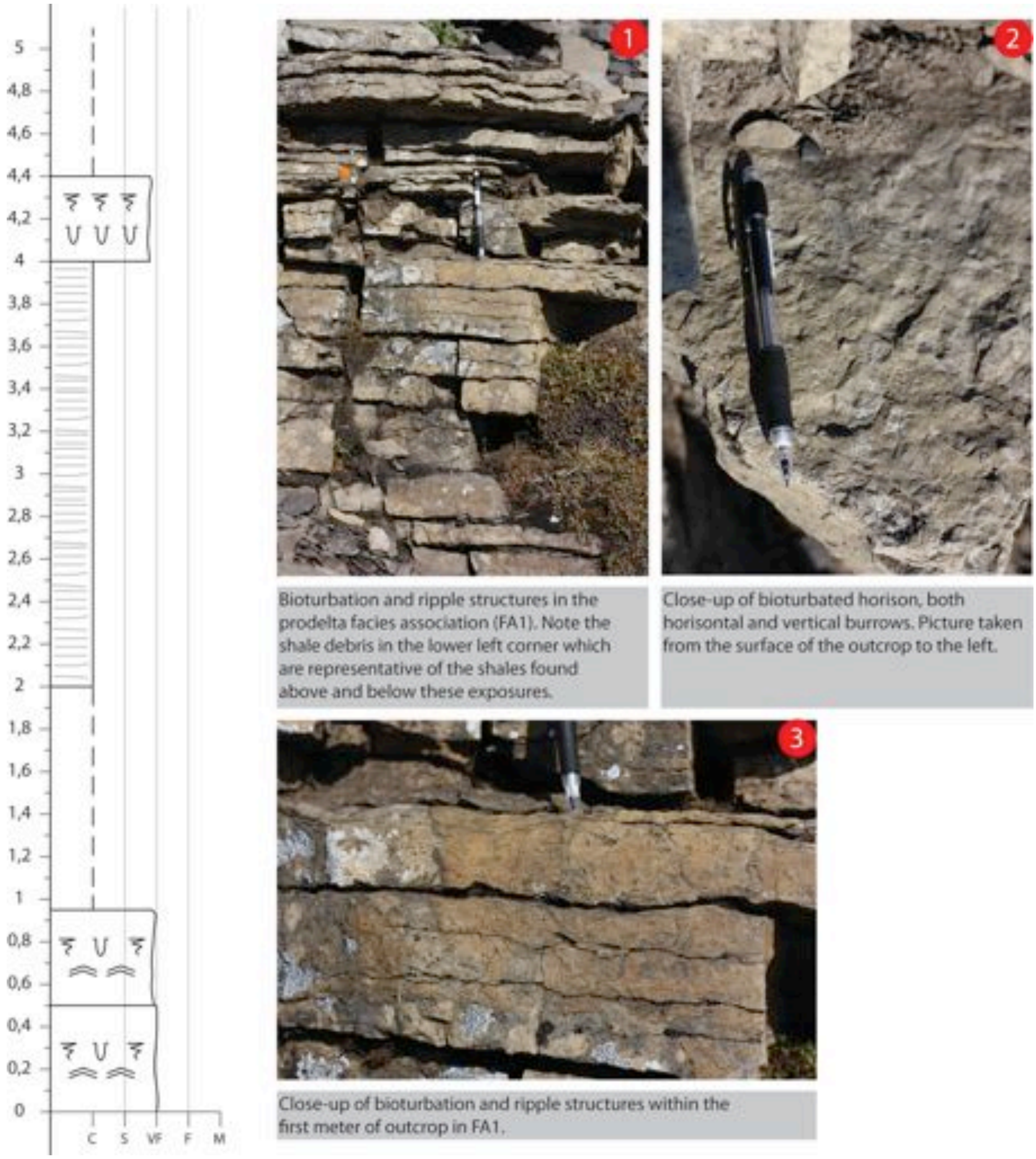

Figure 11 - Lithological log with illustrations and descriptions representing FA1 (1-3): Offshore-transition (Prodelta). The outcrop is from the Passhatten Member and Karentoppen Member of the Bravaisberget Formation on Sørkapp-Land. Legend found in appendix (Figure 68).

Outcrop comments

Facies association 1 includes the upper part of the Passhatten Member (0 - 4m) and the first occurrence of the Karentoppen Member of the Bravaisberget Formation (>4m) (Figure 11). The Passhatten Member is interpreted as deposited in an open marine shelf environment (Mørk et al. 1982).. The exact transition between the two members is difficult to pick at this outcrop. The uncertainty to where the base of this facies association is located is due to scree-cover; therefore the logging commences at the last intermittent siltstone bed close to the lower boundary of the Karentoppen Member (Figure 11).

The measured thickness of facies association 1 at this outcrop is 5m, however the entire Passhatten Member measures a thickness of 53m, whereas the Karentoppen Member is measured 43m in total thickness (Mørk et al. 1982). The Passhatten Member is located further downwards in the outcrop, though scree-cover inhibits further investigation.

Observations

The upper part of the Passhatten Member is dominantly consistent of dark grey, soft shale with intervals of meter-thick siltstone beds increasing in abundance upwards and comprises of lithofacies F1 and F2 (Table 1).

Grain size varies from clay to silt and intermittent beds with very fine-grained sandstones. The shale is dark grey in colour and finely laminated. According to previous studies by Mørk et al. (1982) investigations of the Karentoppen and Passhatten Members comprise of abundant siltstone and silty limestone beds often with phosphate nodular conglomerates. There is an increase in sand-to-silt ratio and increase in abundance of phosphate nodules towards the upper boundary of the Passhatten Member (Mørk et al. 1982).

The facies association coarsens upwards as the abundance of siltstone beds increase relative to the dark grey shale. The intermittent siltstone beds are not found as laterally continuous beds; only sporadic outcrops within the shales of the Passhatten Member are found.

Oscillation ripples are faint and typically distorted by intense bioturbation within the siltstone beds, but is a characteristic feature of FA1. The siltstone beds are further divided by thin lamina of very fine-grained sediments, both silty and shaly (Figure 11),

which makes it easier to see the symmetrical ripples as well as the vertical burrows on the surfaces.
Bioturbation is abundant in the fine-grained sandstone beds (Figure 11), though rather poor within the shales of the Passhatten Member. As the burrows are mostly vertically oriented the origin is suggested to be from suspension-feeders or possible opportunists.

Interpretation

The laminated fine-grained sedimentary rocks together with the intermittent siltstone beds show a clear variation in depositional energy. The laminated, fine-grained beds are deposited from suspension in a low-energy environment below fair-weather wave base. The siltstone beds are most likely distal deposits from periodic storm ventilation of the bottom, where larger grained sediments deposited in the foreshore and shoreface are re-deposited through suspension further seaward.
The symmetrical ripples are possibly generated during the waning stages of the storm. Thus an environment above storm wave base and below fair-weather wave base is a likely for interpretation.
Studies of the Bravaisberget Fm. further north on Spitsbergen suggest that the high organic content and the lack of bioturbation in the shales indicate anoxic sea bottom conditions (Mørk et al. 1982). Bioturbation is lacking in the dark shales and it is not unlikely that it could also indicate anoxic sea bottom conditions at this outcrop. The high degree of bioturbation within the siltstone beds can possibly be due to the oxidation of the sea bottom during storm ventilation. The proposed depositional environment for this facies association is therefore an offshore-transition environment (prodelta) between mean storm wave base and mean fair-weather wave base.

Facies association 2 (FA2) – Distal to proximal delta front

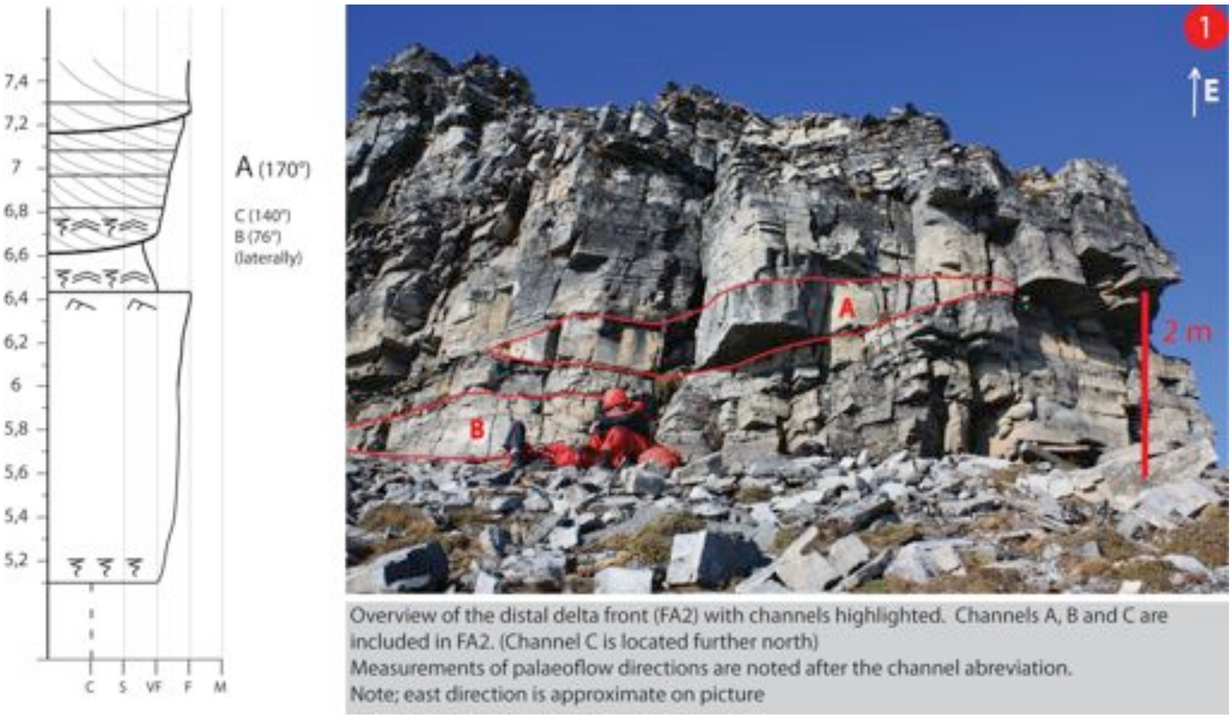

Figure 12 - Lithological log with illustration and description representing FA2 (1): Distal delta front. Palaeoflow directions are indicated next to the log together with the channel abbreviation. (Approximately eastward paleocurrent direction). Legend found in appendix (Figure 68).

Observation

There is a distinct alteration from the offshore-transition, prodelta environment interpreted in facies association 1 (FA1) into a more sandstone prone facies association. Facies association 2 comprises of lithofacies F2-F4 (Table 1).

FA2 has a measured thickness of 2,1m (Fig.4, 5,1-7,2m) where the bed thicknesses range from 20cm to >1m. In comparison with FA1, facies association 2 is coarser grained and contains symmetrical ripples. At approximately 6,5m, lenticular shaped sandstone bodies, interpreted to be channel facies, truncate the underlying wave- and current induced sandstone (Figure 12; Figure 13). The exposed two-dimensional geometry of channel A is roughly 50cm thick and 4m wide, while channel B is 90cm thick and 2m wide. Note the palaeoflow directions measured in degrees; channel A (170°), channel B (76°) and channel C (140°), thus a flow towards E-SE is inferred (Figure 12).

Figure 13 - Lenticular sandstone body (channel B) with tangential cross-bedding (Red) (Modified photo from Snorre Olaussen)

The channel fill consists of tangential cross-bedding, symmetrical- and asymmetrical ripples suggesting both current- and wave-induced structures (Figure 12). The tangential cross-bedding are on the order of tens of centimetres apart and the ripples are on centimetre scale. Faint asymmetrical ripples are found at the upper boundary of the first bed (5,1m - 6,4m), though symmetrical ripples are the overall dominant small-scale structure observed in FA2.
Intense bioturbation is found in a few of the beds, which further distorts the small scale-structures.

Interpretation

Facies association (FA2) is characterised by very fine to fine-grained sandstones divided into two coarsening upwards units (Figure 12). Facies association 2 is interpreted as a transition zone where sediment-laden fluvial currents enter the basin and interact with basinal processes. The basinal processes weaken the energy of the currents and the fluvial processes take over (Reading 1996). The log illustrates two coarsening upwards successions, one in the quite massive sandstone and one in the channel facies (Figure 12). A typical feature in a distal to proximal delta front environment is a coarsening upwards trend, formed as a result of prograding deltaic lobes, which truncate the underlying units (Walker et al. 1992).

The measured set thicknesses of the tangential cross-beds vary from a few centimetres to tens of centimetres. Near uniform dip of forsets suggest paleocurrent flowing towards the NE-SE (Figure 14). The measured dip is approximately 4°. Note the apex angle observed of 92°, which is within normal range of modern delta examples such as Wax Lake delta (100°), Volga delta (90°), Lena delta (175°) and Atchafalaya delta (100°) (Olariu & Bhattacharya 2006).

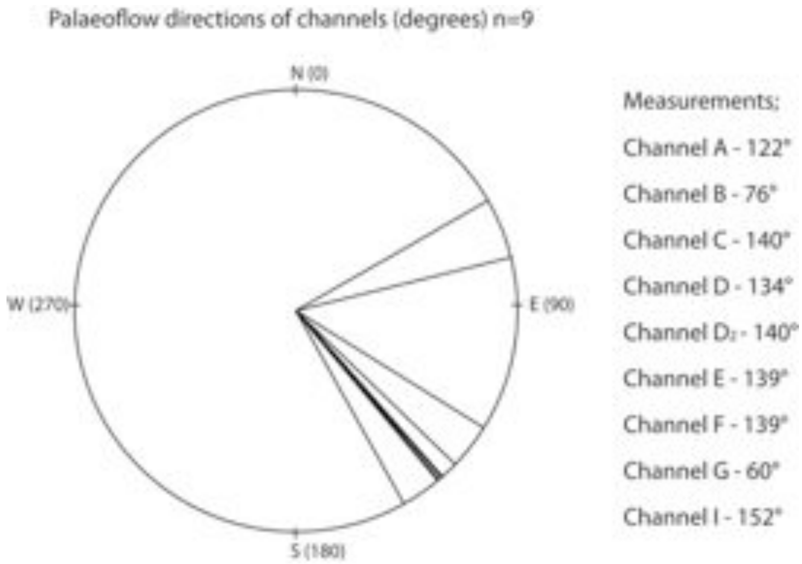

Figure 14 - Nine amalgamated distributary channels were measured. This rose-diagram illustrates the palaeoflow directions of the channels. Note that seven of the channels are within 30° and dip is measured at 4°

The amalgamated channels in this facies association are separated from the channel facies in FA3 as they are deposited in a transitional environment, where intense bioturbation and upwards coarsening channel fills are identified. Based on the observations, this facies association is interpreted to be a part of a distal to proximal delta front environment with amalgamated distributary channels located between SWB and FWB.

Facies association 3 (FA3) – Lower delta plain – lower section

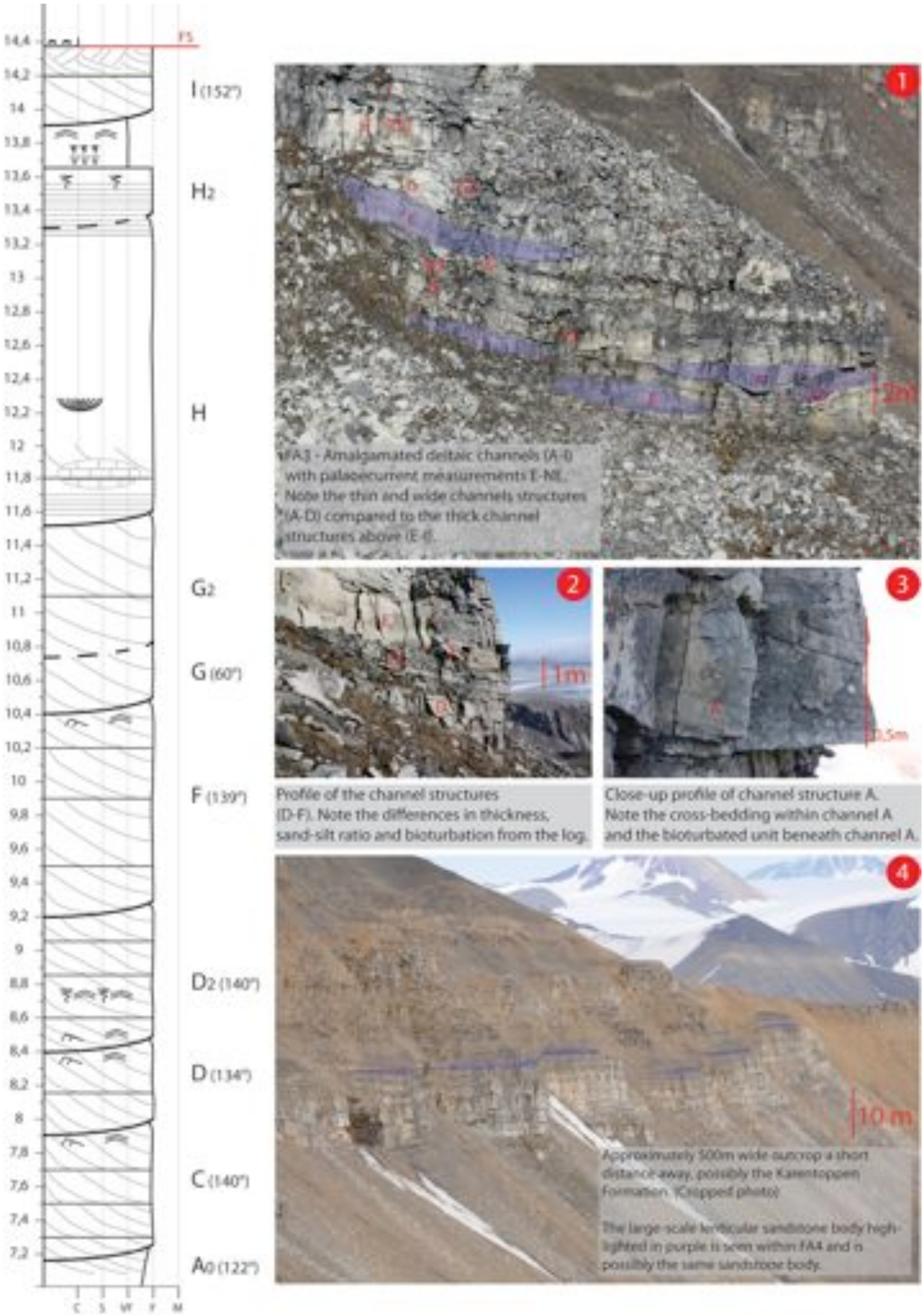

Figure 15 - Lithological log with illustrations representing FA3, Amalgamated distributary channels, lower delta plain. The log shows systematic lettering of the channel facies together with the measured palaeoflow directions. Some of the presentable channels are highlighted

with purple colour in picture 1. Picture 4 possibly represents the same amalgamated distributary channel deposits as FA2-FA3, though at outcrops further east. Note the lenticular sandbody that is characteristic in the Karentoppen outcrop (purple) in picture 4. Legend found in appendix (Figure 68).

Facies association 3 (FA3) – Lower delta plain – upper section

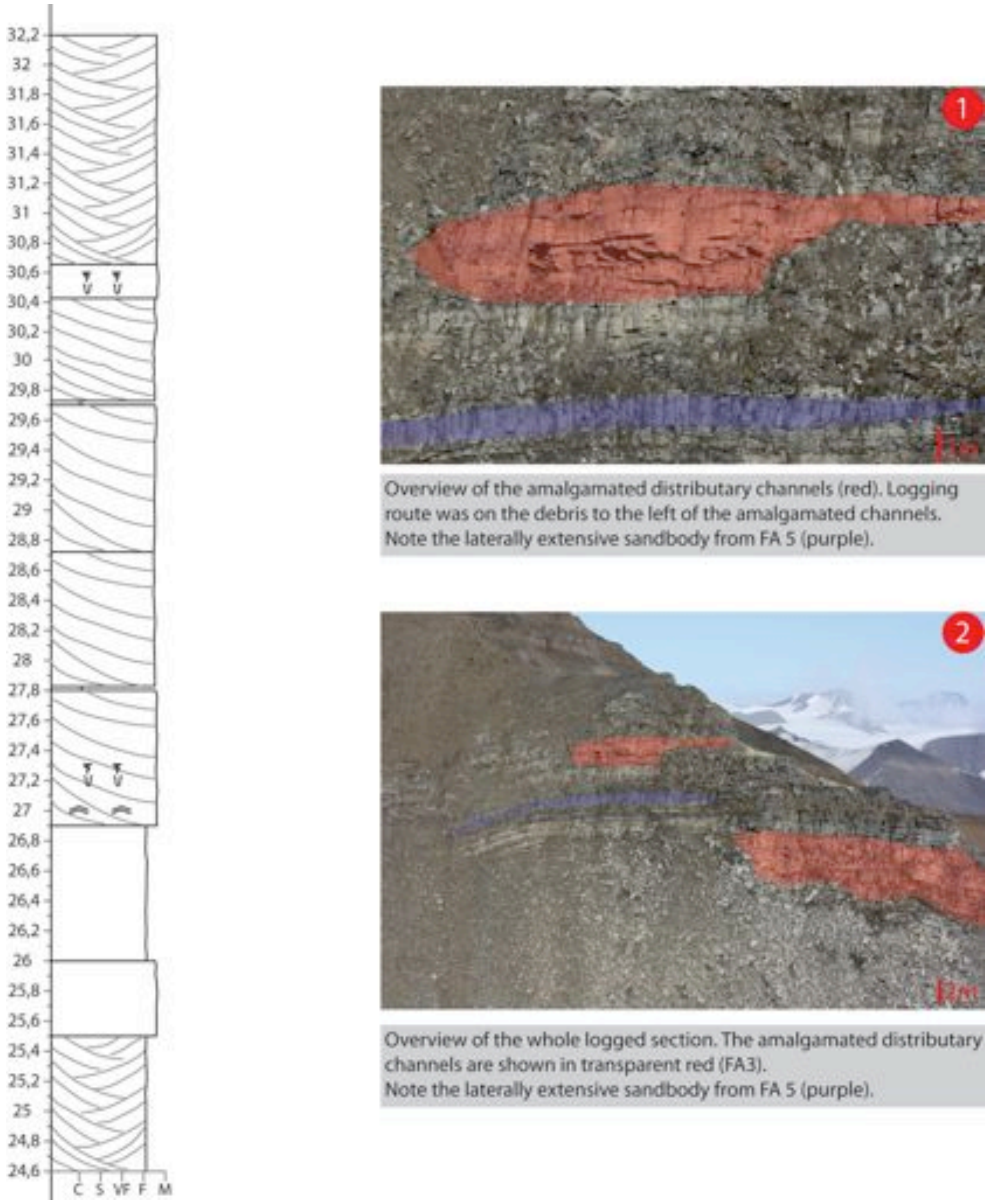

Figure 16 - Lithological log with illustrations representing FA6, amalgamated distributary channels part two. Channel areas are highlighted in red and purple. Note that this log starts at 24,6m, hence upper section. Legend found in appendix (Figure 68).

Observations

Very fine- to fine-to-medium-grained deposits are typical of facies association 3 and in general the grain-size does not vary considerably between the beds. Facies association 3 comprises of lithofacies F4-F8 (Table 1). At the lower reaches (7,2-11,5m) and upper reaches (24,6-32,2m), amalgamated distributary channels dominate facies association 3 (Figure 15; Figure 16). Structural features observed in FA3 are tangential cross-bedding, trough cross-bedding, wave- and current induced features and bioturbation. At the base of each channel structure, a thin layer of finer sediments is present, millimetres to a few centimetres thick.

In total, 15 amalgamated channels are identified within this association and 7 of these are found within the first 4,5 meters of part one (Figure 15). The stacking pattern and channel geometry (width, depth, and internal structures) of the lower part of these facies show similarities to the channels within FA2. The few channels included in FA2 display a coarsening upward channel fill and are therefore included in the distal to proximal delta front environment (FA2). In part one (from 11,5 meters - channels H, H_2 and I) there is a slight change in thickness and channel fill in contrast to the lower reaches of part one in FA3. These three channel fills show plane parallel lamination (Figure 17), trough cross-bedding, wave laminated beds, soft-sediment deformation and limestone concretions.

Figure 17 - Channel H_2: Plane parallel lamination at the base shifting into bioturbation, while distorting the internal structures upwards in the bed

Interpretation

Facies association 3 is distinguished by the presence of amalgamated distributary channels, which are a clear indication of a fluvial system. The channel width and shallow geometry together with the presence of wave-induced structures may imply a marine environment and deposition below sea level. The high width-to-depth ratio of the amalgamated channels indicates a more distal delta environment, where the channels typically shallow further out from the delta (Reading 1996). This is due to the fact that energy from river waters weakens when it enters a marine water body, and marine processes predominate. The occurrence of the thin units of finer sediments present at the base of each channel is a peculiar feature and is not fully understood. The finer sediments might be derived from a delta front environment and suggest a certain distance from the shoreline. The finer sediments may also be derived from deposition into a standing body of water where the sediments deposit from suspension before sands infill the channels.

Studies on oscillatory-flow and combined-flow bedforms in wave tunnel experiments were conducted by Dumas et al. (2005). The studies suggest that the controlling factors of depositional structures as oscillatory- and combined-flow bedforms are grain size, wave period, and unidirectional/oscillatory current velocities. As the grain size between the oscillatory ripples and plane parallel lamination in FA3 does not vary significantly, this factor is not of importance here. A stability field diagram for combined flow depositional structures of very fine-grained sand at a wave period of 8,0s were the result of studies by Dumas et al. (2005) (Figure 18). Their conclusion was that small ripples (>30cm Hanes et al. 2001) are generated at oscillatory velocities (Uo) up to 40 cm/s and unidirectional velocities (Uu) of up to 10 cm/s. On the other hand, plane parallel lamination are generated from Uo = 60-80 cm/s depending on the unidirectional velocities.

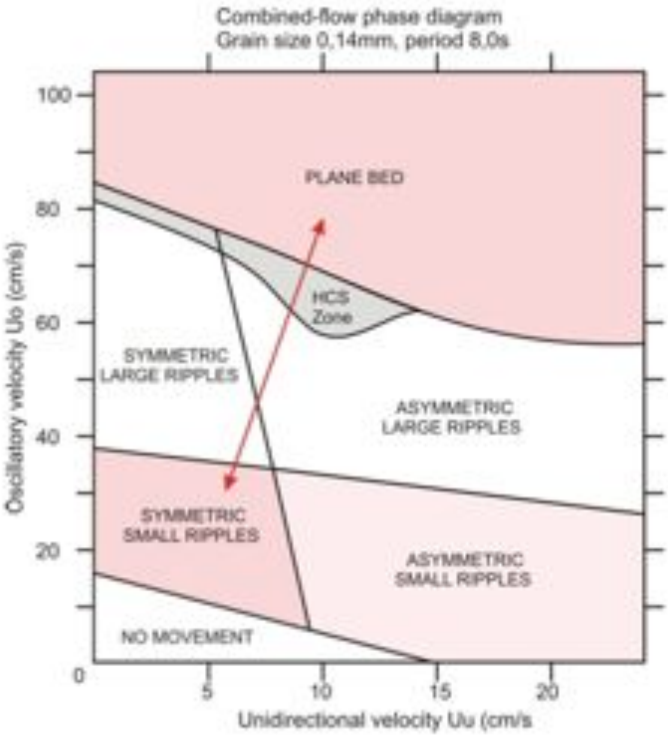

Figure 18 - Stability field diagram for combined flow depositional structures of very fine-grained sand at a wave period of 8,0s. Note that the measured fair weather current velocities of these studies plot within the stability field of small-scale ripples. (Modified from Dumas et al. 2005)

Both plane parallel lamination and small symmetrical ripples are identified in FA3 located at approximately 11,5 and 13 meters within channels H and H_2 (Figure 15;Figure 17). The plane parallel laminations (PPL) appear in the lower bedding plane and in both situations these structures are distorted by bioturbation upwards. Channel H is thick, massive fine-grained sandstone with PPL and soft sediment deformation. According to the studies completed from Dumas et al. (2005), the change from small symmetrical ripples to PPL may be caused by a change in the combined-flow velocities (Uo and Uu).

The question raised is why there are no intermediate deposits such as hummocky cross-stratification, symmetrical- and asymmetrical large-scale ripples within the sediments. A sudden change to higher velocities as well as progradation of the delta could be the answer. An increase in sediment supply together with higher current velocities might favour the transition from small symmetrical ripples to PPL and the formation of soft sediment deformation. Typically soft sediment deformation structures occur when there is a high sand to mud ratio (Reading 1996). Lack of mud in FA 3 suggest that instability of partially consolidated sand within a high energy channel flow, by for example rapid progradation of sand waves within the channel fill, might have caused the soft sediment deformation structures.

The presence of plane parallel lamination, limestone concretions and soft sediment deformation are within the thick, massive, amalgamated channel sandstones. The architecture and stacking pattern of the amalgamated channels are interpreted to be a result of lateral shift within the major or minor distributary channels, with increased current velocity and consequently increase in the rate of sediment supply to the terminal distributary channels. In order to generate the stacking pattern of the amalgamated channels in FA3 a proposed hierarchy of delta lobe shifting is presented in Figure 19.

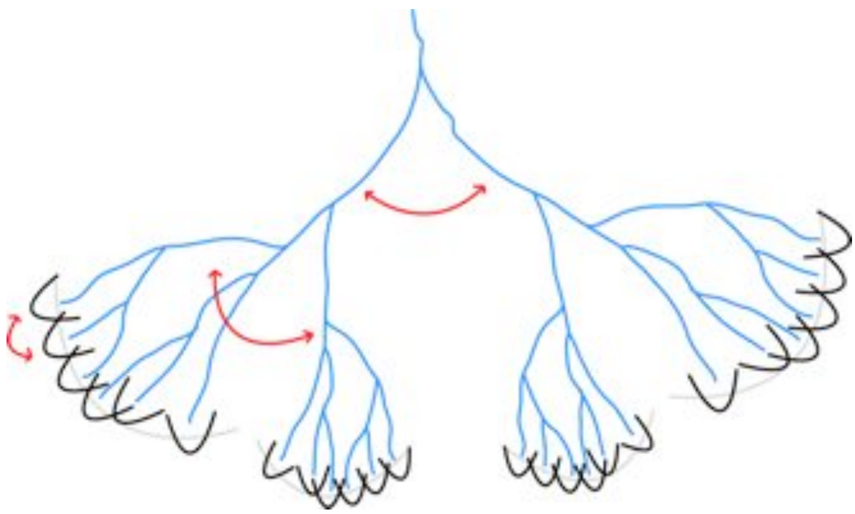

Figure 19 - Hierarchy of lobe shifting mechanisms. The figure illustrates three proposed hierarchy levels; a shift in the entire delta, a shift in delta lobes, and channel shifts within the delta lobes (Modified from Gjelberg, 2011)

The completely bioturbated sandstone beds with high content of organic matter, which are situated between channels H_2 and I and above channel I, suggest small flooding episodes or waning energy (Figure 15; Figure 16). The overlying channel I is interpreted to be part of an amalgamated distributary channel and can possibly imply that the system is quickly restored after the flooding episode. Based on the observations and interpretations, facies association 3 is interpreted as the transition from proximal delta front to lower delta plain.

Facies association 4 (FA4) – Shallow marine shelf sediments

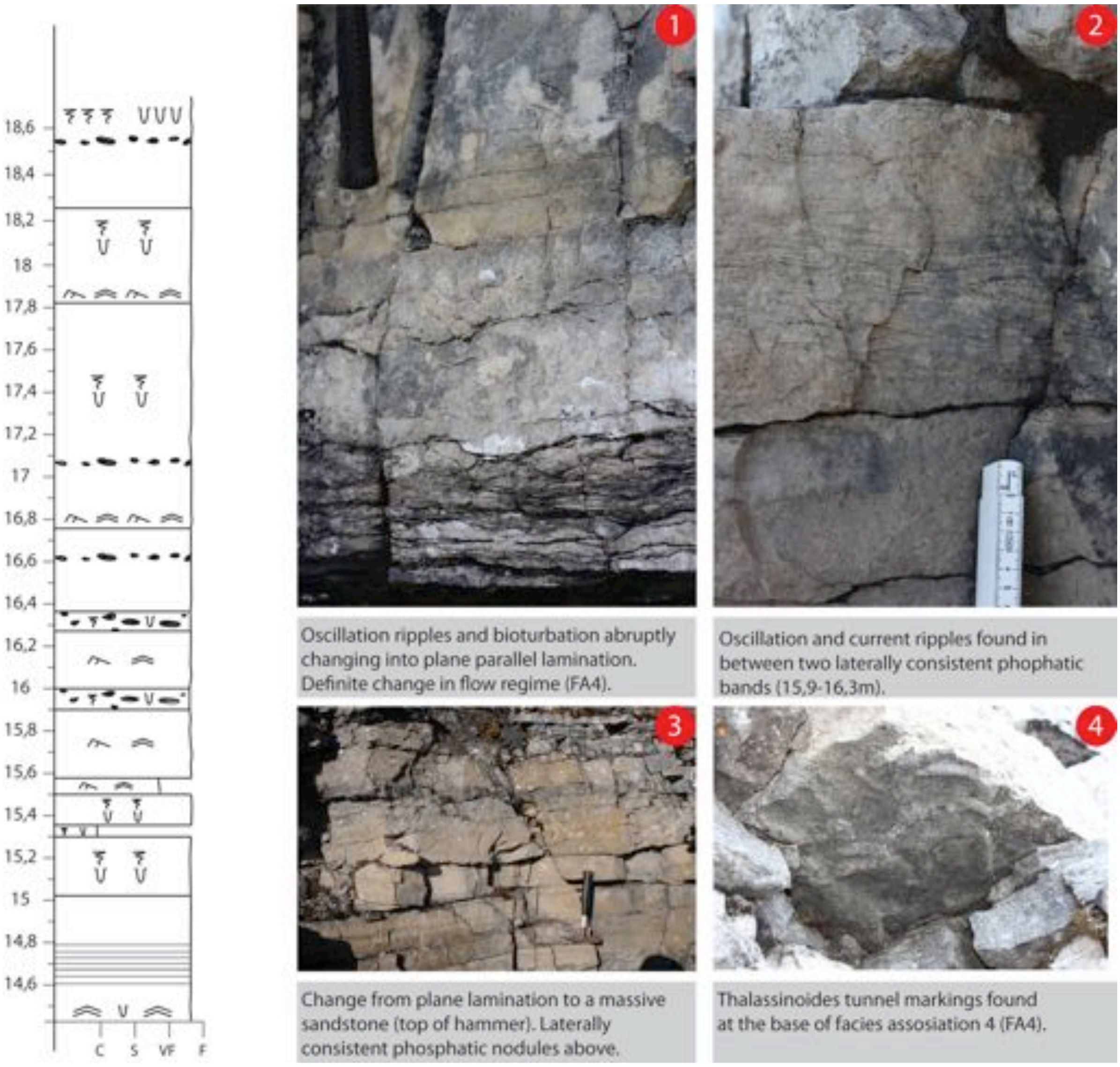

Figure 20 - Lithological log with illustrations representing FA4, Shallow marine shelf sediments. Note the presence of phosphate nodules (3). (4) Thalassinoides trace fossils and combined-flow depositional structures (1-2). Legend found in appendix (Figure 68).

Observations

Facies association 4 consists of very fine-grained sandstone (mediocre sand to silt ratio) with a single bed of a few centimetres bioturbated, mudstone (Figure 20). Facies association 4 comprises of lithofacies F3-F4 (Table 1). Wave- and current lamination structures are common as separate structures as well as together generating combined-flow lamination structures (top right Figure 20). Beds of intense bioturbation gradually decreasing and substituted by small-scale ripples or plane parallel lamination are a common trend throughout FA4 (top left Figure 20).
The most notable feature is the laterally consistent phosphatic nodules, which occur in bands at several stratigraphic levels. The phosphatic nodules are centimetre to tens of centimetre wide with an elliptic shape. Observations suggest that these nodules are not linked to the trace fossils of *Thalassinoides* (Pers. com. Snorre Olaussen).

Interpretations

Very fine-grained deposits together with the presence of combined-flow depositional structures, a high degree of bioturbation and phosphate nodules suggest a somewhat protected environment such as e.g. a deep lagoonal environment or a shallow marine environment.
Phosphatization has been discussed by Krajewski (2000 a,b,c,d,e) within the Middle Triassic succession, and he emphasises the importance of distinguishing between phosphate nodules linked to trace fossils and those which are not. In studies conducted by Mørk et al. (2008), phosphate nodules consisting of silty or muddy sediment cemented by carbonate apatite are a common find today. Mørk et al. (2008) also discussed phosphatization of cemented tunnels of *Thalassinoides* within the Middle Triassic succession such as the Botneheia and Bravaisberget Formations, located east and west on Spitsbergen respectively.
Formation of phosphate nodules typically starts after the burrowing processes have finished, and are a result of sediment filling in fossil traces. The ichnofauna in mention are typical for living in areas of low energy and low oxygen content in the uppermost sediment tier. A high abundance of ichnofauna indicates longer periods or repeated renewal of the favourable living conditions (Mørk et al. 2008).
Thalassinoides ichnocoenoses is mostly restricted to areas below the normal wave base and represents open shelf sedimentation (Mørk et al. 2008). *Thalassinoides* is usually in

conjunction with *Taenidium– Rhizocorallium* and *Polykladichnus* ichnocoenoses, meaning that they all belong to the same faunal community. Unfortunately the latter two are not found in this facies association. According to studies by Pemberton & Frey (1992), *Thalassinoides* are common in firm-ground assemblages, which again explains the depth of their tunnels compared to other infauna. Thus, the presence of *Thalassinoides* and phosphate nodules strengthen the argument for this facies association to be interpreted as shelf sediments in a shallow marine environment contra a deep lagoon environment.

Facies association 5 (FA5) – Proximal delta front (mouth bar progradation)

Figure 21 - Lithological log with illustrations representing FA5, Proximal delta front. Note the laterally extensive sand body, possibly Karentoppen Member, highlighted in picture 3. Legend found in appendix (Figure 68).

Observation

Facies association 5 (FA5) involves beds of different grain sizes, fine- to medium grained sandstone to very coarse-grained sandstone (Figure 21). Facies association 5 comprises of lithofacies F8-F10 (Table 1). Structures as tangential cross-bedding, plane parallel lamination, wave- and current induced structures, and foresets of gravel are identified. FA5 comprises of two channel facies, which are laterally consistent, and not identified previously, as well as two upward coarsening beds with foresets of coarser grains. Laterally consistent sand bodies and channel features are amongst the larger scale structures. Intense bioturbation and the presence of organic material in the finer grain sizes are observed.

Interpretation

Facies association 5 is deposited in a proximal delta front environment with distributary channel facies and interbedded mouth-bars. Studies conducted by Olariu & Bhattacharya (2006) on delta front architecture and terminal distributary channels use examples from both modern and ancient deltas. The ancient, Cretaceous Panther Tongue delta in Utah, USA, is strikingly similar to the studied delta front outcrops of the Karentoppen Member (Figure 22).

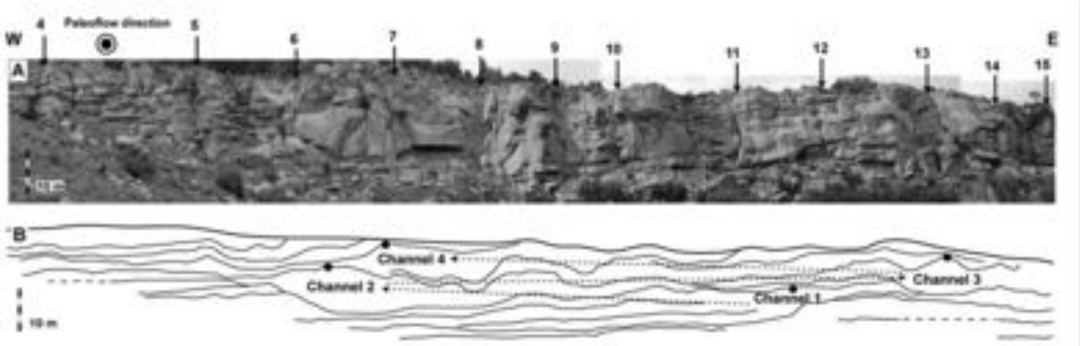

Figure 22 - Cretaceous Panther Tongue delta, Utah, USA. Note the width-to-depth ratio (Olariu and Bhattacharya 2006)

The Panther Tongue delta is interpreted as proximal delta front deposits with distributary channels and laterally migrating mouth-bars. Studies on these channelized features suggest a low topography, with less than 4m relief, and widths of tens to hundreds of meters. The lateral migration of these channels is on the order of hundreds of meters (Olariu & Bhattacharya 2006). The outcrops studied show similar sand body geometries with the channelized features found in these outcrops; hence both terminal distributary channels and large-scale sheet-like channels (Figure 22;Figure 23).

Figure 23 - Possibly Karentoppen Member, as the outcrops appear similar. Note the thick amalgamated channels and the laterally consistent sand body above. This outcrop is not included in this study and the studied Karentoppen Member is seen to left in the picture, though may show the lateral continuity of the sand body.

Interpretations of the Panther Tongue delta suggest that the channels are infilled with fine- to medium sandstone with structureless, plane parallel laminated or trough-cross laminated beds (Olariu & Bhattacharya 2006). Identical structures are seen in previous facies associations and in the present association (FA5). Several sets of plane parallel laminations, tangential cross-bedding and wave- and current induced structures are amongst the main features within FA5.
Figure 24 based on Axelsson (1967), Baydin (1970) and van Heerden (1983), by Olariu and Bhattacharya (2006) shows different evolutionary and formational stages of terminal distributary channels and mouth bar systems. This example can be used to understand facies association 5, where the delta is prograding and terminal distributary channels are being formed and infilled. As a result of the prograding delta, terminal distributary channels extend further seaward and mouth-bar deposits form as the flow condition at the channel mouth changes from confined to un-confined and velocity decreases (Albertson et al. 1950; Bates 1953; Wright 1977; Olariu & Bhattacharya 2006). The eight steps (a-g) in Figure 24, illustrates the formation and evolution of the mouth bar systems and the creation of new terminal distributary channels.

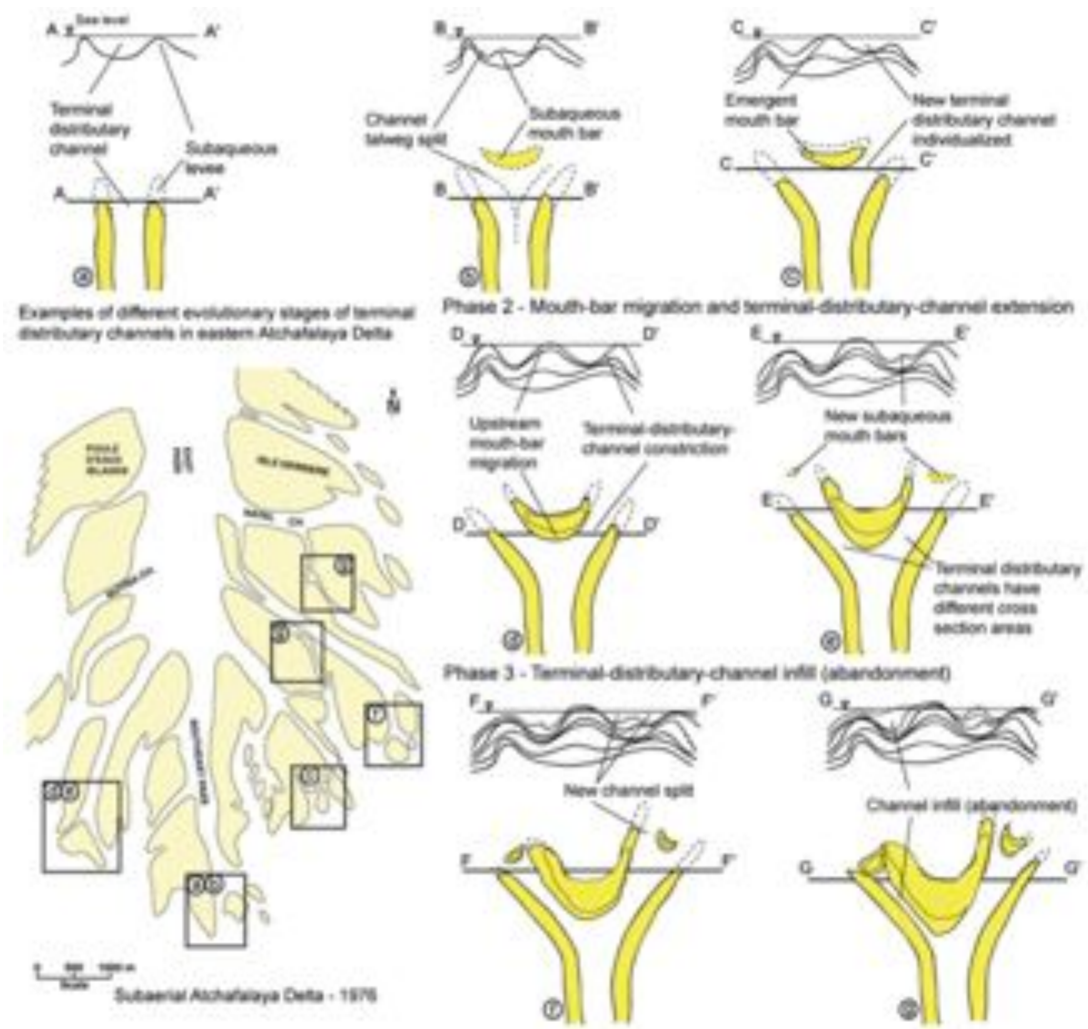

Figure 24 - Conceptional formation and evolution of a terminal distributary channel mouth bar system (based on Axelsson 1967; Baydin 1970; van Heerden 1983) (Illustration taken from Olariu & Bhattacharya 2006)

According to studies by Overeem et al. (2003), mouth-bar deposits are relatively thin (less than 1 m) with a coarsening upward trend for regressive (forced regression) periods. Two similar coarsening upwards trends is found within FA5, though slightly thicker beds than the examples from Overeem (2006). Whether or not this is a regressive period is not yet discussed.

Based on these observations, facies association 5 is therefore interpreted to be a prograding proximal delta front with the formation of terminal distributary channels and mouth bars.

Fieldwork summary of the Karentoppen Formation

The Passhatten and Karentoppen Members are part of an eastward prograding deltaic system (Figure 25). Two coarsening upward trends are interpreted (0-14,4m and 14,4-32,2m) separated by a flooding surface at 14,4 meters. The lower CU- unit comprises prodelta, delta front and deltaic amalgamated distributary channels, which define the first prograding event. A flooding at 14,4m initiates the upper CU unit or second prograding system that comprises an open marine shelf environment, which passes upward and shifts into a delta front and finally into amalgamated distributary channel fills. The last CU unit is capped by a renewed flooding event. Poor exposures at Karentoppen give little information of the overlying unit. But the Karentoppen Member is gradually replaced by offshore mudstone (Mørk et al. 1982) suggeting an overall transgressive unit.

Within the large relative shallow epicontintenal sea in the Triassic Barents Sea internal clinoform geometries on seismic shows that most of the sediments were derived from the Baltic Shield in the south and the Uralian Mountains in the east and southeast (Glørstad-Clark et al. 2011). However the proximal deltaic deposit observed on Karentoppen suggests a nearby land area and drainage from northwest. This is consistent with previous models (Mørk et al. 1982 and Riis et al. 2008) with minor clastic wedges infilling of the larger Triassic basin from west in the Barents Sea (Mørk et al. 1982; Riis et al 2008).

The sandstone/shale ratio and the architecture of the sandstone bodies are originally a very prolific potential reservoir unit. Based on observations from a distance on outcrops not yet studied (Figure 23), this prolific facies is supposed to be laterally continuous in kilometre scale parallel to the paleocoastline (in this case probably a northeast – southwest directed coastline). Due to previous deep burial, late diagenetic processes, the member appear now as a very tight (probably less than 5 -7% porosity) and impermeable sandstone unit.

The outcrop seems to be a good analogue to part of the reported proximal deposits of the Kobbe Formation in the Goliat Field. Hopefully this analogue will improve a prediction of sandstone body geometry, sequence stratigraphic resolution and facies models of the Kobbe Formation in the Goliat Field.

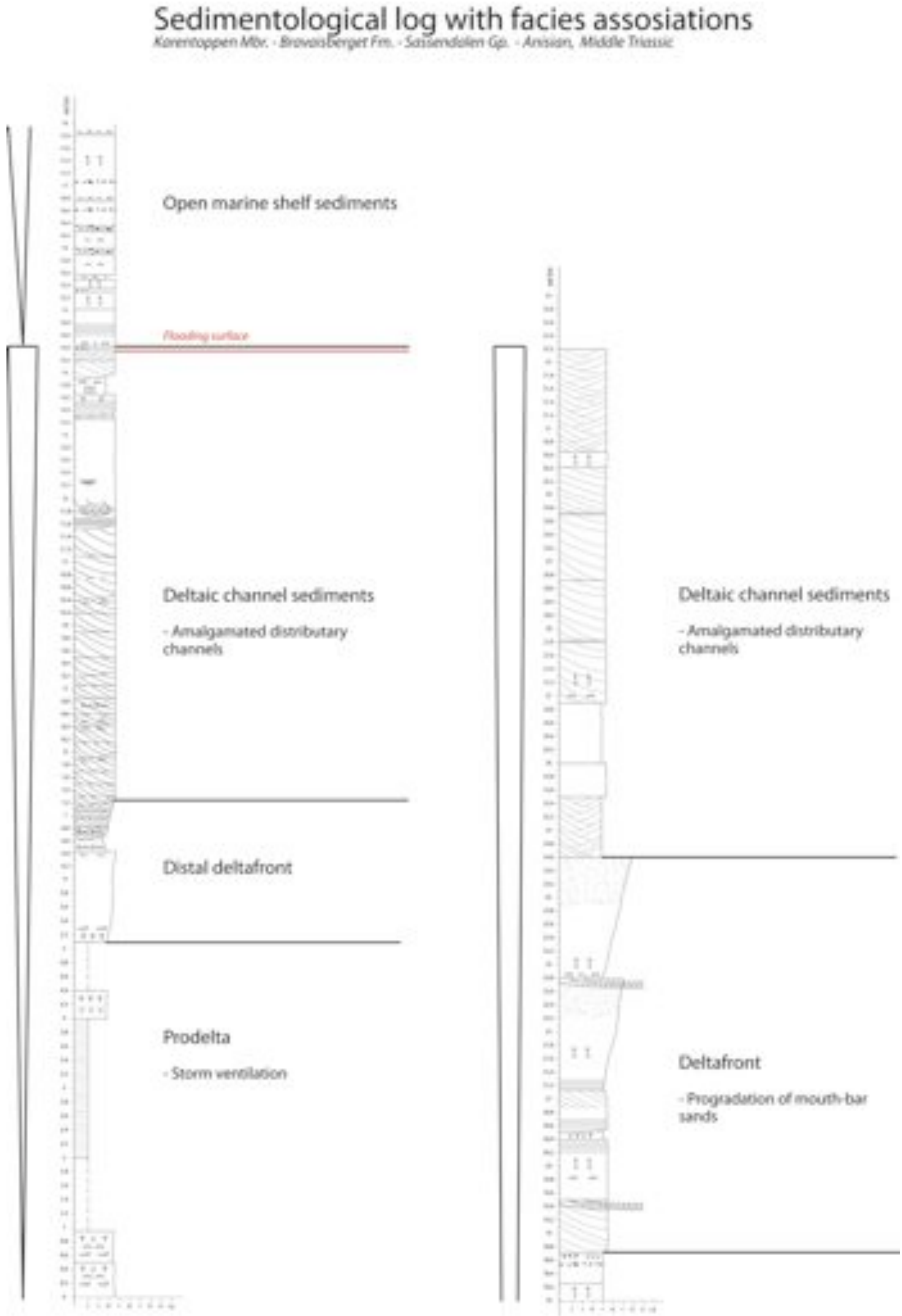

Figure 25 – Sedimentological log with facies associations from Karentoppen Member, Spitsbergen. Legend found in appendix (Figure 68).

4. Facies association - Cores

Well 7122/7-3

General information

The following information on well 7122/7-3 (cores 5 and 6) is taken from the Norwegian Petroleum Directorates fact pages (factpages.npd.no). The total depth of the well is 2726 MD (mRKB) with a maximum inclination of 4,7°, and is considered an exploration well. The depth in focus in this assignment is 1835MD – 1824MD, penetrating the Kobbe Formation in the Goliat Field. The core diameter is approximately 13cm.
A table of facies associations with interpreted depositional environments is presented below in Table 3.

Table 3 - Six facies associations and lithofacies (FA1-FA6) with interpreted depositional environments

Facies associations:	Interpreted depositional environments:
FA1 (F1-F2)	Offshore shales
FA2 (F3-F5)	Inner estuary fluvial channels
FA3 (F6-F7, F9)	Bay-head delta
FA4 (F1-F2)	Estuarine mud
FA5 (F5, F7, F9)	Tidal-influenced fluvial channels
FA6 (F9-F10)	Estuarine mouth bars

Well 7122/7-3 – Core 6

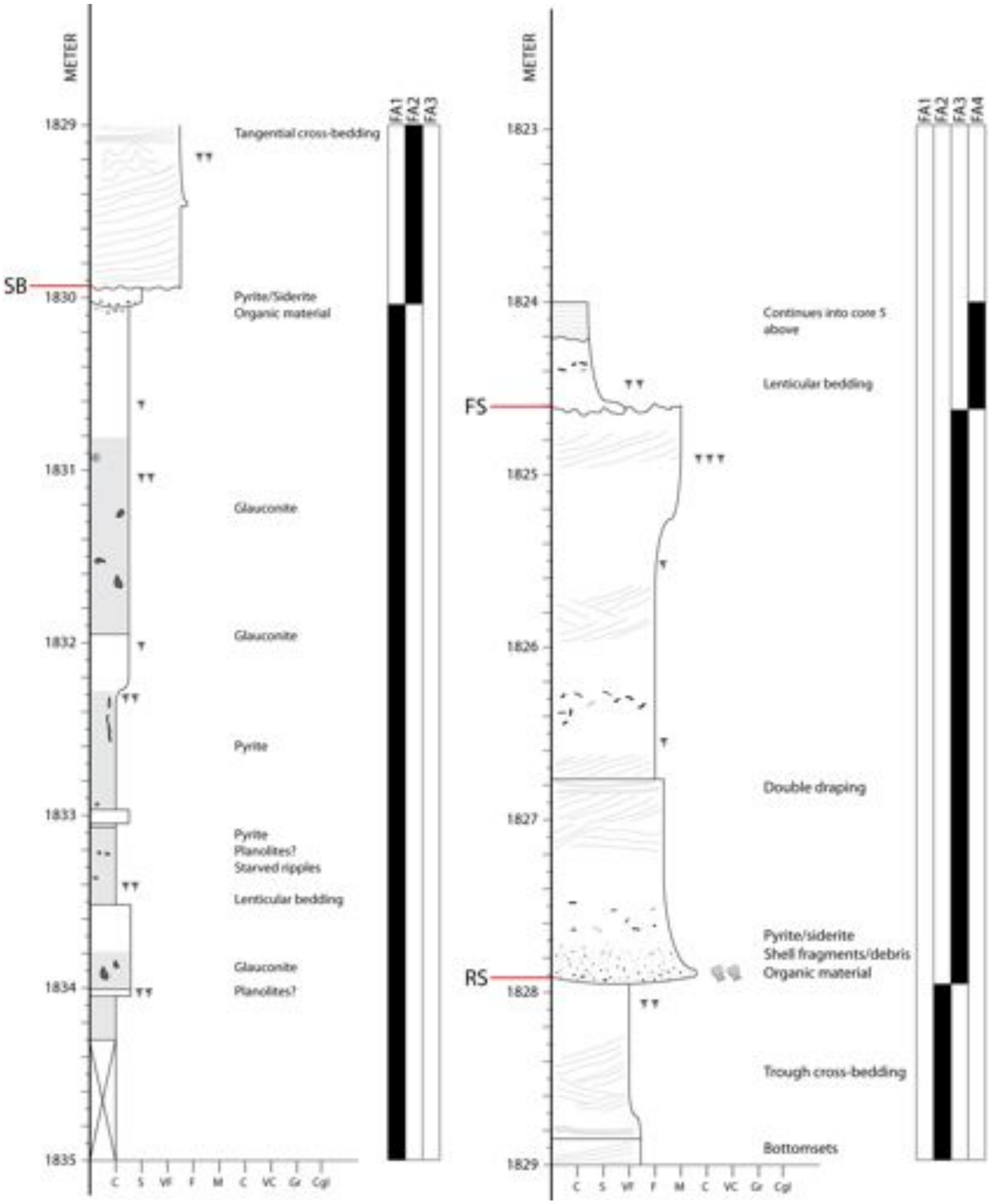

Figure 26 - Lithostratigraphic log with facies associations from well 7122/7-3 - core 6. SB; Sequence boundary. FS; Flooding surface. RS; Ravinement surface. Legend found in appendix (Figure 68).

Facies association 1 (FA1) - Offshore

Observation

Facies association 1 (FA1) consists of laminated claystone and striped silty claystone (Figure 26;Figure 27) (1835-1830m). Grain size varies between clay and clay-to-silt and the facies is black and dark grey in colour, comprising of lithofacies F1-F2 (Table 1). Discontinuous seams and lenses of siltstone with starved ripple structures are observed within the first few meters (Figure 27). The seams and lenses of siltstone are lenticular shaped and on millimetre- to centimetre scale. Claystone lamination and scarce ripple structures as well as pyrite, siderite and glauconite features dominate the internal structure of facies association 1.

The clay mineral glauconite is observed at three stratigraphic levels in this association (Figure 27). Glauconite appears as a green tint on the claystone and gradually increases in tone upwards at each level. In all three appearances the glauconitic claystone is suddenly abrupt by black laminated claystone above (Figure 27).

Figure 27 - Close-up features of FA1. (1) Discontinous seams and lenses of siltstone and bioturbation. (2) Vertical pyrite nodules. (3) Glauconite abrupt by black laminated claystone

Pyrite and siderite are found as nodules and possibly as pyrite-replacement of certain burrows (Figure 27). The pyrite-replaced burrows are seen as both vertical and horizontal traces in centimetre-scale. Pyrite is a common iron disulphide mineral and is

observed at several outcrops of Middle Triassic age on Spitsbergen (Krajewski et al. 2007; Mørk et al. 1982; Riis et al. 2008).
The degree of bioturbation fluctuates as unburrowed beds are intercalated with burrowed beds. Millimetre-scale, white-circled, horizontal burrows are observed within the striped silty claystone and are a prominent feature as the diversity of ichnofossils is low in this part (Figure 27). Both the diversity and intensity of bioturbation increases further upwards in the succession.

Interpretation

The striped silty claystone beds containing starved ripples can indicate periods of higher depositional energy, whereas the black laminated claystone can indicate periods of lower depositional energy. The laminated claystone and striped silty claystone may have been generated during periods of repeated activity of bottom currents and changes in depositional energy.
The lamination within the claystone is only preserved in the unburrowed beds and may also indicate differentiated bottom conditions.

Pyrite is observed throughout the association both as nodules and vertical features. According to studies by Gingras and MacEachern (2011) , pyrite can replace bioturbated textures as they observed from studies on tidal ichnology of shallow-water clastics. Though the ichnologic nature in this study is not identified, a vertical trend of pyrite is observed and could indicate replacement of burrows. Krajewski (2008) describes the Botneheia Formation on Spitsbergen, which is the eastern time-equivalent to the Bravaisberget Formation, and finds that common authigenic pyrite is seen in anoxic sulphidic environments below the water/sediment interface. Based on these studies, the interpretation of reducing and dynamic bottom conditions can be likely.

As observed, the glauconitic sequences are intensely burrowed and are abrupt by black laminated claystone. Previous encounters with green-tinted claystone has shown that glauconite forms in marine-shelf environments, as e.g. (Gjelberg et al., 2005) interpreted from studies on the Ormen Lange gas field. Glauconite is also observed from the upper Ladinian Sentralbanken in the transition between an open marine to a tidal channel complex environment (Riis et al. 2008). Glauconite can form in many environments,

though due to the interpreted lithostratigraphy of this association, it is likely that the clay mineral formed in a marine setting.
The white-circled burrows within the striped silty claystone are not identified; though resemble the burrows of *planolites*, which can be an indicator of oxygen-stressed environments (Gingras and MacEachern, 2011). This interpretation is further strengthened by the low diversity of ichnofossils in this part of the association.

The absence of storm-generated structures and the suggested reducing bottom conditions may indicate deposition below storm-wave base. Therefore, the depositional environment of facies association 1 is interpreted as an offshore environment with changing depositional rates and dynamic bottom environments shifting between dysoxic and anoxic conditions.

Facies association 2 (FA2) – Inner estuary fluvial channels

Observation

Facies association 2 (FA2) comprises of sharply bounded units of very fine-to-fine grained, well-sorted sandstones with amalgamated trough cross-bedding as the prevailing internal structure (Figure 26) (1830,1-1828,1m). Facies association 2 comprises of lithofacies F3-F5 (Table 1). Facies association 2 erodes into facies association 1 by a disconformity (Figure 26;Figure 28). Plane parallel lamination, tangential cross-beddings and distinct bottomsets are observed at certain levels of the association (Figure 28).
FA2 is part of a fining upwards sequence, where the upper and lower boundary surfaces contain siderite- and pyrite nodules and organic matter (Figure 28). As the unit slightly fines upwards the cross-bedding structures are distorted by intense bioturbation. The cross-bedding is gradually less pronounced as well as a gradual shift in colour from dark brown to light grey with smaller variations in between. The foresets of the cross-beddings may show tidal influenced processes, where the result is double and single mud drapings, and in places distorted by intense bioturbation (Figure 28).

Figure 28 - Close-up of the features of FA2 with red and white markings. (1) Erosional surface between FA1 and FA2. (2) Bioturbation below and tangential cross-bedding above. (3) Trough cross-bedding. (4) Bioturbation and siderite nodules together with organic matter. (Note the gradual fining upwards from pictures 1 to 4.)

Interpretation

Facies association 2 is interpreted as amalgamated channels with trough cross-bedding as the dominant internal structure. The alluvial channels truncate the marine shales of facies association 1 generating a sequence boundary, which by definition, is an erosional surface that separates cycles of deposition (SB) (Figure 26;Figure 28). The internal structures together with the overall fining upwards trend suggests migration and gradual infilling within a confined channelized setting (Dalrymple and Zaitlin, 1994; Dalrymple et al., 1992). The differences in internal structures such as plane parallel lamination and trough cross-bedding suggest fluctuating depositional energy, hence the stability diagram by e.g. (Dumas et al., 2005) (Figure 18).
Decimetre-scale intervals of bioturbation are present within the association (Figure 28). Intermittent bioturbation may suggest differential depositional energy and/or the increase of salinity into the system. The trace fossils are difficult to sort and remain unidentified.

The amalgamation of channels may be a response to base level rise balanced by sediment supply, which again implies that vertical aggradation played a major role in forming these sand bodies (Løseth et al., 2009). Based on the observations and interpretations of facies association 2, and the overlying association (FA3), facies association 2 is interpreted as an inner estuary, fluvial channel environment.

Facies association 3 (FA3) – Bay-head delta

Observation

Facies association 3 consists of fine-to-medium and fine-grained sandstones with an erosional base truncating the underlying facies association (FA2) (Figure 26) (1828,1 – 1825,4m). FA3 comprises of lithofacies F6, F7 and F9 (Table 1). Decimetre thick lag sediments are deposited onto a sharp surface. The lag sediments consist of shell fragments, coal pieces, siderite nodules and larger grained sediments (Figure 29). The siderite nodules and shell fragments are constrained within the first meter of facies association 3.

The primary sedimentary structures are trough cross-bedding with single and possible double drapes on foresets, sets of low-angle lamination and possibly mud rock partings (Figure 29).

The facies association is divided into one fining upwards and one coarsening upwards sequence (Figure 26). The fining upwards sequence is characterized by sharply based lag sediments, which grade vertically into primary sedimentary structures. The coarsening upwards sequence contains the same primary sedimentary structures though without shell fragments and siderite nodules, as well as bioturbation seems to be more pronounced upwards in the sequence (Figure 29).

The coal pieces vary both in size and distribution as some pieces have root shapes with no preferred alignment and others cluster and align the foresets (Figure 29). The presence of organic matter is decreasing vertically as bioturbation intensity increases. Bioturbation is generally modest though variable and occasionally absent through the association.

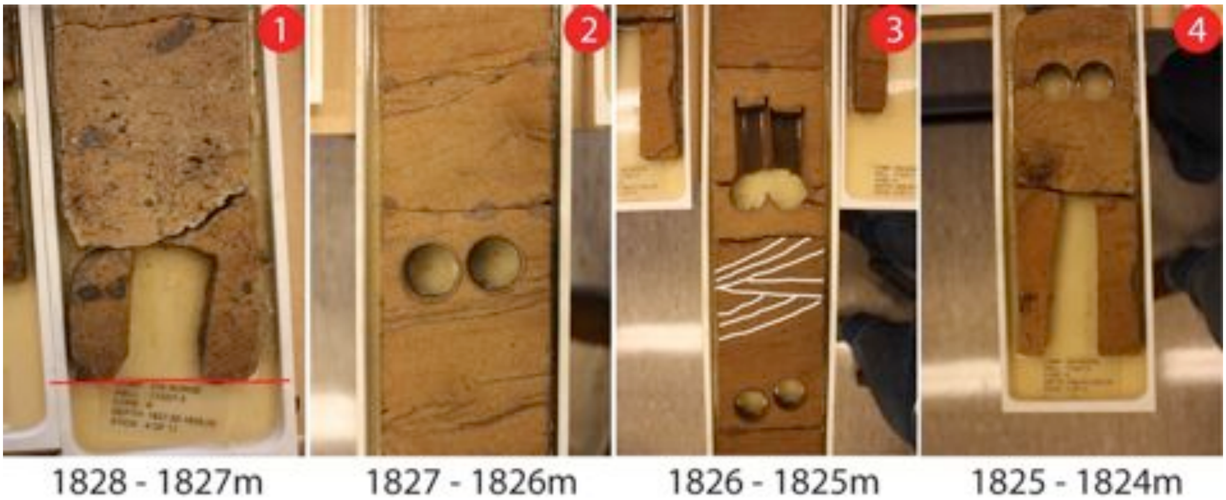

Figure 29 - Close-up of the features of FA3 with red and white markings. (1) Transgressive lag sediments. (2) Foresets of double and single drapes. (3) Trough cross-bedding. (4) Bioturbation towards the top of FA3

Interpretation

Facies association 3 is initiated by a transgressive lag that truncates the underlying association (FA2) and generates a ravinement surface. A ravinement surface is a key-bounding surface formed by shoreface erosion during transgressive conditions (Helland-Hansen and Gjelberg, 1994; Nummedal and Swift, 1987), or at the coast, both as tidal ravinement at river mouths and as wave ravinement along the open-coast shoreface (Davis, 2011). Studies by (Willis, 1997)on fluvial-dominated valley-fill deposits, suggests that as relative sea level rises, the accommodation space increases and the valley-infilling commences, gradually becoming more estuarine in character.

The sediments, shell fragments and coal pieces comprising the transgressive lag are interpreted as allocthonous and are coarser-grained than the overlying units.
The coarse-grained nature of the sediments, together with the internal primary structures, suggests deposition in a relatively high-energy environment. Trough cross-bedding and low-angle lamination with single and paired drapes indicates influence from tidal processes (Dalrymple et al., 1992; Pattison and Walker, 1994). The presence of bioturbation in between the preserved cross-bedding suggest influx of saline water.

(Dalrymple et al., 1992) defines an estuary as "*the seaward portion of a drowned valley system which receives sediment from both fluvial and marine sources and which contains* *facies influenced by tide-, wave- and fluvial processes". (Dalrymple et al., 1992)* further distinguishes between the end-members, tidal- and wave-dominated estuaries. The evolution of a wave-dominated estuary commonly initiates with a transgression and further the progradation of a bay-head delta. Bay-heas deltas have a scale and geometry superficially like inclined heterolithic point bars, but they coarsen upwards (Davis, 2011). The fluvial sediments are distinguished from the bay-head delta facies by the lack of tidal structures and/or a brackish-water fauna (Dalrymple et al., 1992). In tide-dominated estuaries, the tidal currents can redistribute the sediment supplied by the river and marine sources, and cause rapid infilling of the deeper and wider parts (Dalrymple et al., 1992). Although these end-members are readily distinguishable, this association alone is insufficient to define the dominant estuarine character.

Based on these observations and the interpretation of the underlying FA2, a bay-head delta environment within the upper estuary is proposed for facies association 3.

Facies association 4 (FA4) – Estuarine mud

Observation

Facies association 4 comprises of two fining upwards sequences of very-fine grained sandstones to claystones (1825,4 – 1823,3m) (Figure 26). As a side note, the transition between core 6 (1835-1824m) and core 5 (1824-1812m) in well 7122/7-3 divides facies association 4 at 1824 meters measured depth (MD). The first 80cm of core 5 are missing, though the assumption that facies is more or less the same as the underlying is made. FA4 comprises of lithofacies F1-F2 (Table 1).
Core 6 comprises one of the two fining upwards units and is approximately 60cm thick. The base of facies association 4 is erosional and grades vertically with decreasing sand and silt content (Figure 30). As a result the sedimentary bedding patterns grade from flaser- to lenticular bedding to laminated claystone. Bioturbation is intense at the base and decreases as the clay content increases.

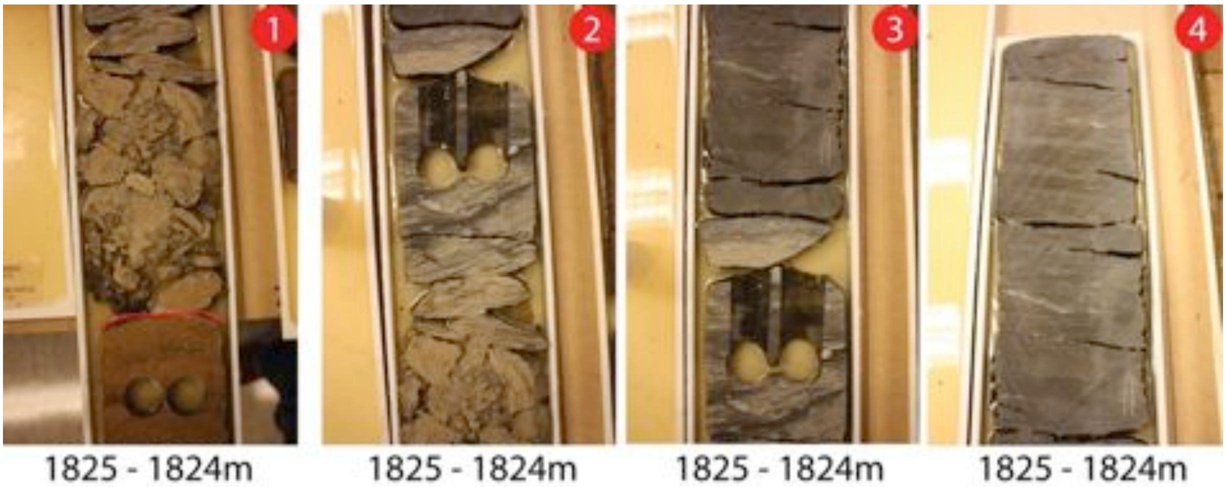

Figure 30 - Close-up of the features of FA4, core 6. (1) Erosional base onto FA3 (2-3) Decreasing siltstone content. (4) Black laminated claystone

Core 5 initiates with a fining upwards sequence with grain sizes ranging from silt to clay. The siltstone dominates the lower boundary and grades into claystone vertically. Internal structures as flaser- and lenticular bedding, pyrite nodules, organic matter and bioturbation are present (Figure 31). Bioturbation is intense at the lower boundaries and decreases upwards, similar to the fining upwards sequence of core 6.

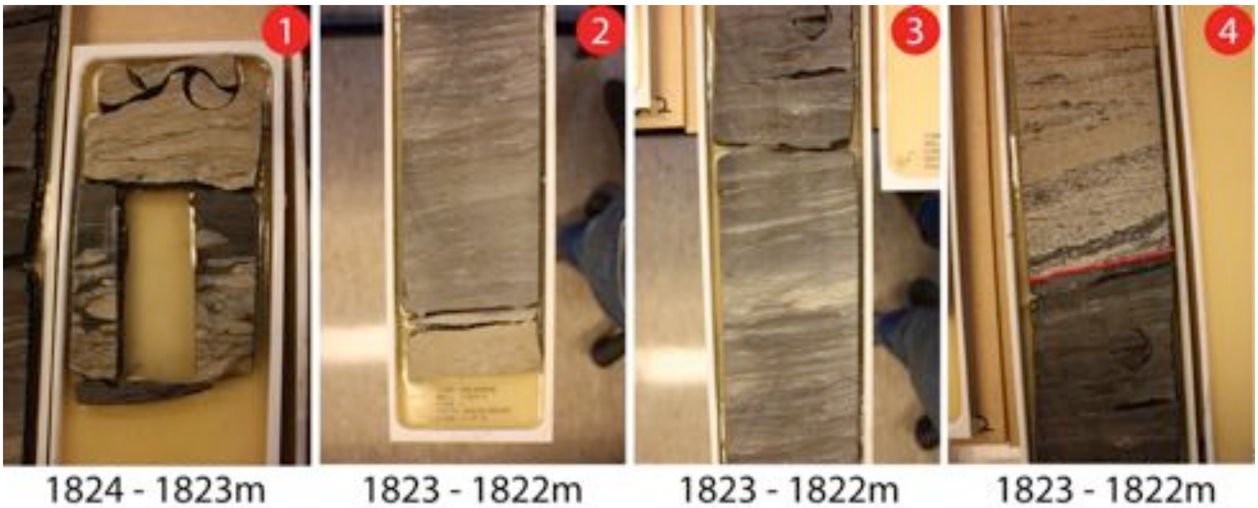

Figure 31 - Close-up of the features of FA4, core 5. (1-3) Fining upwards sequence with decreasing siltstone content. Flaser to lenticular bedding. (4) Black laminated claystone with the boundary to FA5 marked in red. Note the rip-up clasts in FA5

Interpretation

The deposits of facies association 4 overlay the sandstones of facies association 3 by a sharp disconformity. Both fining upwards units are similar in internal structure and increasing mud content. There are many ways to interpret this association, and two possible interpretations will be discussed below:

- Estuarine mud deposits
- Mud flat deposits

As end-members, wave-dominated and mixed-energy estuaries commonly form barriers/spits preventing most of the energy from entering the estuary. As a consequence, the finest sediments are deposited in the area where the river-dominated currents mix with the marine-dominated currents (Figure 32) (Dalrymple et al., 1992). The finest sediments in tide-dominated estuaries are commonly deposited as tidal meanders and/or mud flats in the mixed energy-zone. According to Dalrymple et al. (1992), it is commonly a higher total energy in the mixed zones of idealized tide-dominated estuaries than wave-dominated estuaries (Figure 32).

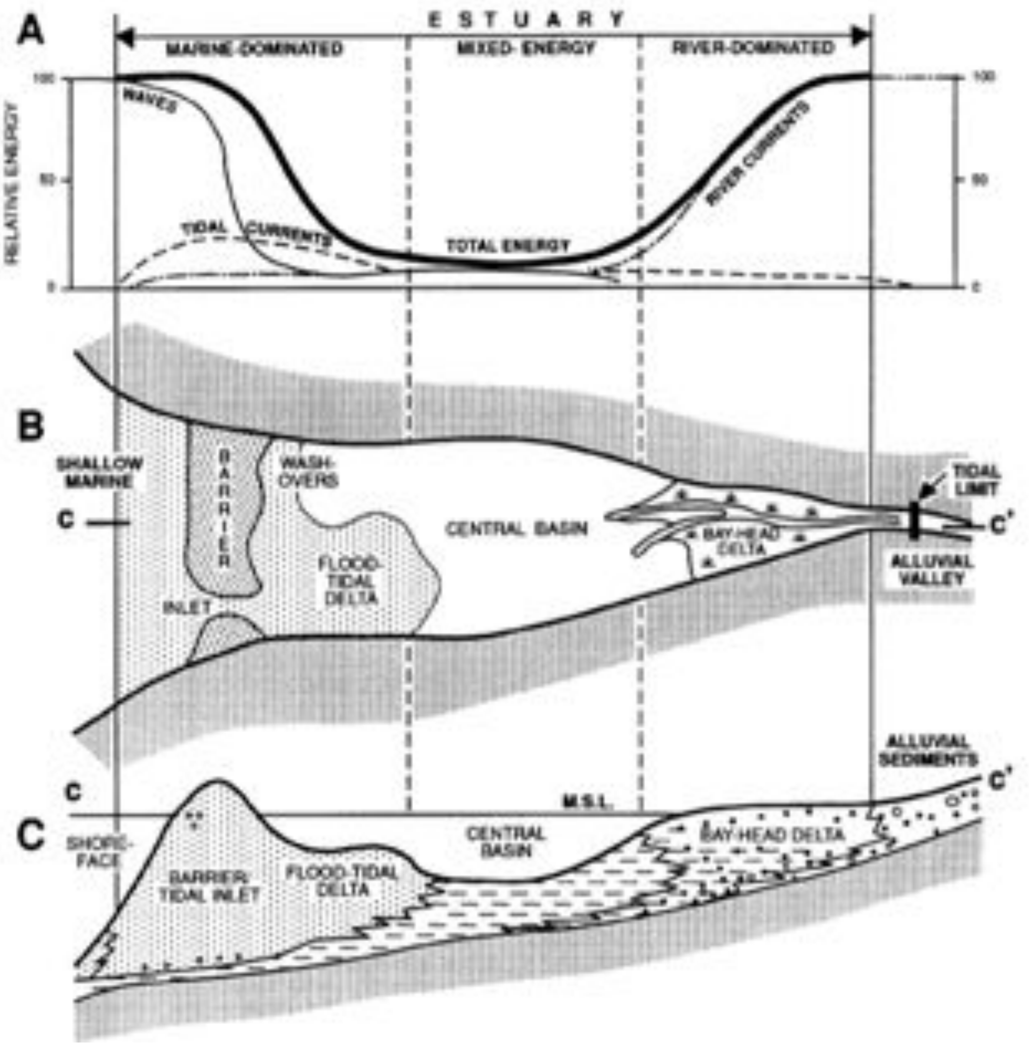

Figure 32 - Idealized wave-dominated estuary from (Dalrymple et al., 1992). (A) Distribution of energy types. (B) Distribution of morphological components in plan view. (C) Distribution of sedimentary facies in an idealized wave-dominated estuary

The upwards-fining nature of facies association 4 proposes a gradual transition from the sandstones of a bay-head delta into an estuarine mud environment. As (Dalrymple et al., 1992) states, the upwards-fining trend may represent a passage from a transgressive, fluvial and bay-head delta deposit to an estuarine mud deposit environment.
Based on the observations and the adjacent associations, facies association 4 is interpreted as a transition from a bay-head delta into an estuarine mud deposit environment. Therefore, an estuarine mud depositional environment is proposed for facies association 4. A compilation of core 6 with core photos is presented in Figure 33 below.

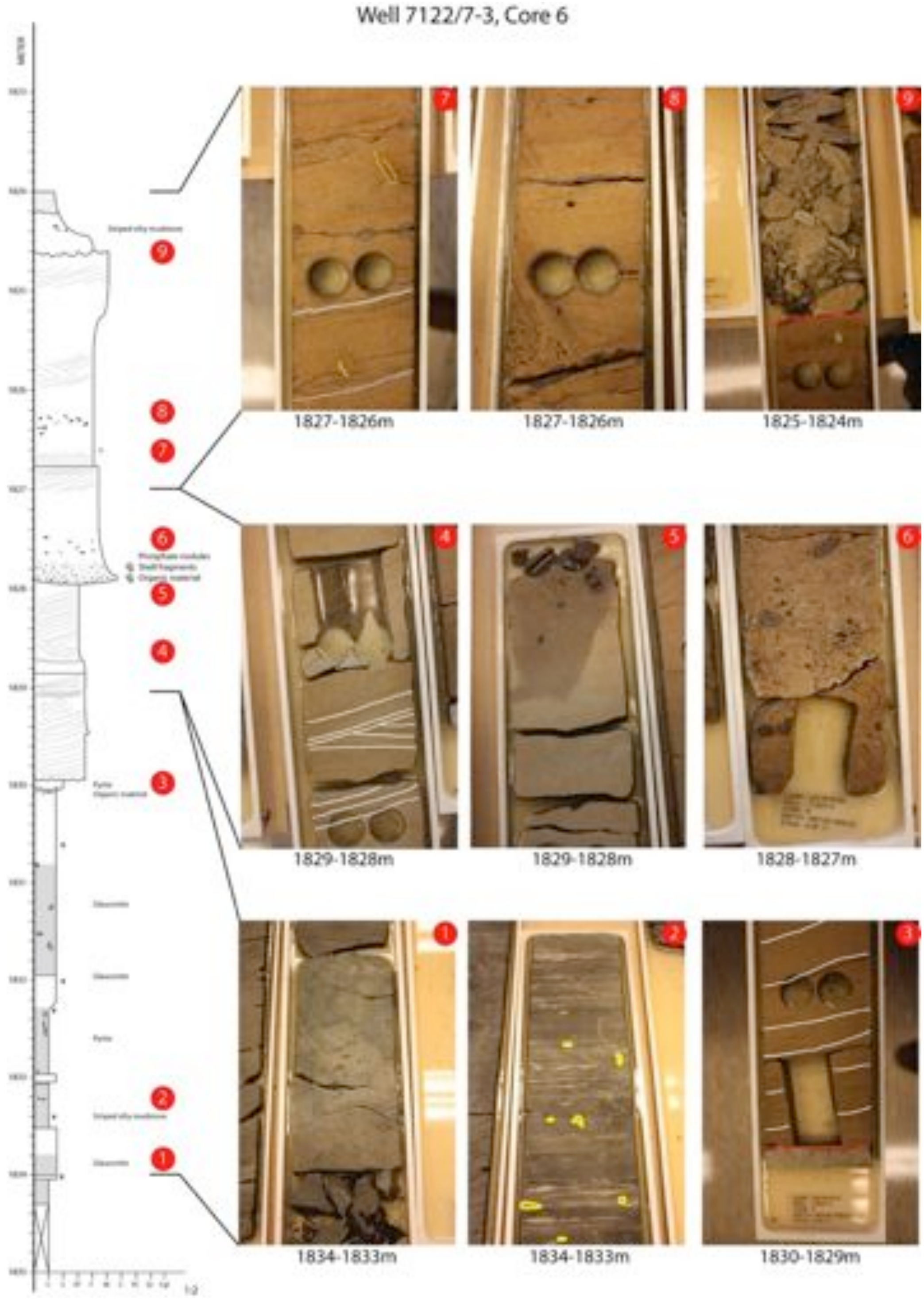

Figure 33 - Compilation of log and photos from well 7122/7-3, core 6. (1) Bioturbated glauconite. (2) Striped silty claystone with bioturbation (yellow) and starved ripple structures. (3) Sequence boundary between FA1 and FA2. (4) Trough cross-bedding in FA2. (5) Bioturbated bed with siderite nodules in FA2. (6) Ravinement surface - transgressive lag with shell fragments, coal pieces and siderite nodules at the base of FA3. (7) Low-angle cross-bedding with double drapes and burrows (yellow). (8) Coal horizons and possible water escape. (9) Flooding surface between FA3 and FA4. Note the bioturbation at the upper boundary of FA3. Legend found in appendix (Figure 68).

Well 7122/7-3 – Core 5

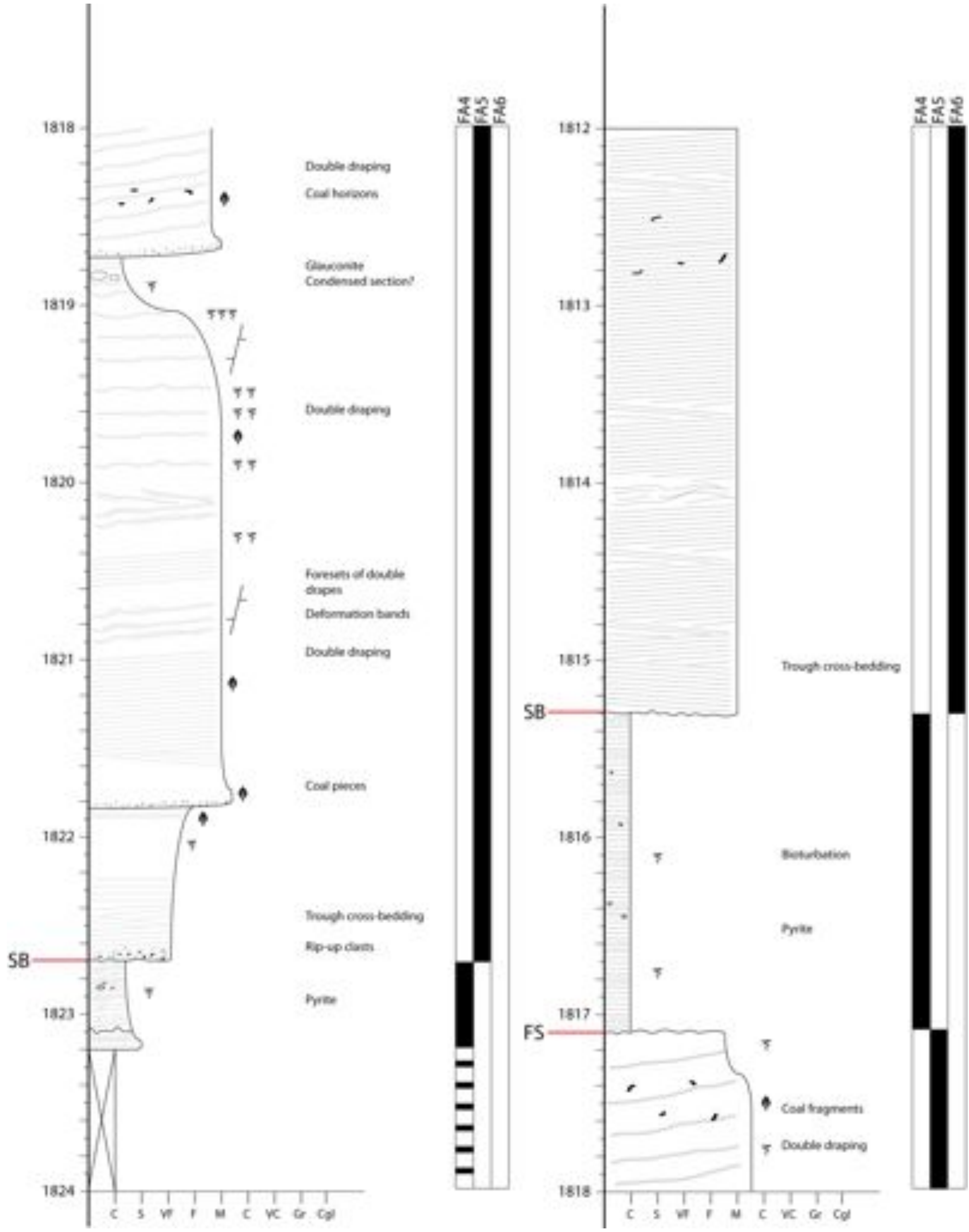

Figure 34 - Lithostratigraphic log with facies associations in well 7122/7-3, core 5. SB; sequence boundary, FS; Flooding surface. Legend found in appendix (Figure 68).

Facies association 5 (FA5) – Tidal-influenced fluvial channels

Observation

Facies association 5 comprises of one coarsening upwards and two fining upwards sequences of very fine to medium-grained sandstone (1823,3 – 1818,9m) (Figure 34). FA5 comprises of litofacies F5,F7,F9 (Table 1). Facies association 5 sharply erodes into the underlying association (FA4) by a disconformity (Figure 35). An 80cm thick, coarsening upwards section of rip-up clasts, coal pieces, trough cross-bedding and possible shell fragments initiates facies association 5 (Figure 35). The rip-up clasts comprise of claystone and are situated at the lower boundary together with possible shell fragments. The trough cross-bedding is partially distorted by bioturbation, but are visible when the foresets contain single mud drapes and organic matter.

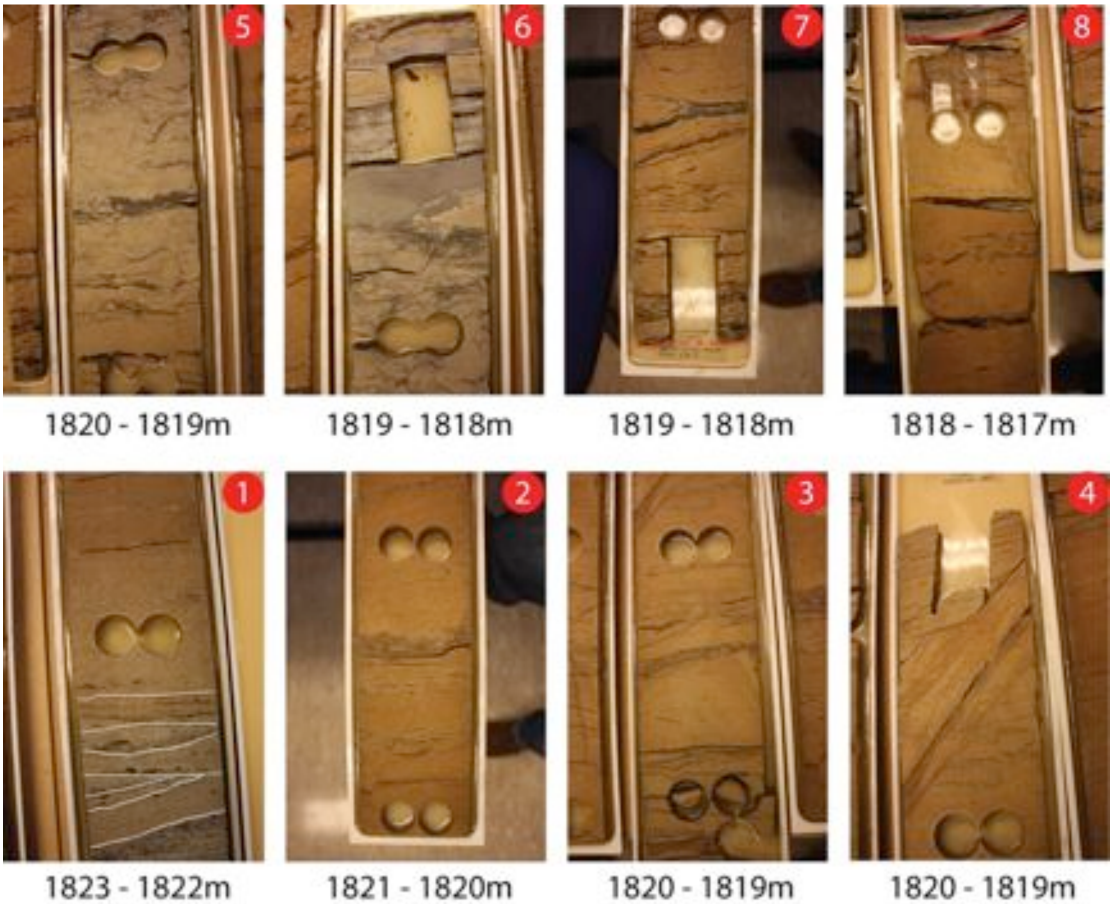

Figure 35 - (1) Rip-up clasts and trough cross-bedding. (2) Deformation band with bioturbation. (3) Foresets of single and double drapes. (4) Deformation band with bioturbation. (5) Intense bioturbation, foresets of single and double drapes and mud partings. (6) Condensed section with glauconite, claystone and sandstone. (7) Coal pieces,

mud parting, double and single drapes. (8) Intense bioturbation, coal pieces and a flooding surface to FA4 above

The medium-grained sandstone truncates the lower, upwards coarsening unit and comprises of coal horizons and trough cross-bedding with foresets of both single and double mud drapes. The intensity of the mud drapes, coal fragments and bioturbation are fluctuating.
Bioturbation is increasing towards the upper boundary of the first fining upwards channel complex. Horizontal grazing traces and vertical burrows are present (Figure 35). A possible condensed section is located at the upper boundary of the first fining upwards channel complex. The section begins with a laminated claystone together surrounded by large (up to 5 cm) glauconite nodules. Two divisions of rip-up clasts and organic matter overlay the claystone before being truncated by the second fining upwards channel complex.
The second fining upwards channel complex is similar to the underlying, comprising of trough cross-bedding, foresets of single and double drapes, increasing bioturbation intensity vertically and organic matter.
Deformation bands are restricted to porous granular media, where the individual deformation bands rarely host offsets greater than a few centimetres even when the bands themselves are hundreds of meters long (Figure 35) (Fossen et al., 2007). The types of deformation bands observed in facies association 5 are identified as phyllosilicate deformation bands (Pers. com. Alvar Braathen).

Interpretation

Facies association 5 comprises a coarsening upwards unit and two fining upward units. The association (FA5) is initiated by an erosional surface, which generates a sequence boundary above the underlying shales of facies association 4.
Trough cross-bedding, allochthonous coal fragments and foresets of single and double drapes may indicate an inner estuary environment influenced by tidal processes.
The first coarsening upward sequence grades vertically into a potential condensed section consisting of glauconite, laminated claystone, sandstone, rip-up clasts and is further truncated by the medium grained sandstone unit of the second coarsening upwards sequence.
A condensed section commonly represents a section of fine-grained sedimentary rocks

that accumulated slowly, thus covering a condsiderable time-span by a thin layer. Phosphate and glauconitic material is usually concentrated in these layers. The condensed sections are generally deposited during transgressions and in such cases are associated with maximum flooding surfaces (MFS).
The phyllosilicate deformation bands identified occur as individual bands and zones of bands (Figure 35). Deformation bands are found in several upper crustal tectonic and non-tectonic regimes, and it is important to distinguish deformation bands from ordinary fractures (Fossen et al., 2007). Firstly they are thicker and exhibit smaller offsets; secondly they tend to exhibit a reduction in porosity and permeability, whereas slip surfaces and tension fractures typically increase permeability (Fossen et al., 2007). Deformation bands occur as isolated structures, linked systems, complex zones of multiple, interconnected deformation bands, and in fault damage zones (Aydin and Johnson, 1983; Fossen et al., 2007). As a summary, the mixing and alignment of platy minerals mainly cause permeability reduction, and these factors, amongst others, typically vary along the deformation bands. The exact effect deformation bands have on fluid flow is therefore difficult to estimate (Fossen et al., 2007).
Bioturbation intensity is variable throughout the association, and increases upwards in both fining upwards sequences. All the deformation bands are located at intensely burrowed sections, though this is most likely a coincidence.

Based on these interpretations and the surrounding associations, facies association 5 is interpreted as an inner estuarine, tidal-influenced fluvial channel system, with a condensed section possibly representing a maximum flooding surface.

Facies association 6 (FA6) – Estuarine mouth bars

Observation

Facies association 6 comprises of well-sorted, medium-grained sandstones with trough-cross bedding as the dominant internal structure (1816,7 – 1812m) (Figure 34;Figure 36). FA6 comprises of lithofacies F9-F10 (Table 1). The association truncates onto the underlying shales of facies association 4, and a sequence boundary (SB) is generated (Figure 36). A few horizons of coal pieces and coal horizons are present, though generally absent throughout the association (Figure 36). Bioturbation is absent and the structural laminations are preserved in the entire association.

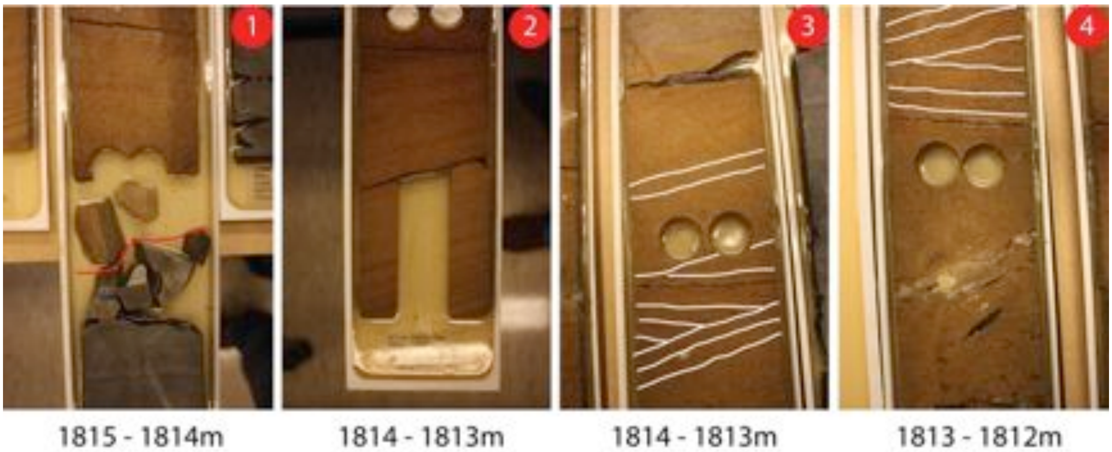

Figure 36 - (1) Erosional base generating a sequence boundary. (2-4) Trough cross-bedding and coal pieces

Interpretation

Facies association 6 is a thick, well-sorted sandstone unit of predominantly trough cross-bedding structures (Figure 36). The unit is difficult to interpret, as there are few internal structures that clearly define the nature of deposition. The fact that the underlying facies associations of core 5 and 6 are of estuarine nature, a proximal depositional environment within an estuarine setting is likely.
Bioturbation is completely absent, which may indicate a high-energy environment or low influx of saline water. Therefore, based on the underlying facies associations and the observations within FA6, an estuarine mouth bar depositional environment is proposed.

Summary of well 7122/7-3

According to (Dalrymple et al., 1992), estuaries are initially formed at the beginning of a transgression and migrate landward as transgression proceeds. Well 7122/7-3 is interpreted to exhibit estuary evolution in agreement with conceptual models and idealized lithofacies by e.g. (Dalrymple et al., 1992). Defining the evolutionary classification of estuaries is complex and difficult. A tripartite division of coastal environments is proposed by e.g. (Dalrymple et al., 1992) (Figure 37). Three end-members, river-, tide- and wave-dominated estuaries are organized to classify and predict the depositional environment of an estuarine system.

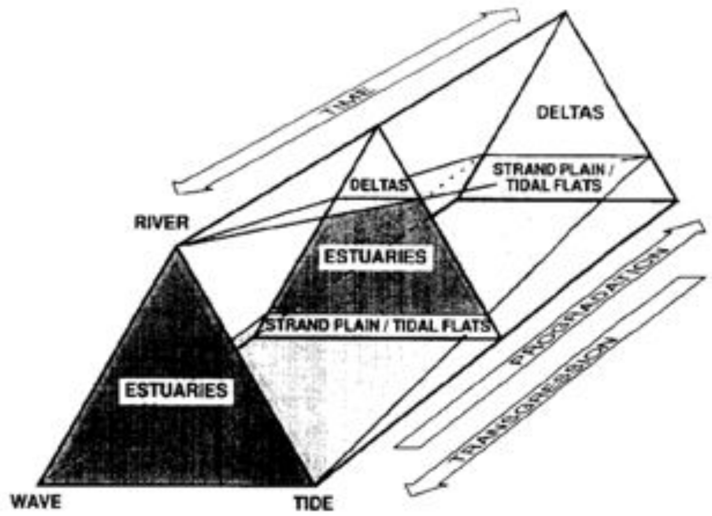

Figure 37 - Evolutionary classification of coastal environments. A tripartite division with relative time and references to changes in relative sea level and sediment supply (i.e. transgression and progradation) (Dalrymple et al., 1992)

Well 7122/7-3 is interpreted as six facies associations (Table 3;Figure 38). Core 6 initiates with an offshore environment (FA1) with dynamic bottom conditions. A sequence boundary is generated as the valley is transgressed and fluvial channels initiate the deposits of the valley-fill (FA2). A bay-head delta continues to prograde seaward and constitutes facies association 3 (FA3). Flooding of the bay-head delta generates a flooding surface and deposits the finer estuarine muds (FA4) onto the bay-head delta of the underlying association. Progradation of tidal-influenced channels occurs as the flooding wanes (FA5), and tidal processes supress the wave processes in the estuary. A second flooding event caps the underlying tidal channels and a proposed mouth bar sequence is deposited (FA6).

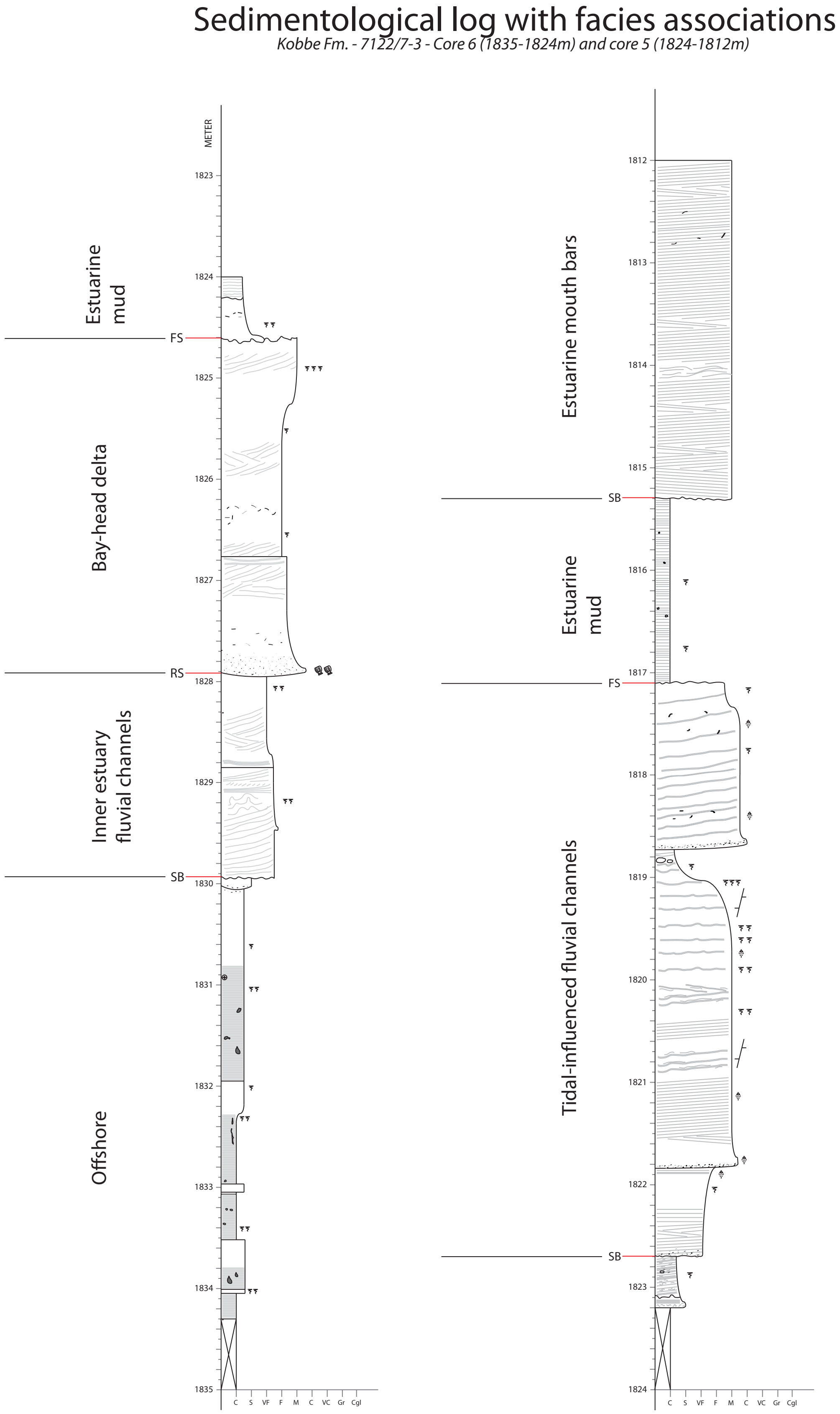

Figure 38 - Sedimentological log with facies associations from well 7122/7-3, Goliat Field. Legend found in appendix (Figure 68).

Well 7122/7-4S

General information

Information on well 7122/7-4S (core 3) is taken from the Norwegian Petroleum Directorates fact pages (factpages.npd.no). The total depth of the well is 2550 MD (mRKB) with a maximum inclination of 33°, and is considered an exploration well. The well is logged as it is observed, thus with and inclination. The depth in focus in this assignment is 1819MD – 1794MD, penetrating the Kobbe Formation in the Goliat Field. The core diameter is approximately 13cm.
A table of facies associations with suggested depositional environments is presented below in Table 4.

Table 4 - Five facies associations (FA1-FA5) with interpreted depositional environments

Facies associations:	Interpreted depositional environment:
FA1 (F3-F4)	Prodelta
FA2 (F1-F3)	Floodplain/crevasse splay
FA3 (F4, F5, F8, F9)	Proximal to distal tidal-fluvial channels
FA4 (F5, F9, F10)	Coarse-grained proximal tidal-fluvial channels
FA5 (F1-F3)	Channel abandonment

Well 7122/7-4S – Core 3

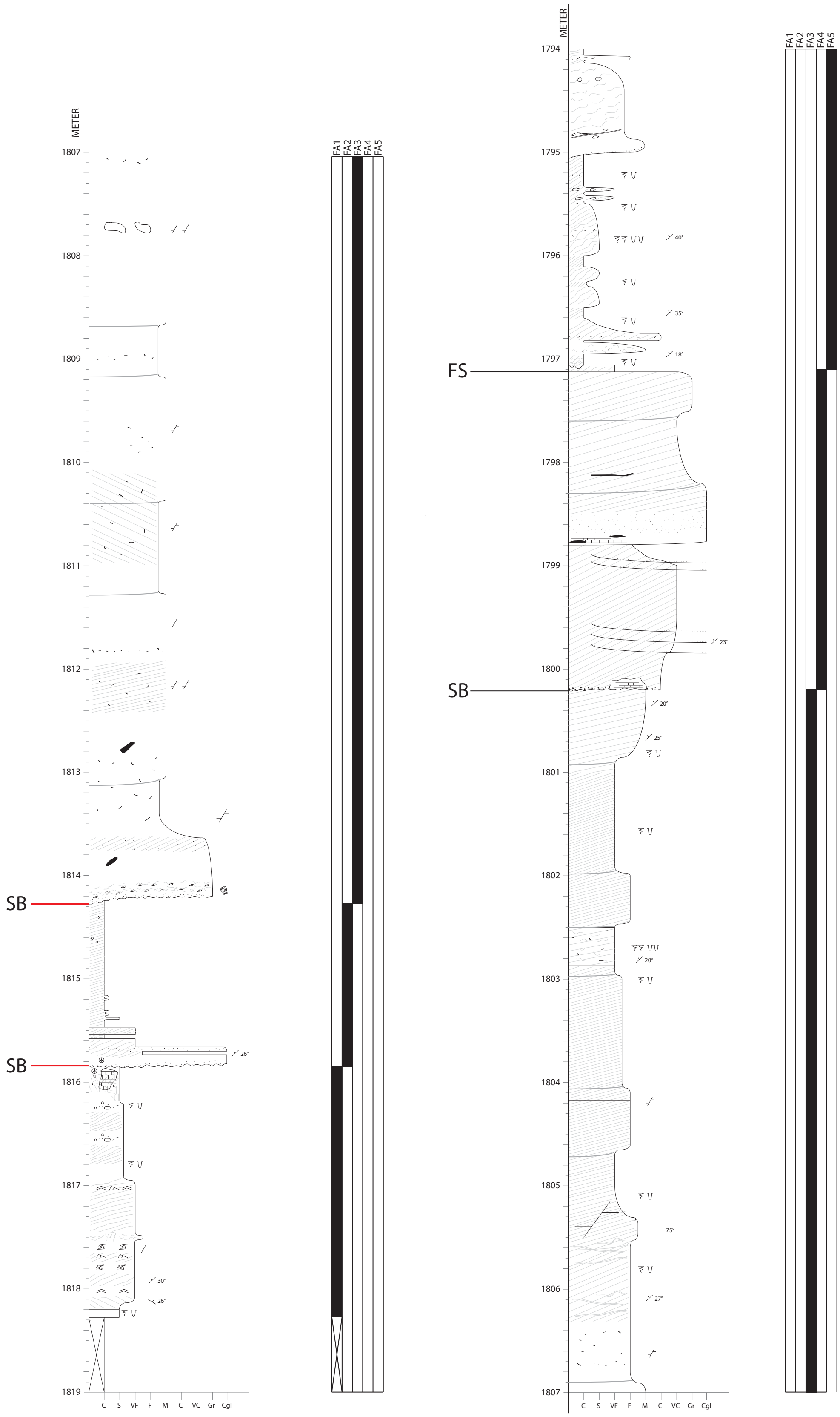

Figure 39 - Lithostratigraphic log with facies associations from well 7122/7-4S - core 3. SB; sequence boundary. FS; Flooding surface. Legend found in appendix (Figure 68).

Facies association 1 (FA1) - Prodelta

Observation

Facies association 1 comprises of a thick, light grey sequence of siltstone to fine sandstone in a fining upwards nature (Figure 39) (1818,1 – 1815,8 m). FA1 comprises of lithofacies F3-F4 (Table 1). The association overlies and truncates a black, bioturbated shale, though only a few centimetres are present in this core. Wave- and current induced ripples dominate the internal structures (Figure 40). Soft sediment deformation, pyrite and siderite nodules are present further upwards as the sequence fines (Figure 40). Limestone concretions are pronounced as the upper boundary of facies association 1 (Figure 40). Bioturbation intensity is variable and increases upwards in the association.

Figure 40 - (1) Erosional boundary generating a sequence boundary. (2) Bioturbation and limestone concretion. (3) Limestone concretion. (4) Erosional boundary between FA1 and FA2

Interpretation

Facies association 1 comprises a grey/dark grey, heterolithic alteration of siltstone and silty sandstone. The general nature of the association is fining upwards together with an increased degree of bioturbation upwards. The internal structure is dominated by wave- and current induced structures, which is a marine indicator, though the siltstone content suggests a certain proximity to the source. As the succession fines upwards, bioturbation also increases, which could be a result of more favourable conditions or a relatively lower sedimentation rate. Soft sediment deformation, e.g. slumping or water

escape, is observed at the lower boundary. The latter structures develop either at deposition or shortly after deposition during the initiation of consolidation. The structures result from displacement and movement of unconsolidated material.
Based on the observations and interpretations, a prodelta environment is proposed for facies association 1.

Facies association 2 (FA2) – Floodplain/Crevasse splay

Observation

Facies association 2 comprises of a fining-upward sequence of conglomerate and claystone grain sizes (1815,8 – 1814,3 m) (Figure 41). FA2 comprises of lithofacies F1-F3 (Table 1). The base of facies association 2 initiates with a conglomerate and truncates the underlying facies association 2 (Figure 41). The conglomerate comprises of angular, poorly sorted grain sizes containing organic material, rip-up clasts, limestone concretions, pyrite nodules and abundant bioturbation (Figure 41).
Above the conglomerate, laminated claystone comprising of lenticular bedding and pyrite nodules are observed. The lenticular bedding is scarce and of millimetre- to centimetre scale. Further upwards, black laminated claystone dominate the association together with pyrite nodules and organic material (Figure 41). Bioturbation appears absent in the claystone above the conglomeratic unit. The overlying facies association 3 initiates with rip-up clasts from association 2, which truncates the succession.

Figure 41 – (1) Sequence boundary. (2) Poorly sorted conglomerate with organic material. (3) Lenticular bedding. (4) Bioturbation (yellow circles)

Interpretation

Facies association 2 initiates with a mixed conglomerate of coarse-grained sediments, organic material and limestone concretions. The conglomerate resembles transgressive lag sediments as the association fines upwards and deposits suspended finer-grained sediments. The erosive surface onto the underlying facies association 1 generates a sequence boundary. The amount of coarse-grained material and organic material may suggest a certain proximity to the source, although the overlying fine-grained material may suggest a relatively distal deposition. Overbank areas are associated with channel facies of all types and are commonly divided into proximal and distal areas. Levees and crevasse splays are usually deposited close to active channels, whereas floodplains are deposited in distal areas with some distance from the active channel (Reading 1996). The suggested depositional environment for facies association 2 is therefore either floodplain fines or crevasse splay. As floodplains commonly dry out and exhibit subaerial- or wet swamp features (Reading 1996). However, isolated crevasse splays may be interbedded with floodplain fines a certain distance away from the channel (Reading 1996).

Based on the observations and the overlying facies association, a floodplain/crevasse splay environment is proposed for facies association 2.

Facies association 3 (FA3) – Tidal-fluvial channels

Observation

Facies association 3 (Figure 42, 1814,3 – 1798,8 m) comprises thick, sandstone units of very fine to conglomerate grain size, in a general fining upward trend. FA3 comprises of lithofacies F4, F5, F8, F9 (Table 1). The sandstone units are in the range of 40cm to 1,2m thick. The association initiates with a conglomeratic base, which truncates the underlying association. The lower conglomeratic unit consists of foresets of coarser-grained sediment, organic material, rip-up clasts, shell fragments and sporadic bioturbation (Figure 42). Facies association 3 grades vertically into thick, well sorted, structureless sandstone units that comprise of shale clasts, organic material and deformation bands (Figure 42) (1813,6 -1806,4m). Units of faint cross-bedding are insinuated due to the preferred alignment of the coal horizons and coal pieces (Figure 42).

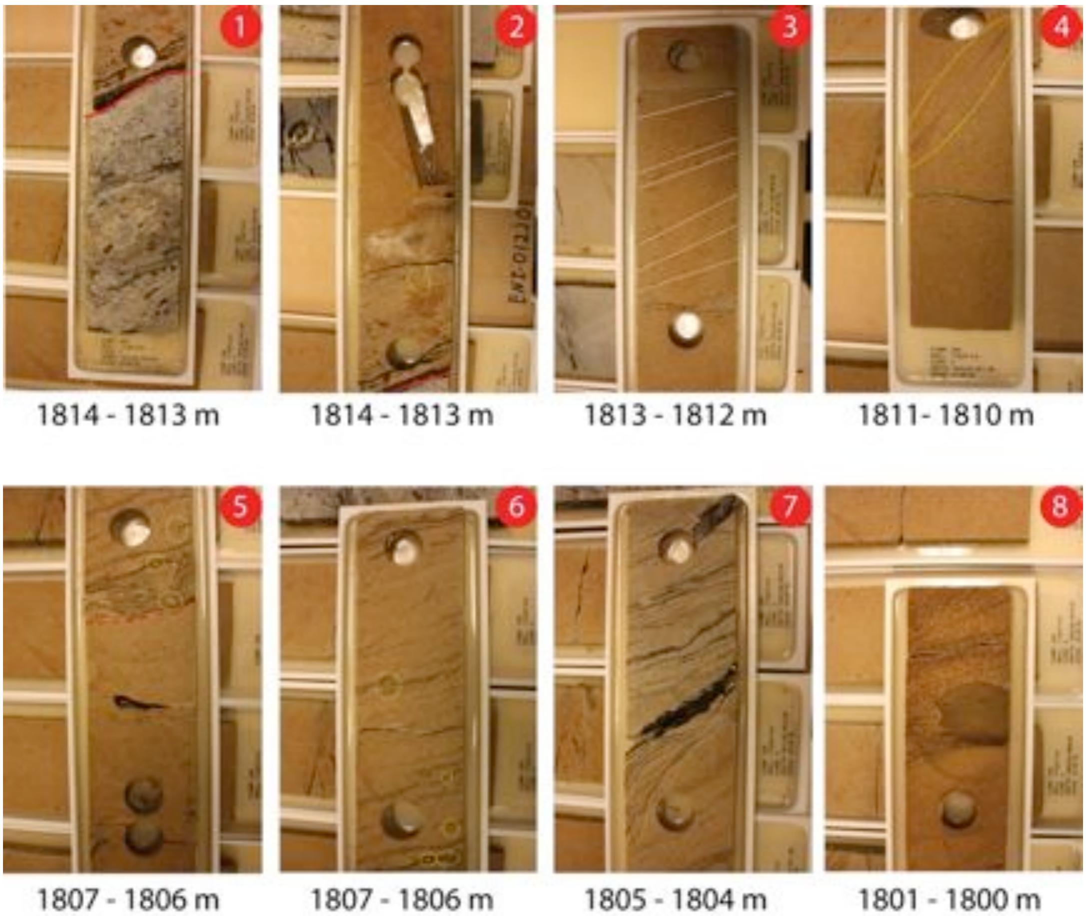

Figure 42 – Compilation of facies association 3. (1) Rip-up clasts, organic material, shell fragments. (2) Bioturbation and organic material. (3) Faint cross-bedding due to preferred

alignment of coal fragments. (4) Deformation band. (5) Shift in grain size and bioturbation. (6) Bioturbation and mud parting. (7) Finer grain size and more organic material. (8) Coarse-grained upper boundary.

Above the structureless units the internal structures gradually change, where the units shift from fine to very fine grain size. However, there is no apparent erosion, truncation or break in sedimentation onto the underlying structuresless units (Figure 42). Internal structures as trough cross-bedding with foresets of single and double drapes dominant from 1806,4 – 1798,8m. Increased organic material and mud partings appear on foresets as millimetre- to centimetre thick continuous bands (Figure 42).

Bioturbation is hard to identify in the structureless unit and thus appears absent. However as the trough cross-bedding and the double drapes emerge, either the degree of bioturbarion increases or the internal structures make the burrows more visible (Figure 42). Nevertheless, bioturbation is intense where the single- and double drapes first appear (1806,4m), though gradually decreases upwards. The degree of bioturbation increases in areas where the clay content is higher as the association fines.

Interpretation

Facies association 3 is initiated by a transgressive lag that truncates the underlying facies association 2 and generates a sequence boundary (SB) (Figure 42). The transgressive lag sediments comprise of shell fragments, organic material and rip-up clasts, which are interpreted as allocthonous and in a high-energy environment (Figure 42).

The structureless sandstone units show faint trough cross-bedding indicated by the preferred alignment of coal pieces and the overlying internal structures (Figure 42). The structureless sandstone units appear absent of bioturbation. This could be due to the high-energy environment and/or lack of salinity.

At approximately 1806m, the structureless sandstone units are dominated by trough cross-bedding and tidal-processes such as single- and double drapes of mudstone and organic material (Figure 42). Trough cross-bedding and low-angle lamination with single- and double drapes of mudstone and organic material indicate influence from tidal processes e.g. (Dalrymple et al., 1992; Pattison and Walker, 1994). Bioturbation is increased in these units and may be an effect of increased salinity due to tidal influence.

Note that as there is no apparent break in sedimentation between the two latter sandstone units, therefore both units are interpreted within the same facies association 3. Based on the observations of this association and over- and underlying associations, a tidal-fluvial estuarine channel complex is proposed. The interpreted depositional environment shifts from relatively proximal to distal as the channel complex changes from fluvially dominated to tidally influenced deposition.

Facies association 4 (FA4) – Proximal tidal-fluvial channels

Observation

Facies association 4 consists of several thick, fining upwards sandstone units of poorly sorted, fine to conglomerate grain sizes (Figure 43, 1800,2 – 1797,1m). FA4 comprises of lithofacies F5, F9, F10 (Table 1). Facies association 4 truncates and erodes into the underlying association 3 (Figure 43). The conglomeratic base that initiates the sequence comprises of varying sizes of clastic foresets and organic material (Figure 43). The second conglomerate based sandstone unit erodes and truncates into the latter sandstone units (Figure 43). This conglomeratic unit comprises of foresets of varying grain sizes, organic material and limestone concretions. Both successions embrace varying degrees of bioturbation, from moderate to intense.

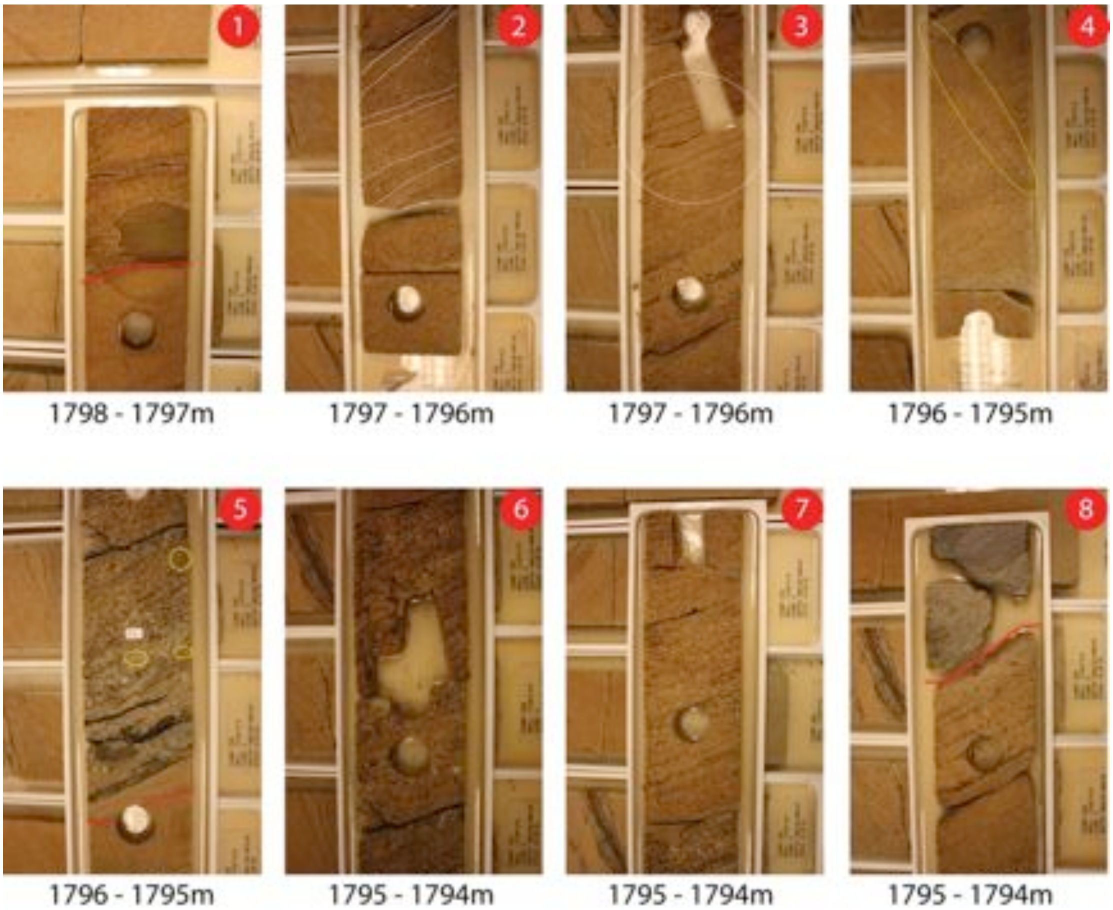

Figure 43 – Compilation of facies association 4. (1) Conglomeratic base. (2) Foresets of cross-bedding. (3) Single and double drapes. (4) Deformation band. (5) Conglomerate and bioturbation. (6-7) Coarse-grained sequence with organic material. (8) Upper boundary of FA4.

Regarding the internal structure, trough cross-bedding with foresets of coarse, poorly sorted grain sizes dominates this association. The foresets comprise of both single and double drapes of organic material and mudstone. Coal horizons and deformation bands (Figure 43) are additionally distributed throughout the succession. This facies association is structurally similar to the underlying association (FA3), apart from the coarser grained nature of this association.

Interpretation

Facies association 4 is inititated by a conglomerate that truncates the finer sediments of the underlying association (FA3). The truncation generates a sequence boundary/ravinement surface and the accommodation space fills with transgressive lag deposits. As the nature of the lag deposits and the overlying sandstone units are coarser grained than the association below, deposition in a higher energy environment is likely. The coarse grained nature of these deposits suggest a certain proximity to the source, though also a certain distal position, as the tidal processes dominate the internal structure. In the more proximal reaches of the fluvial-tidal transition, coarser fluvial deposits are observed (Davis, 2011). However, as the conceptual models of (Dalrymple et al., 1992) demonstrate, tidal processes in an estuary can reach relatively far upstream of the fluvial-tidal channel complex (Figure 32).

Thin muddy or organic drapes are common in most tidal cross-stratal foresets, because of the frequency of slack-water periods in tidal settings (Davis, 2011). The tidal cross-stratal foresets show no cyclical evidence.

Varying degree of bioturbation from moderate to intense propose a certain salinity and a mixing between marine and river water allowing tidal energy to penetrate into the inner estuary (Dalrymple et al., 1992).

Based on these interpretations and the latter facies association, a proximal, coarse-grained tidal-fluvial channel complex is proposed for facies association 4.

Facies association 5 (FA5) – Channel abandonment

Observation

Facies association 5 comprises of several fining upward sequences of coarse-grained sandstone to claystone (Figure 44, 1797,1 – 1795,1m). FA5 comprises of lithofacies F1-F3 (Table 1). Lenticular bedding, organic material, pyrite nodules and varying degrees of bioturbation are the most prominent features of this association (Figure 44). The pyrite nodules are observed in areas where the clay content is the highest, and commonly in the upper boundary of the fining upwards sequences.
An erosional surface overlays the upper claystone and infills with medium-grained sandstones containing abundant organic material and pyrite nodules. The intensity of organic material increases vertically and has no preferred alignment. At the upper boundary, the succession fines and claystone caps the facies association (Figure 44). Bioturbation varies from moderate to intense in this section where the most intense bioturbation is located in the turbulent and organic rich area (Figure 44) (1795 - 1794m).

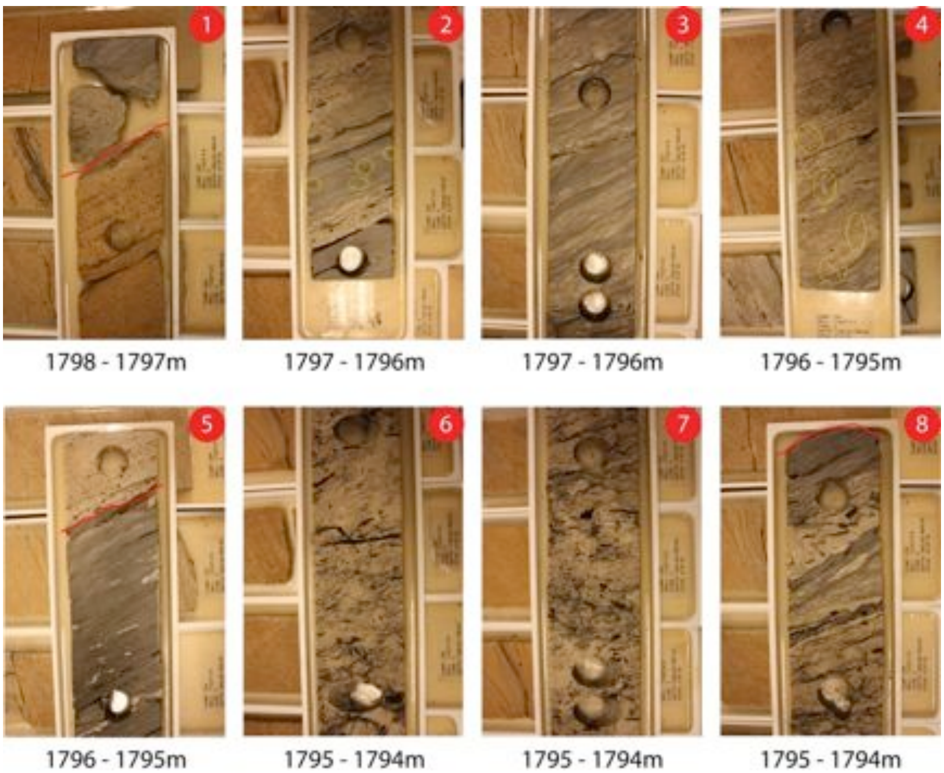

Figure 44 – Compilation of facies association 5. Lenticular bedding, organic material, pyrite nodules and varying degrees of bioturbation are present.

Interpretation

Facies association 5 truncates the underlying tidal-fluvial channel complex and in fills the accommodation space with sediments ranging from coarse-grained sandstone to claystone. The surface between the two facies associations (FA4-FA5) is interpreted as a flooding surface. Fine-grained suspended sediment is deposited together with irregular influx of silt- and sandstone, generating lenticular bedding structures (Figure 44). Deposition of fine-grained sediments and abundant organic material suggests a lower energy regime.

The upper unit of coarser-grained sandstone and claystone truncates the underlying claystone and contains abundant organic material and pyrite nodules. An interpretation is that the sediments are being deposited under turbulent conditions, insinuated by the non-preferred alignment of organic material and lack of preserved structures (Figure 44). Minor crevasse splays occur as discrete coarse beds in the bay muds and silts, and may also occur in levee sequences (Elliot 1974). Based on the observation and interpretation, a channel abandonment sequence with a levee/crevasse splay sequence is proposed for facies association 5.

Summary of well 7122/7-4S

Well 7122/7-4S is divided into five associations (Table 4, Figure 45) comprising different depositional environments. Core 3 initiates with a fining upward, prodelta environment (FA1) and is truncated by an overlying floodplain/crevasse splay environment (FA2), generating a sequence boundary between the two associations. Tidal-fluvial channels overlie and truncate the underlying association, generating another sequence boundary. The channels are amalgamated and of varying thickness and preserved internal structures. As the channel complex fines upwards there is a shift into a coarse-grained, proximal tidal-channel complex (FA4), which erode into the underlying association (FA3). The last facies association in core 3 is interpreted as a channel abandonment succession that generates a flooding surface.

A general coarsening upward trend is present in the core 3, with the exception of the channel abandonment sequence interpreted in facies association 4. A progradation of the entire system is proposed for core 3 as the sediments deposited gradually coarsen and the internal structures exhibit certain proximity. Well 7122/7-4S is suggested to be relatively more proximal than well 7122/7-3 and 7122/7-5.

Figure 45 - Sedimentological log with facies associations from well 7122/7-4S, Goliat Field. SB; Sequence boundary. FS; Flooding surface. Legend found in appendix (Figure 68).

Well 7122/7-5

General information

Information on well 7122/7-5 (core 1) is taken from the Norwegian Petroleum Directorates fact pages (factpages.npd.no). The total depth of the well is 2228 MD (mRKB) with a maximum inclination of 2,4°, and is considered an exploration well. The depth in focus in this assignment is 1911MD – 1900MD, penetrating the Kobbe Formation in the Goliat Field. The core diameter is approximately 13cm.
A table of facies associations with interpreted depositional environments is presented below in Table 5.

Table 5 – Facies associations with interpreted depositional environments

Facies associations:	Interpreted depositional environments:
FA1 (F1-F2)	Offshore/Prodelta
FA2 (F4,F5,F7,F9,F10)	Distributary channels/mouth bars (lower delta plain - delta front)
FA3 (F4,F6)	Shallow marine shelf sediments
FA4 (F2-F4)	Proximal shoreface

Well 7122/7-5 - Core 1

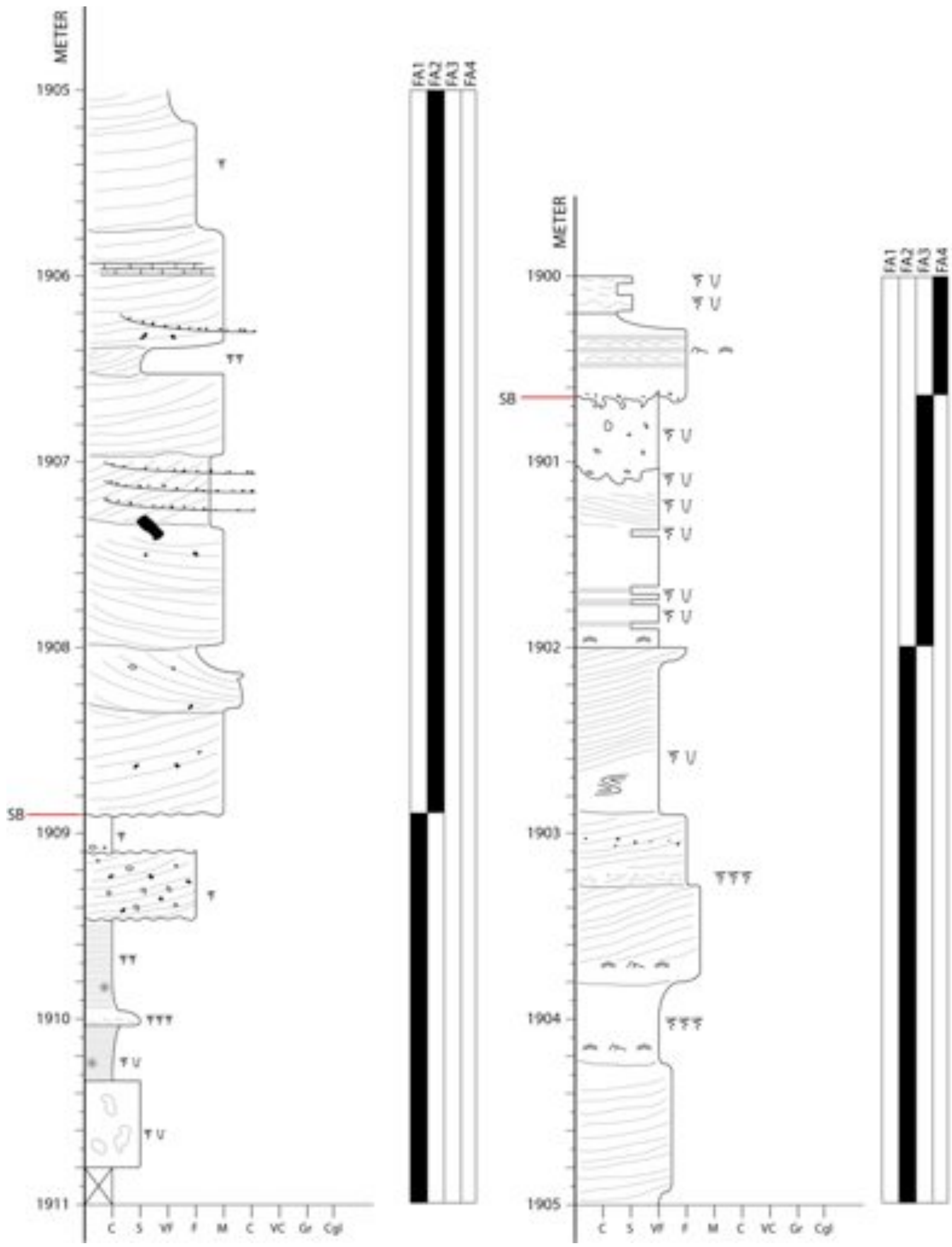

Figure 46 - Lithostratigraphic log with facies associations from well 7122/7-5 - core 1. SB; sequence boundary. Legend found in appendix (Figure 68).

Facies association 1 (FA1) – Offshore/Prodelta

Observation

Facies association 1 (FA1) consists mainly of light grey/green and purple siltstones and claystones (Figure 46, 1911 – 1908,9m). FA1 comprises of lithofacies F1, F2 (Table 1). The internal structures are discontinuous seams and lenses of siltstone together with the laminated claystone (Figure 47), though the silt content decreases relatively upwards in the association. Well-rounded phosphate nodules as well as limestone concretions are seen towards the upper boundary (Figure 47). There is a varying degree of bioturbation from scarce to intense and both vertical and horizontal burrows are observed (Figure 47). The overlying sandstones of facies association 2 truncate facies association 1 (Figure 47).

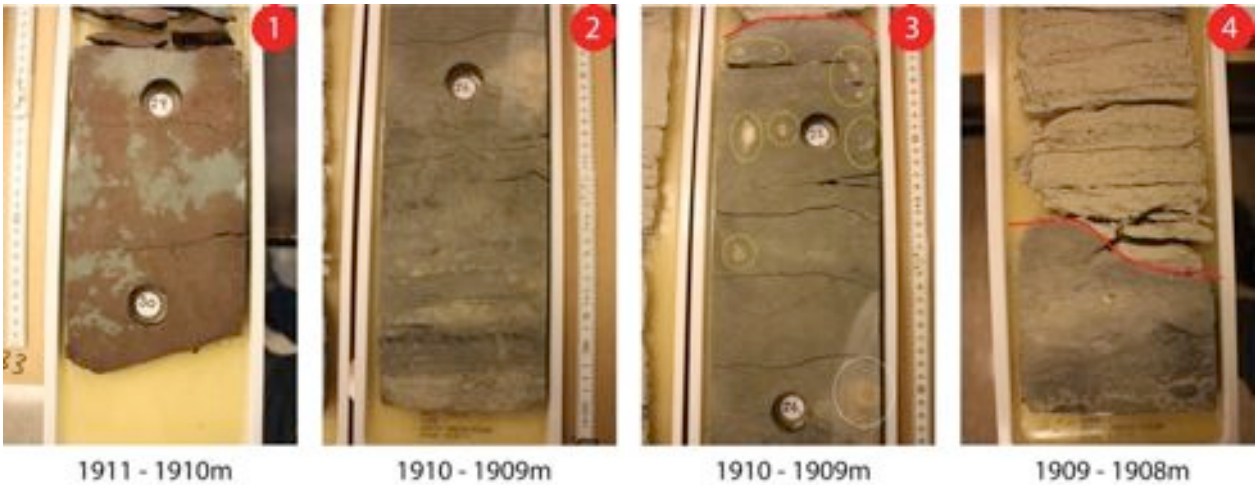

Figure 47 – Compilation of facies association 1. (1) Light grey/purple siltstone and claystone. (2) Intense bioturbation. (3) Limestone concretions. (4) Bioturbated upper boundary.

Interpretation

Facies association 1 lacks depositional structures that indicate wave- and current induced flow, which can be expected in an environment subjected to storm processes. The fine-grained nature of these sediments together with the latter observation proposes an environment below storm weather wave base. The presences of siltstone as beds and within the claystones indicate a relatively shallower water depth.

Moderate to intense bioturbation suggests favourable bottom conditions and a relatively stable depositional environment.
Based on the observations and interpretations made, facies association 1 is interpreted as an offshore environment below storm weather wave base.

Facies association 2 (FA2) – Distributary channels/Mouth bars

Observation

Facies association 2 (FA2) comprises of thick, sandstone units varying from very fine to medium grain sizes, with the exception of a few foresets of coarse-grained sediments (Figure 46, 1908,9 – 1902,0 m). FA2 comprises of lithofacies F4, F5, F7, F9, F10 (Table 1). Facies association 2 truncates the underlying association (FA1) and the first 40cm comprise of trough cross-bedding with foresets of organic material and mudstone, pyrite nodules and some bioturbation (Figure 48).
The sandstone units embrace a large-scale fining upward trend from medium-grained sandstone units at the lower boundaries to very fine-grained sandstone units at the upper boundary (Figure 48). The sandstone units are moderately sorted within their respective trough cross-bedded packages.
The dominant internal structure consists of trough cross-bedding with foresets of organic material, mudstone and a few coarser-grained foresets (Figure 48). Wave- and current induced ripples are also present towards the upper boundary (Figure 48). Phosphate nodules, organic material, a limestone horizon and bioturbation are observed (Figure 48).

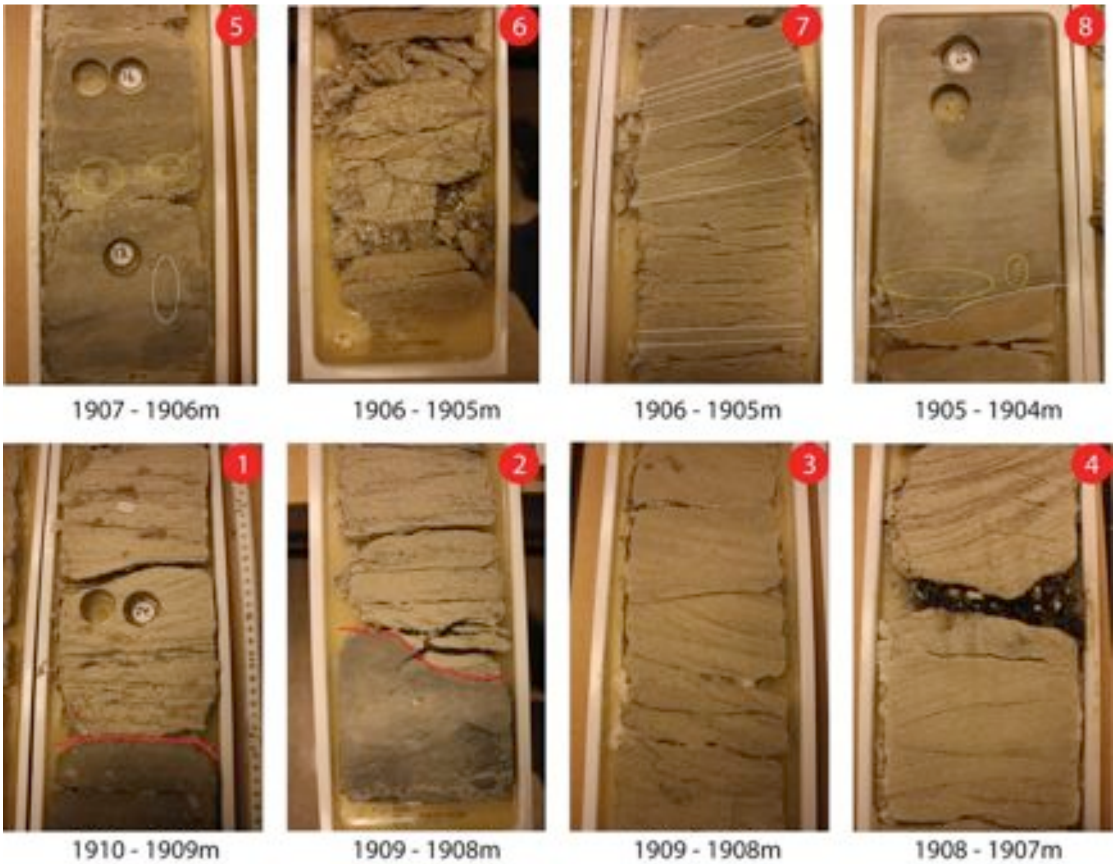

Figure 48 – Compilation of facies association 2 (1-8). Bioturbation, trough cross-bedding with foresets of organic material and mudstone, pyrite nodules and wave- and current induced ripples are many of the characteristic structures.

Interpretation

Facies association 2 is characterized by the presence of amalgamated distributary channels, which is a clear indicator of a marine environment. Some deltas have only one channel, but commonly more than one, and often diverge >60° from the overall basinward direction (Reading 1996). The dominant internal structures are trough cross-bedding with foresets of organic material and mudstone and wave- and current induced structures (Figure 48). The individual channel units vary between fining upwards and coarsening upwards. However there is a general fining upward trend and the proposed interpretation is a transition from distributary channels to mouth bars. Distributary channels have many characteristics of fluvial channels, though hard to differ in cores as the lateral overview is absent.

The coarse-grained nature of these channel facies and the presence of organic material suggests a certain proximity to the shoreline. As the association fines upwards, wave-

and current induced structures prevail together with trough cross-bedding. A slightly more distal environment, or distributary channel shift, with deposition as mouth bars is interpreted. An increase in degree of bioturbation and finer-grained nature in the interpreted mouth bars propose a slight decrease in depositional energy.
Based on these observations and interpretations, a lower delta plain environment comprising of amalgamated distributary channels as well as a shift into a delta front environment with deposition of mouth bars is proposed for facies association 4.

Facies association 3 (FA3) – Shallow marine shelf sediments

Observation

Facies association 3 comprises of decimetre thick units of very fine sandstone to siltstone character (Figure 46, 1902,0 – 1900,6 m). FA3 comprises of lithofacies F4, F6 (Table 1) The units are dark grey at the lower boundaries and gradually greens upwards. The dominant internal structure is plane parallel lamination and trough cross-bedding (Figure 49). Three zones of plane parallel lamination of centimetre thicknesses are observed at the lower boundary of the association. The base of one of these laminations is initiated by very fine sandstone, however all are laminated by mudstone and organic material (Figure 49). Organic material as fragments and phosphate nodules are a prominent feature of the association (Figure 49).
Bioturbation varies from moderate to intense and some of the burrows are quite protruding (Figure 49). White-circled horizontal burrows and thick vertical burrows are frequently observed (Figure 49). Towards the top of the association, a green tint is observed in the very-fine sandstone together with pyrite/siderite nodules (Figure 49).

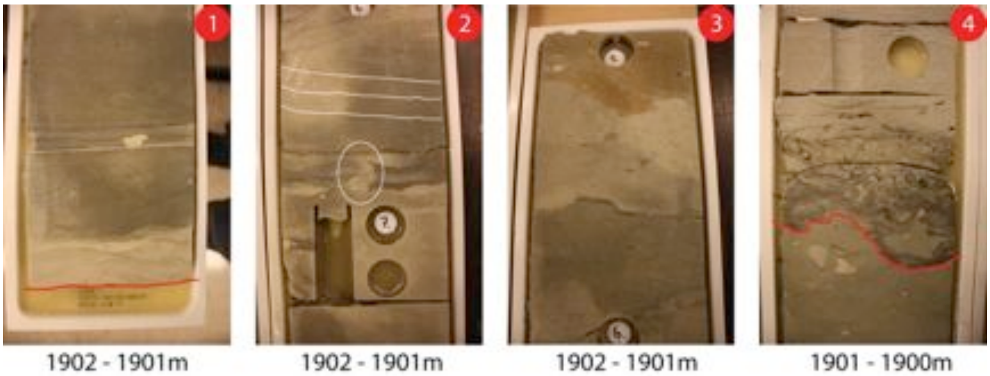

Figure 49 – Compilation of facies association 3. (1) Base of the association with PPL and bioturbated. (2) Vertical burrow and cross-bedding. (3) Bioturbated siltstone. (4) Upper boundary with conglomeratic base of FA4.

Interpretation

Facies association 3 is characterized by a quite uniform, very-fine grain size although a few fluctuations into siltstone are present. The facies association has a sharp base to the underlying mouth bars sands, though does not appear to be erosive (Figure 49). Wave ripples initiate the sequence along with plane parallel lamination and intense bioturbation, which distorts the internal structures (Figure 49). The combined flow diagram by Dumaas et al. (2004) (Figure 18) suggests a dynamic depositional environment due to the different internal structures observed in this association. A thin bed of trough cross-bedding is observed towards the upper boundary and appears undistorted by bioturbation (Figure 49). The fine-grained nature of the sediments together with intense bioturbation suggests periods of relatively low energy and sedimentation rate. Possible glauconitization of the sandstone is observed towards the top of the succession.

As seen from the previous well (7122/7-3), glauconite can form in marine-shelf environments, as e.g. in the Ormen Lange gas field (e.g. Gjelberg et al., 2005).

Based on the observations and interpretations, a shallow marine shelf environment is proposed for facies association 3.

Facies association 4 (FA4) – Proximal shoreface

Observation

Facies association 4 (Figure 46, 1900,6 – 1900 m) comprises of fine sandstone to alternating layers of mud- and siltstone. FA4 comprises of lithofacies F2-F4 (Table 1). Facies association 4 truncates the underlying facies association 3 (Figure 50). The sediments deposited at the base of FA4 are a mixture of mud- and sandstones together with pyrite nodules and organic material as well as bioturbation (Figure 50). The internal structures within the sandstones above are dominated by alternating plane parallel lamination (PPL) and current induced ripples (Figure 50). The thicknesses of the structures are on centimetre scale and there is no apparent difference in grain size between the two latter. In general the association fines upwards and above the PPL and ripple structures, alternating layers of mud- and siltstone generate lenticular shapes. Bioturbation is absent in the section dominated by PPL and ripples, whereas the section above is moderately bioturbated of horizontal and vertical burrows (Figure 50).

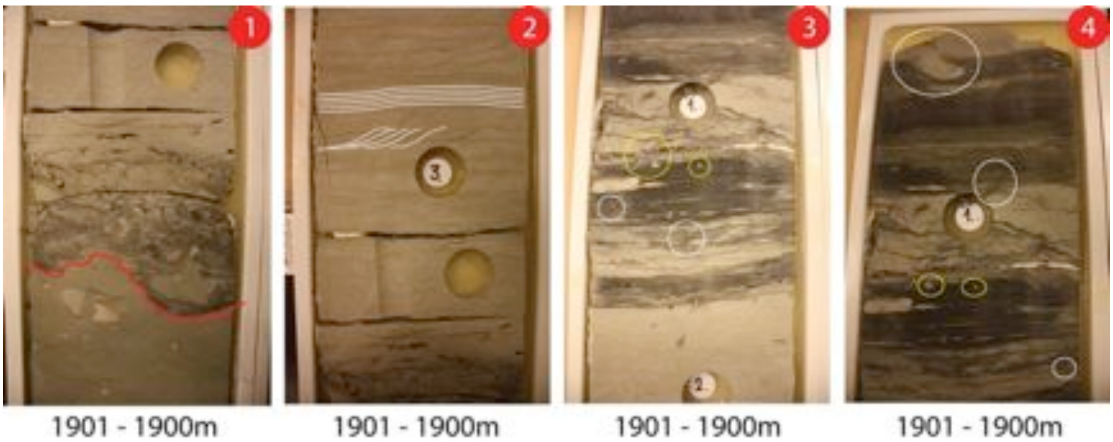

Figure 50 – (1) Conglomeratic base with pyrite nodules and organic material. (2) PPL and asymmetric ripples. (3) Bioturbation and pyrite nodules in mixed grain sizes. (4) Vertical burrows and pyrite nodules in more claystone dominated sequence.

Interpretation

Facies association 4 truncates the underlying sandstones of facies association 3 depositing lag sediments and rip-up clasts (Figure 50). Above the lag sediments, plane parallel lamination and current induced structures alternate in the fine-grained sandstone unit. Plane parallel lamination and small-scale ripples are deposited in different energy environments. The absence of intermediate structures such as hummocky cross-stratification and large-scale ripples suggest a rapid shift in depositional energy (Dumas et al. 2005). The lack of preserved large-scale ripples in between the small-scale ripples and PPL has been observed in many shoreface environments (Hill et al. 2003). Unidirectional and oscillatory current velocities are controlling factors along with wave period and grain size in a shoreface environment (Dumas et al. 2005). A proximal shoreface environment is suggested due to a longer waning period in distal environments, giving time for preservation of larger-scaled structures. Based on the observations and interpretations, a proximal shoreface environment is suggested for facies association 4.

Summary of well 7122/7-5

Well 7122/7-5 is divided into four facies associations (Figure 51) (FA1-FA4) and initiates with an offshore/prodelta environment of bioturbated clay- and siltstone (FA1). Facies association 1 is truncated by amalgamated distributary channels, which are situated in a lower delta plain environment (FA2), and generates a sequence boundary. As the association fines upward, a transition into mouth bar sediments is suggested. A continued upward fining of bioturbated very-fine siltstone comprises the proposed shallow marine shelf environment of facies association 3 (FA3). The suggested proximal shorface environment of facies association 4 (FA4) truncates the underlying and generates a sequence boundary.
In general, a progradational sequence of prodelta environment to distributary channel complex followed by a regressive sequence of mouth bars and shoreface environment is proposed.

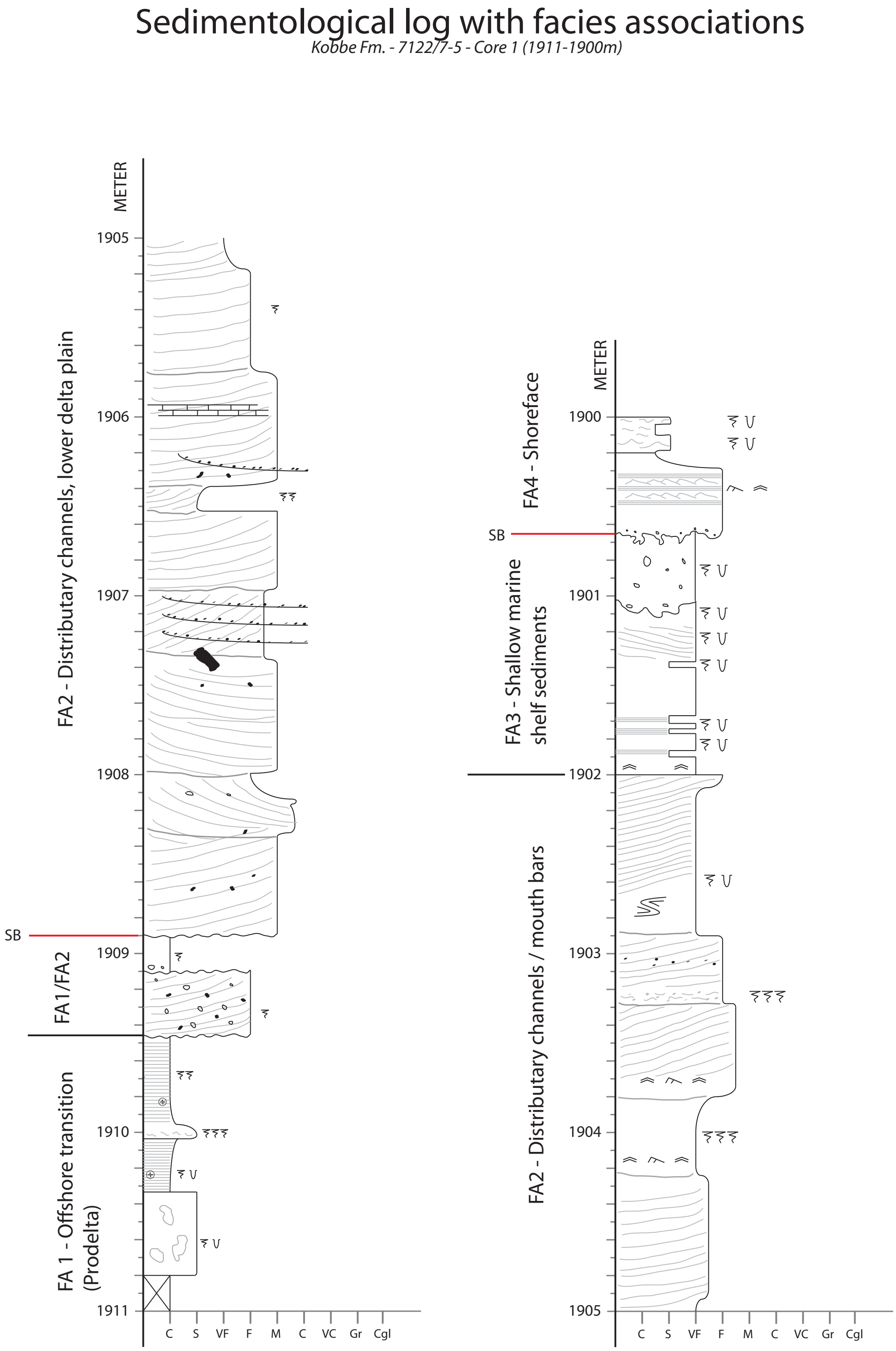

Figure 51 - Sedimentological log with facies associations from well 7122/7-5, Goliat Field. SB; Sequence boundary. Legend found in appendix (Figure 68).

5. Well correlation

Well log measurements and transects

This chapter is based on Bjørlykke (2010) brief introduction to well logs, giving the reader a short overview of the main concepts of well log measurements.
Well logging is used to record the physical properties of rocks penetrated by a well (Bjørlykke 2010). The measurements of importance in this chapter are the gamma, neutron porosity and density logs. Gamma and neutron porosity logs are united under radioactivity logs where the gamma logs measure the natural emission of gamma rays from the rocks, while the neutron log sends radiation into the rock. The absorption of neutrons, mostly by hydrogen atoms, commonly occurs in water and hydrocarbons (Bjørlykke 2010). The density log measures the density and pore fluid of the rock.
Well log measurements can be used directly for interpreting depositional environments in addition to provide information on porosity and permeability (Bjørlykke 2010). Well logs are also used as a visual tool to identify the main rock types and as a basis for sedimentological and stratigraphic interpretation (Bjørlykke 2010). A simplified log response to different lithologies is presented in Figure 52 below.

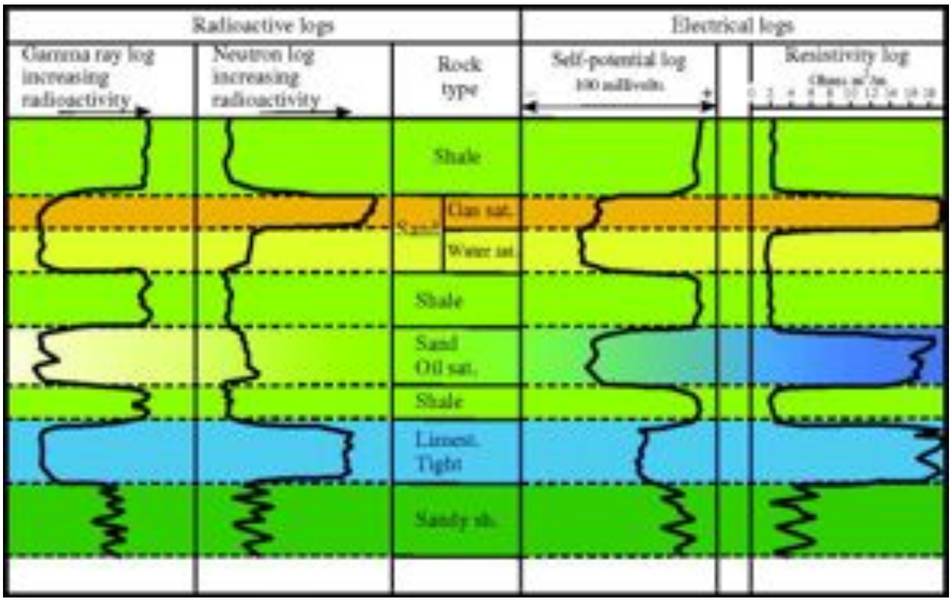

Figure 52 - Simplified log response to different lithologies. Note the sensitivity to oil saturation (Hobson and Tiratsoo 1981, Bjørlykke 2010)

The gamma radiation (GR) is typically measured between 0 and 150 API units, the neutron porosity (NPHI) range is between 0,45 and -0,15, and the density (RHOZ) range is between 1,95 and 2,95. As a side note, the hydrogen index of sandstones can be converted into neutron porosity units (NPHI) and used as a tool for determining the porosity of reservoir rocks (Bjørlykke 2010). The latter units are used instead of pure neutron measurements in these interpretations.

A correlation panel between wells 7122/7-4S, 7122/7-3 and 7122/7-5 in the Goliat Field and corresponding Kobbe Formation is presented in the section below. Two transects between the wells are created in PETREL with data from wireline logs, which are provided by Eni Norge A/S. The well data comprises of gamma ray (GR), neutron porosity (NPHI), and density (RHOZ) measurements from well strings. Sequence stratigraphic concepts are essential for a complete and detailed interpretation and correlation of each well. Therefore, a classification into facies associations with interpretations of key surfaces, such as sequence boundaries, flooding surfaces and ravinement surfaces are important elements in order to create 3D conceptual models.

One transect is created between wells 7122/7-4S and 7122/7-3 (4S-3), and the other between 7122/7-3 and 7122/7-5 (3-5). The term transect is used as a straight line along which observations are made or measurements are taken. All wells are measured in measured depth (MD).
The two transects are therefore generated on the basis of core interpretation, wireline measurements, key surfaces and extrapolation on the basis of well log measurements. The chosen transect order is based on the facies interpretation and proximity to the source. Results from the wireline logs are listed as highs and lows within the individual facies associations in the respective tables below to get a general overview of the different lithologies.

7122/7-4S - 7122/7-3 transect

Transect 4S-3 is generated from one core in well 4S (core 3) and two cores in well 3 (core 5-6), together with corresponding well data. Well 4S is deviated downward and situated approximately 1,8km east (from the seabed) of well 3. Well 3 is vertically drilled with a maximum inclination of 4,7°. Measurements of the highest and lowest values from wireline readings in wells 3 and 4S are listed in Table 6 below.

Table 6 - Results from wireline logs. Gamma ray, neutron porosity, density are listed with respect to the highest and lowest readings of individual facies associations and lithologies

Well 7122/7-4S						
	Gamma ray		Porosity		Density	
Facies association	High	Low	High	Low	High	Low
Offshore/prodelta	128	60	0,16	0	2,68	2,35
Channel complex	59	35	0,31	0,21	2,4	1,96
Channel abandonment	95	46	0,2	0,05	2,52	2,19

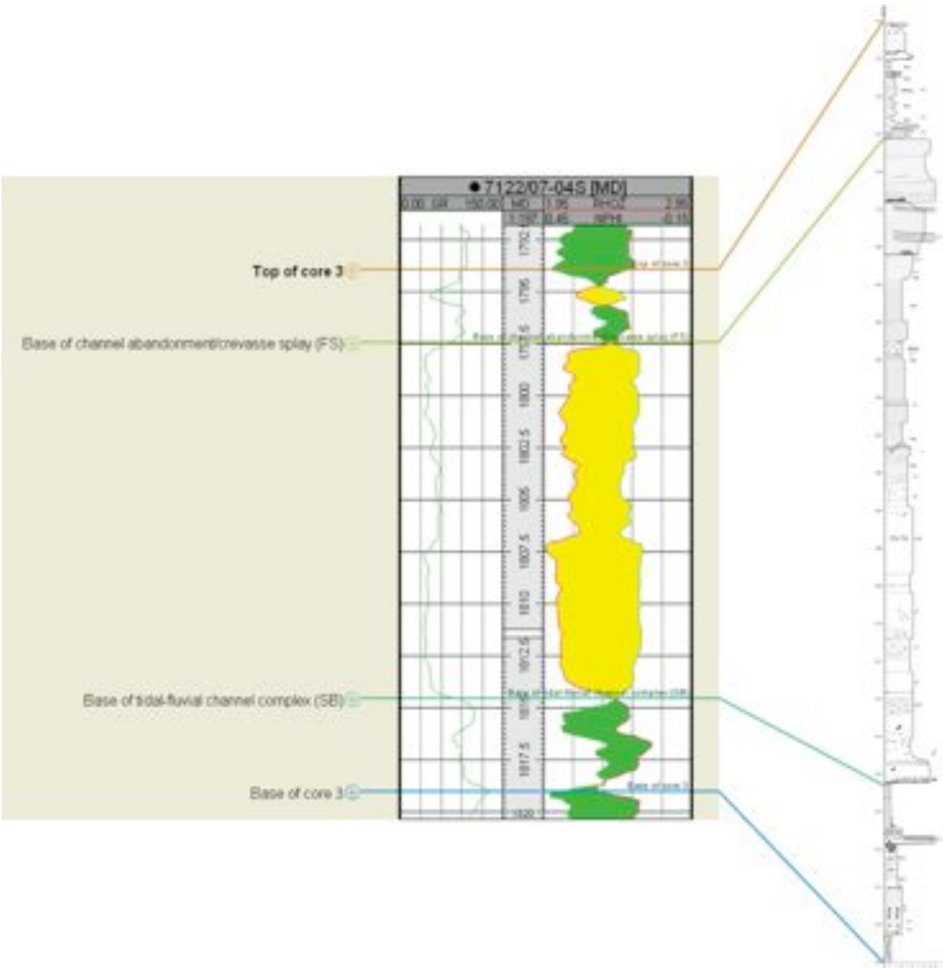

Figure 53 - Well 7122/7-4S. Data collected from wireline logs and the interpreted core. GR = Gamma ray, RHOZ = Density, NPHI = Neutron porosity. Log not to scale

Well 4S is cored from 1819-1794m MD and terminates together with the Kobbe Formation (Figure 53). Well 4S is interpreted as the most proximal deposited core compared to the neighbouring wells and comprises of five facies associations (Figure 53). Well 3 is cored from 1835-1824m MD and comprises of six facies associations. The offshore shales at the base of core 6 are comparable to the offshore/prodelta succession of core 3 in well 4S, generating a correlative flooding surface within both wells. The offshore/prodelta associations in both wells comprise of high gamma ray readings and low neutron porosity readings. The respective values appear normal for shale-rich rock successions in accordance with the readings of the simplified log response model and other examples from Løseth (2009) and Bjørlykke (2010) (Figure 53). In shales and sandstones, calculation of porosity based on neutron porosity logs can be quite tricky as there are many different aspects to consider. There are several effects, e.g. shale- and gas effect, which may have impact on readings due to the presence of hydrocarbons or bounded hydrogen within clay minerals in the rock (Bjørlykke 2010).

The sandstone successions interpreted in cores 5 and 6 (well 3) are interrupted by estuarine muds (Figure 54 - Well 7122/7-3. Data collected from wireline logs and the interpreted core. GR = Gamma ray, RHOZ = Density, NPHI = Neutron porosity. Log not to scale), whereas the sandstone succession in core 3 (well 4S) is a continuous amalgamated channel complex (Table 6; Figure 53). In the channel complex of both wells, the density range is low and the porosity range is high. These readings are in accordance with other examples of sandstone responses (Løseth 2009, Bjørlykke 2010). The neutron porosity readings are generally high and ranges between 0,2 and 0,3, which is good, though the permeability readings are an important factor as well.
The channel abandonment facies in well 4S and the estuarine fine facies are not correlative comparable in this transect.

7122/7-3 - 7122/7-5 transect

Transect 3-5 is generated from two cores in well 3 (core 5 and 6) and one core in well 5 (core 1), together with corresponding well data. Both wells are vertically drilled and situated approximately 2,1km apart. Well 5 is situated approximately straight north of well 3. Measurements of the highest and lowest values from wireline readings in wells 3 and 5 are listed in Table 7 below.

Table 7 - Results from wireline logs. Gamma ray, neutron porosity, density are listed with respect to the highest and lowest readings of individual facies associations and lithologies

Well 7122/7-3						
	Gamma ray		Porosity		Density	
Facies association	High	Low	High	Low	High	Low
Offshore/prodelta	111	76	0,06	0,02	2,62	2,49
Channel complex	74	36	0,3	0,21	2,37	2,13
Estuarine fines	110	90	0,11	0,07	2,57	2,51

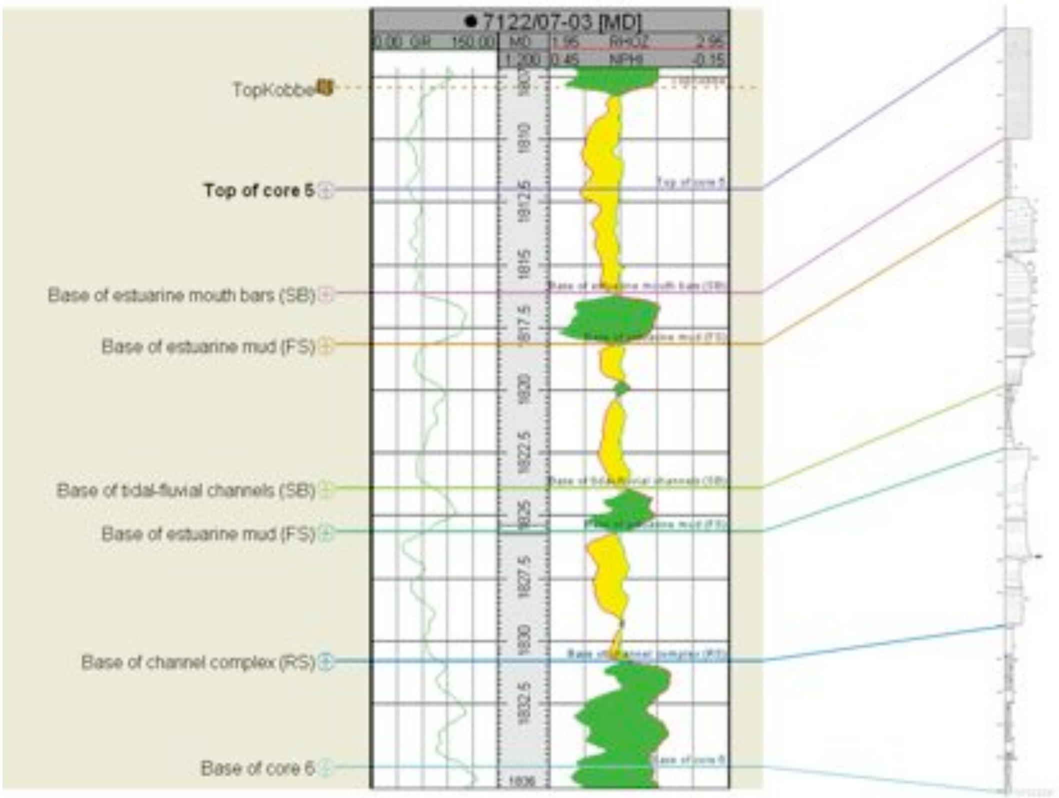

Figure 54 - Well 7122/7-3. Data collected from wireline logs and the interpreted core. GR = Gamma ray, RHOZ = Density, NPHI = Neutron porosity. Log not to scale

Well 3 is cored from 1835-1824m MD and comprises of six facies associations (Figure 54). Well 5 is cored from 1911-1900m MD and comprises of four facies associations. The interpreted offshore/prodelta shales of core 6 (well 3) are comparable with the facies above the interpreted core 1 (well 5). The offshore/prodelta facies generates a flooding surface at the top of core 1, and the interpreted distributary channel facies generates a sequence boundary at the base of core 1. This correlation is primarily based on wireline measurements and lithological similarities, as there is no core retrieved from the latter section (Figure 54). The distributary channel complex, shallow marine shelf sediments, and shoreface facies interpreted in well 5 are extrapolated based on the similarities below the offshore shale succession. Therefore, well 5 is correlated on the basis of the upper offshore succession that is present in all three wells. A detailed correlation between the two wells in mention is therefore based on similarities and speculation. The wireline measurements above the cored section of well 5 are interpreted as a more distal depositional environment than wells 3 and 4S (Figure 55; Table 8). This interpretation and correlation is based on the increased shale successions and decreased sandstone successions together with lithological similarities in wireline measurements (Figure 55).

Table 8 - Results from wireline logs. Gamma ray, neutron porosity, density are listed with respect to the highest and lowest readings of individual facies associations and lithologies

Well 7122/7-5						
	Gamma ray		Porosity		Density	
Facies association	High	Low	High	Low	High	Low
Offshore/prodelta	86	81	0,12	0,07	2,55	2,35
Channel complex	88	40	0,28	0,09	2,56	2,25
Shallow shelf sed.	81	65	0,2	0,14	2,46	2,35

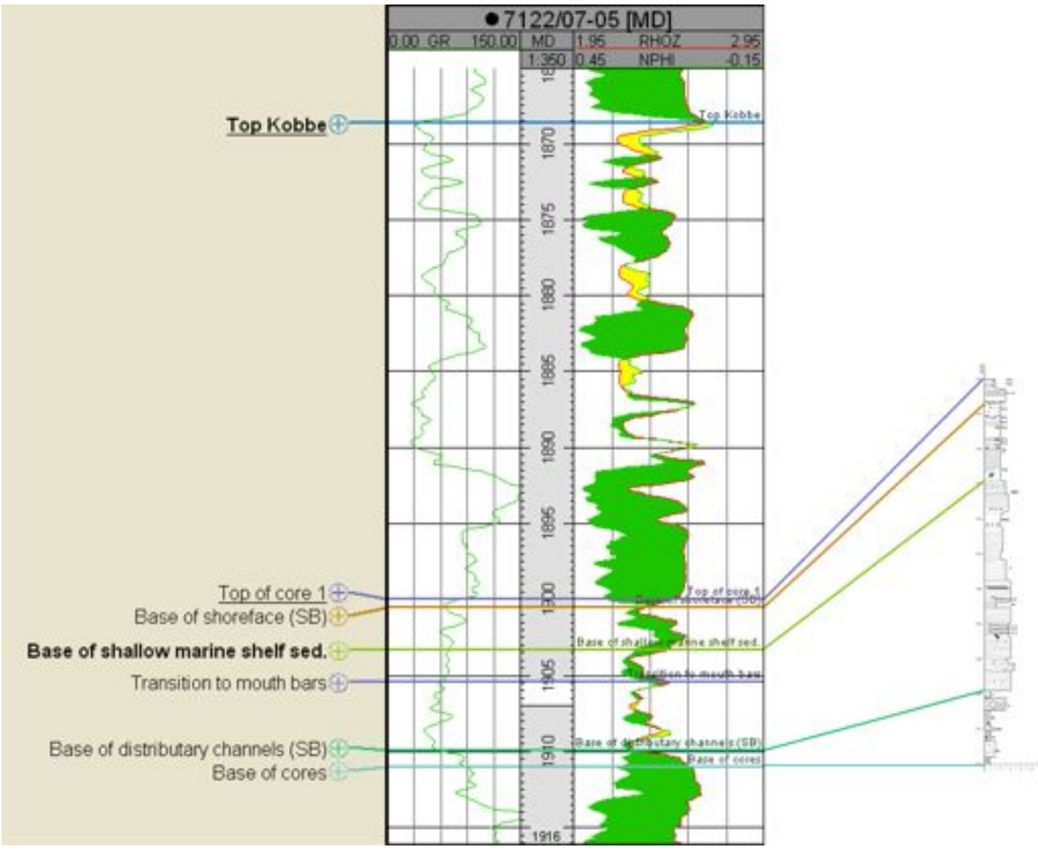

Figure 55 - Well 7122/7-5. Data collected from wireline logs and the interpreted core. GR = Gamma ray, RHOZ = Density, NPHI = Neutron porosity. Log not to scale

An overview of the correlation between the three wells, divided into two transects, is shown in Figure 56. All wells are shown in 1:350 scale and correlated on the basis of the top Kobbe Formation. The correlation between all wells show a definite proximal to distal depositional environment from well 4S to well 5. The thick sandstone succession of well 4S shows a more distal depositional environment in the two preceding wells along with a gradual separation by estuarine shales. As shown from the wireline readings, and based only on the measurements presented, a general proximal to distal trend is seen from well 4S to well 5. This trend may represent the palaeodepositional direction as approaching from the E-SE or variations in the delta distribution. Further discussion on depositional environments and palaeogeography is presented in the following chapter.

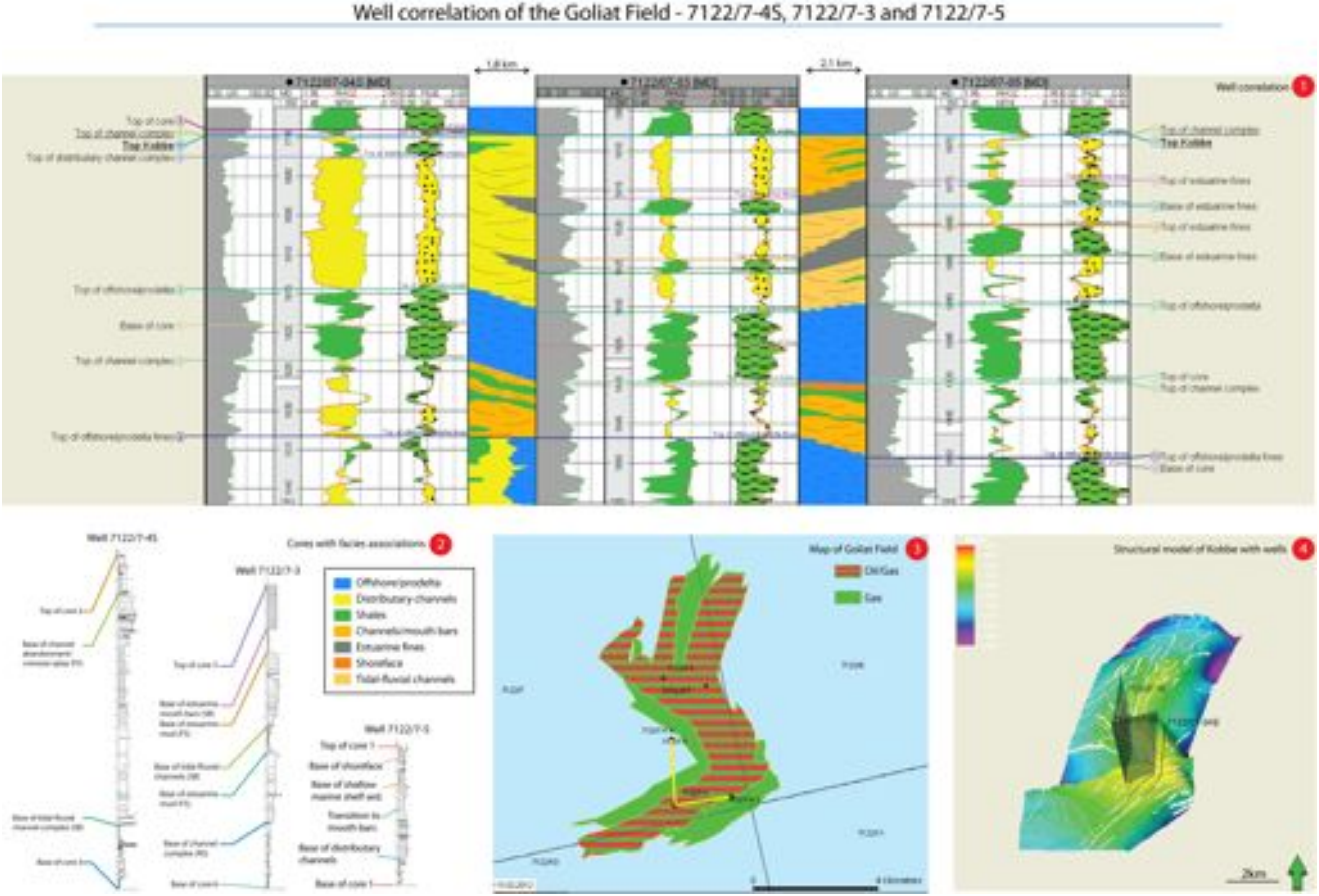

Figure 56 – (1) Well correlation of the Goliat Field. Well 7122/7-3, Well 7122/7-4S, Well 7122/7-5. (2) Cores with respective facies associations. (3) Map of the Goliat Field (npd.no). (4) Structural map of the Upper Kobbe Formation with wells and transects.

6. Depositional environments and conceptual models

Introduction

Facies associations and the depositional environments proposed therein are described in the latter chapters. This chapter is meant to summarize the facies associations and create conceptual models based on the interpreted depositional environments from the respective wells and cores, along with the fieldwork conducted on Spitsbergen. Depositional environments and conceptual models are created for each well and are divided into their respective subchapters.

Results from Karentoppen Member, Spitsbergen

Fieldwork conducted on the Karentoppen Member, SW Spitsbergen, exhibits two coarsening upward sequences. The first sequence is divided into prodelta shales of facies association 1 (FA1), the distal deltafront of FA2 and the deltaic channel complex of FA3. This sequence is abrupt by a flooding surface, which initiates the second coarsening upward sequence. The second sequence starts with a shallow marine shelf environment (FA4) and is further overlain by a proximal delta front (FA5) and back into a deltaic channel complex (FA3). The sediments constituting the Karentoppen Member are deposited in relatively proximal and paleocurrent measurements acquired show deposition towards E-SE, as the outcrop is approximately parallel with the palaeo-shoreline. These results are in accordance with Worsley´s (2008) mid-Triassic palaeogeographic model of the Barents Sea, showing deposition from the west and northwest (Figure 57). The depositional model for Karentoppen Member suggests an overall progradation from the west/northwest comprising of two parasequences.

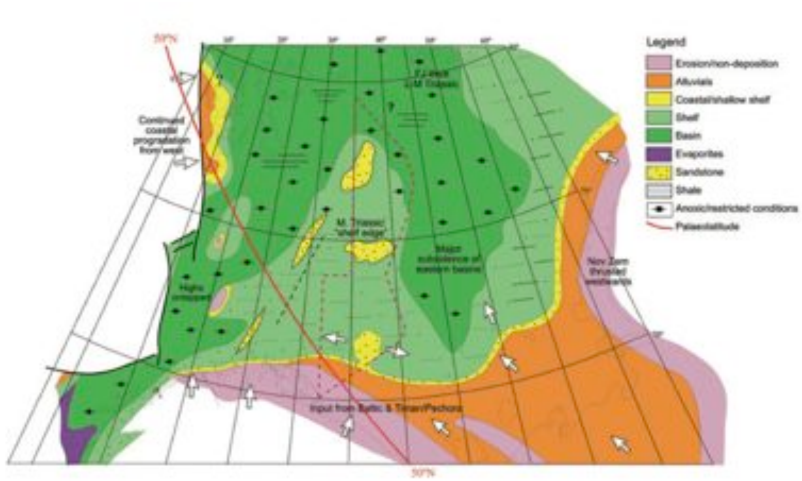

Figure 57 - Mid-Triassic regional palaeogeography of the Barents Sea. Note the coastal progradation from the northwest (Worsley 2008).

Delta type and modern analogue of the Karentoppen Member

The deltaic origin of the Karentoppen Member is evident from the downcutting of distributary channels into delta front deposits. This observation is further supported by previous studies of Karentoppen by Mørk et al. (1982), showing a deltaic depositional environment. These studies also revealed a N-S trending coastline with sediment transport to the E-SE (Mørk et al. 1982). The Mid-Triassic Bravaisberget Formation, which comprises Karentoppen Member, shows an overall coarsening upward sequence where the coarsest sediments are found in Sørkapp-Land (Mørk et al. 1982).
Proposing a lateral size of the delta system at Karentoppen is difficult based on scarce data, although the Karentoppen Member is only outcropped at the fieldwork site. Figure 23 gives a slight overview of the overall outcropped deltaic system. Worsley (2008) proposes a laterally extensive delta system throughout the Mid-Triassic, although this model comprises of all the deltaic formations and members deposited in Mid-Triassic (Figure 57). The size of the individual parasequences may give a rough estimate to the individual delta lobes, though the exact delta size is not given due to the limited study area.
The east-facing delta off the coast of Italy is proposed as a modern analogue for the delta system of the Karentoppen Member (Figure 58). The suggested Po delta has been used as a modern analogue for other studies e.g. the deltaic system of Battfjellet Formation on Svalbard (Olsen, 2008; Helland-Hansen, 2010; Skarpeid, 2010). The combined wave- and fluvial interactions of the Po delta might make it a good analogue for many ancient delta systems, including the Karentoppen Member.

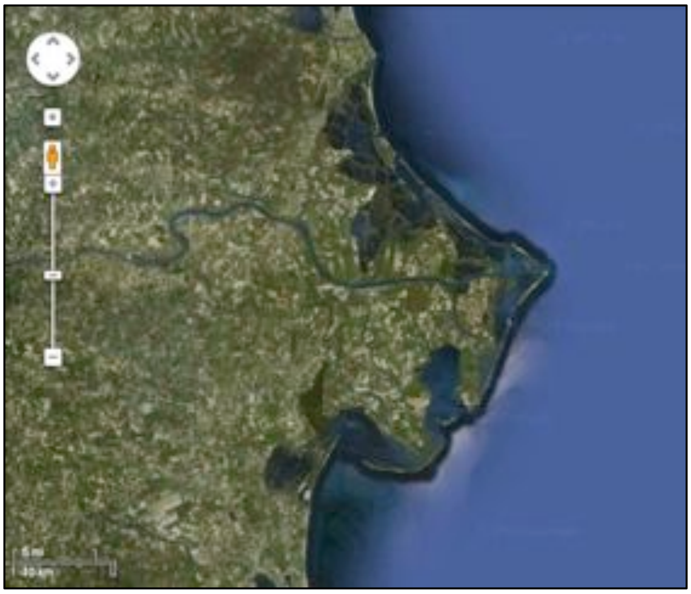

Figure 58 - Modern analogue. Satellite image of the Po delta at the coast of Italy (maps.google.no)

Sequence stratigraphy of the Karentoppen Member

Applying traditional sequence stratigraphic concepts is difficult due to the limited extent of the study area and the apparent absence of major flooding events and bypass during relative sea-level fall (Emery and Myers 2008). A model primarily based on regressive and transgressive shoreline trajectories is applied here (Helland-Hansen and Gjelberg 1994). Shoreline trajectories are defined as the cross-sectional migration path along depositional dip and are a function of sediment supply, relative sea-level change and basin physiography (Helland-Hansen and Gjelberg 1994). The Karentoppen Member is interpreted to be part of an overall regressive pattern. The Karentoppen Member shows progradation and aggradational features as the parasequences exhibit by stepping basinward.

The downcutting of the distributary channels onto the delta front deposits may be indicative of descending regression, often abbreviated regressive surface of fluvial erosion (RSFE). Commonly during descending regression, incision occurs behind the downward migrating shoreline, although fluvial channels may erode below sea level (Helland-Hansen and Gjelberg 1994; Bhattacharya 2006). A relatively high depositional rate is evident during falling sea level, as the regression is accretionary. A minor flooding event is interpreted at 14,4m, which creates accommodation space and deposition of shallow marine shelf sediments. A renewed progradation of the system overlies the shallow marine shelf sediments and delta front deposits. Downcutting of the distributary channels onto the delta front deposits is repeated. A conceptual model based on the interpreted facies associations and palaeocurrent measurements are shown in Figure 59. Note the two parasequences of amalgamated distributary channel complex (FA3) and the flooding surface dividing the two sequences (FA4).

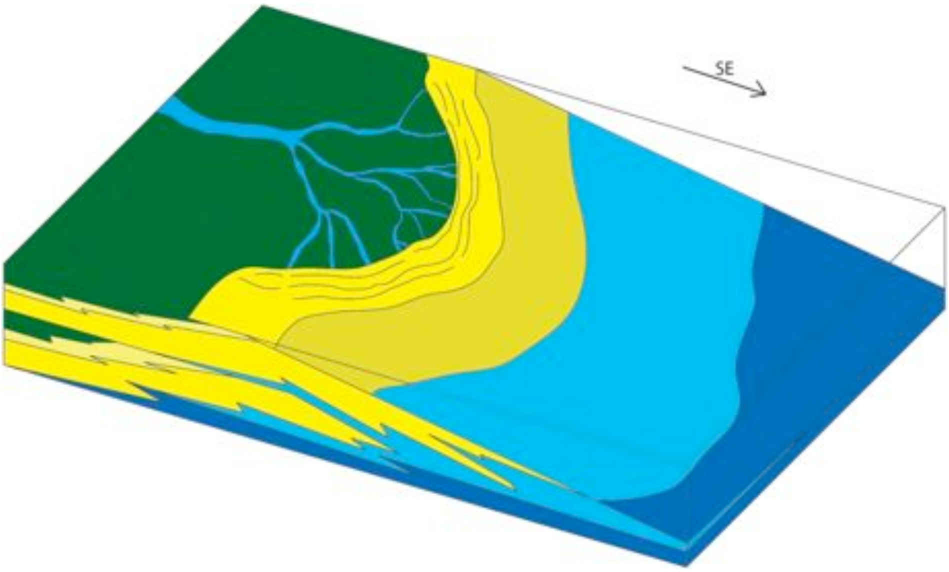

Figure 59 - A deltaic conceptual model of the Karentoppen Member with two parasequences

Well 7122/7-4S

Core 3 in well 7122/7-4S initiates with a wave-influenced prodelta sequence (FA1), which is truncated by a coarse-grained lag unit initiating a floodplain environment (FA2). The unit consist dominantly of claystone and is abrupt by a tidal-fluvial channel complex (FA3), generating a sequence boundary (SB). The unit is thick and gradually shifts into a tidal-dominated channel complex. As the unit succession progrades, another sequence boundary is generated as a proximal, coarse-grained tidal-fluvial channel complex truncates the underlying association (FA4). A flooding surface is generated as the channel complex is abandoned in facies association 5 (FA5).
A proximal part of an estuarine environment is proposed as an overall depositional system in core 3 of well 7122/7-4S (Figure 60). The conceptual model is based on the Gironde estuary in southwestern France, and is modified from Dalrymple et al. (1992).

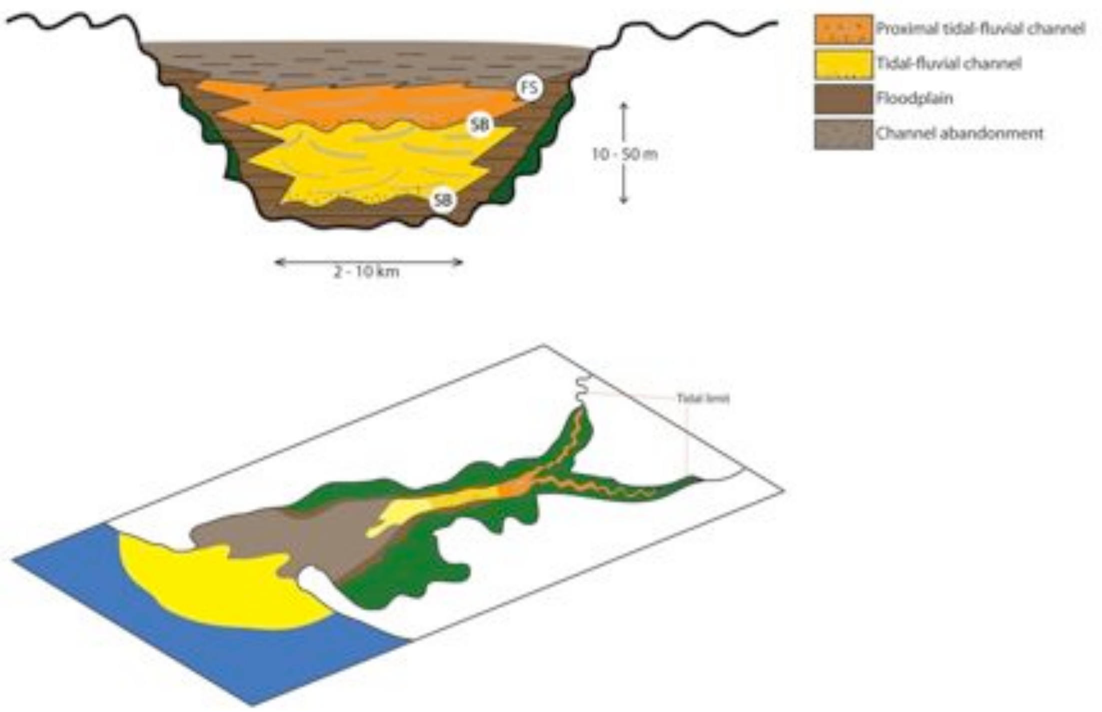

Figure 60 – (1) Conceptual model of depositional succession from well 7122/7-4S. SB – Sequence boundary, FS – Flooding surface. Model modified from (Dalrymple, 2010b)
(2) Conceptual model of depositional succession from well 7122/7-4S. Model modified from the Gironde estuary, a mixed-energy system, from (Dalrymple et al., 1992)

Well 7122/7-3

Cores 5 and 6 in well 7122/7-3 comprise of a total of six facies associations, and initiates with an offshore environment (FA1). A sequence boundary divides the offshore environment infilling the valley with alluvial channels (FA2). Progradation of a bay-head delta (FA3) above the alluvial channels generate a ravinement surface with a conglomeratic base. A flooding event causes deposition of estuarine fines (FA4), which generates a flooding surface above the bay-head delta. As the flood wanes, renewed progradation and tidal-influence of the estuary is evident, depositing tidal-fluvial channel sediments (FA5). A repeated flooding event generates a new flooding surface as it deposits estuarine fines (FA4). The last key-bounding surface is a sequence boundary generated by deposition of mouth bar sands (FA6) above the estuarine fines. An estuarine environment is proposed as an overall depositional system in cores 5 and 6 of well 7122/7-3 (Figure 61). The conceptual model is based on the Gironde estuary in southwestern France, and is modified from Dalrymple et al. (1992).

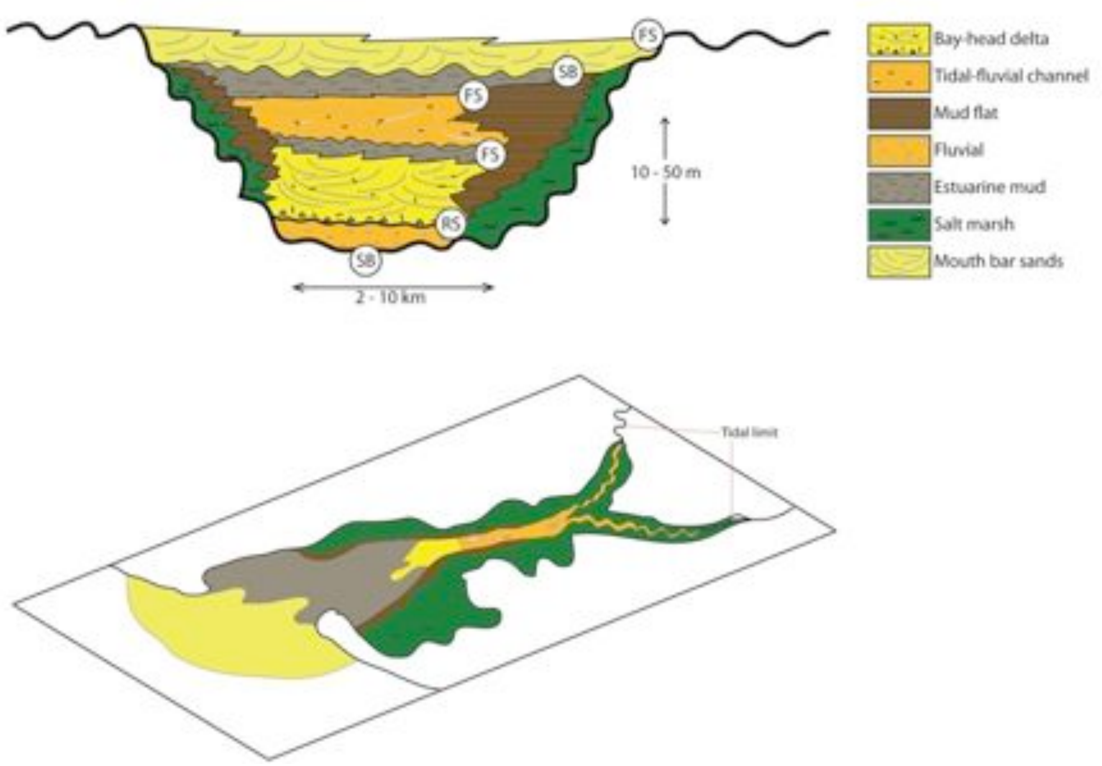

Figure 61 - (1) Conceptual model of depositional succession from well 7122/7-3. The succession begins with fluvial valley-fill deposits and is capped by mouth bar sands. RS - Ravinement surface, SB – Sequence boundary, FS – Flooding surface. Model modified from (Dalrymple, 2010b)

(2) Conceptual model of depositional succession from well 7122/7-3. Model modified from the Gironde estuary, a mixed-energy system, from (Dalrymple et al., 1992)

Well 7122/7-5

Core 1 in well 7122/7-5 is initiated by an offshore/prodelta environment below storm weather wave base (FA1), and is truncated by amalgamated distributary channels (FA2), generating a sequence boundary (SB). The thick sandstone package of distributary channels gradually changes into mouth bar deposits, without any break or erosive surface. Wave- and current induced structures along with extensive bioturbation are shown in the mouth bar deposits. Facies association 3 is interpreted as shallow marine shelf sediments and is truncated by a thin package of shoreface deposits (FA4), generating a sequence boundary (SB). In general, progradation of channel sediments onto the offshore shales initiate the core and are further overlain by more distal deposits. As shown in the well correlation panel (Figure 56), the cored section in well 7122/7-5 is below the interpreted estuarine observed in the two latter wells. The estuarine environment is interpreted to be present in well 7122/7-5, though not in the cored section (Figure 55). A deltaic origin is the basis for the conceptual model created to give a better visual overview (Figure 62).

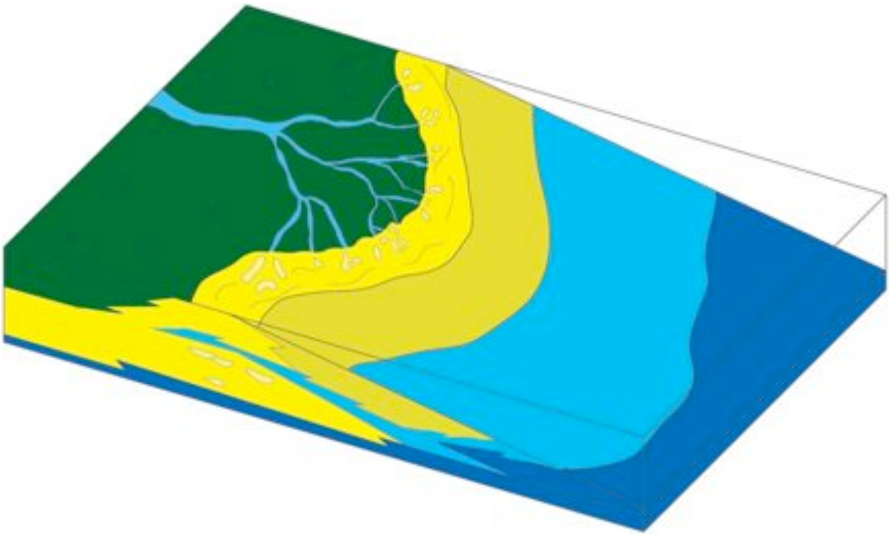

Figure 62 - A deltaic conceptual model of well 7122/7-5 with two parasequences and mouth bars

Delta type and modern analogue from the Kobbe Formation, Goliat Field

The Gironde estuary is used as a modern analogue in all three wells, and is considered a mixed-energy system (Figure 63). As all three wells in mention exhibit both wave- and tidal-influence of the estuary, the Gironde estuary is suggested as a good analogue. Dalrymple et al. (1992) presents the Gironde estuary as an example for a mixed-energy system where an increase in tidal-influence within a mixed-energy system may cause the bay-head delta to change from a fluvial-dominated morphology to a tide-dominated morphology. This transition may be observed in well 3 as the estuary changes into a tide-dominated morphology after a flooding event.

Classifying the nature of the estuary based on dominance and/or influence is difficult to decide. An estuarine environment is interpreted for all the wells above the thick shale sequence at the top of well 5, however a deltaic environment is interpreted for the wells below the thick shale sequence, within well 5. All the wells show influence of both tidal and wave action, which makes it difficult to put the system into an end-member branch. Therefore, the Po delta, which is a fluvio-wave delta, and the mixed-energy Gironde estuary are both good analogues for describing the environments in all three wells.

As a sidenote, core 1 in well 5 does not include the interpreted estuarine environment observed from well 3 and wireline measurements. Therefore, the Po delta analogue described in the fieldwork section can be used as an analogue for core 1 in well 5.

Figure 63 - Modern analogue - Satellite image of the Gironde estuary of southwestern France (maps.google.no)

Sequence stratigraphy from the Kobbe Formation, Goliat Field

Sequence stratigraphic concepts and principles was originally defined by Mitchum et al. (1977) as: "*A stratigraphic unit composed of relatively conformable succession of genetically related strata bounded at its top and base by unconformities or their correlative conformities*". A classification into systems tracts comprising of a number of different distinct depositional packages is reviewed within all three wells in this section. An idealized systems tract sequence is shown in Figure 64 below.

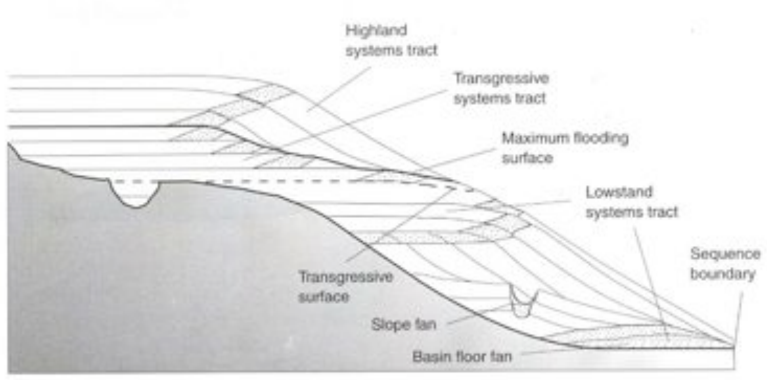

Figure 64 - Idealized type 1 sequence showing the different systems tracts and key bounding surfaces (Emery and Myers 2008)

All three wells are divided on the basis of a type 1 sequence, representative of a shelf-break margin. The basal part of all three wells is initiated with a lowstand systems tract, which is deposited during an interval of relative sea-level fall, and further, a slow relative sea-level rise (Figure 64) (Emery and Myers 2008). During such conditions, rivers incise into previous deposits and stabilize as the relative sea level low point is reached (Emery and Myers 2008). As observed, all wells exhibit an alluvial succession above the offshore/prodelta succession below.

As all three wells display an estuarine setting, a transgressive systems tract is a reasonable proceeding, as it is deposited during a relative sea-level rise cycle. Accomodation space increases faster than the rate of sediment supply, therefore creating volumes in incised valleys or commonly known as drainage systems (Emery and Myers 2008). The systems tract ends as the accommodation space decreases and matches sediment supply, generating progradation of the system. The progradational cycle starts as the influx of the thick sandstone packages overlie the offshore successions. Many authors define this point as the maximum flooding surface (Emery and Myers 2008 and references therein). The maximum flooding surface in the

correlated wells, is therefore somewhere towards the top of the thick offshore shale package just as the progradation begins (Figure 56).
Following the transgressive systems tract is the initial aggradation and later progradation of the highstand systems tract. This is where the rate of accommodation space is less than the rate of sediment supply (Emery and Myers 2008). The thick channel- and estuarine complexes overlying the offshore shale packages are interpreted as a shift between a transgressive systems tract and highstand systems tract.

The interpreted estuarine fines are deposited during minor flooding events within this transition, and are a part of a parasequence set. A parasequence set was defined by Van Wagoner et al. (1990) as: *A succession of genetically related parasequences forming a distinctive stacking pattern bounded by major marine-flooding surfaces and their correlative conformities.* The end-members of parasequence sets are progradational-, aggradational- and retrogradational parasequence sets (Figure 65). The retrogradational parasequence set is characteristic of transgressive systems tracts (Emery and Myers 2008), which is interpreted for these wells. However, the characteristics of progradational parasequence sets are highstand systems tracts and lowstand prograding wedges. Classifying the correct parasequence within such a limited lateral overview and few parasequences is difficult, and a combination of the two latter sets is suggested.

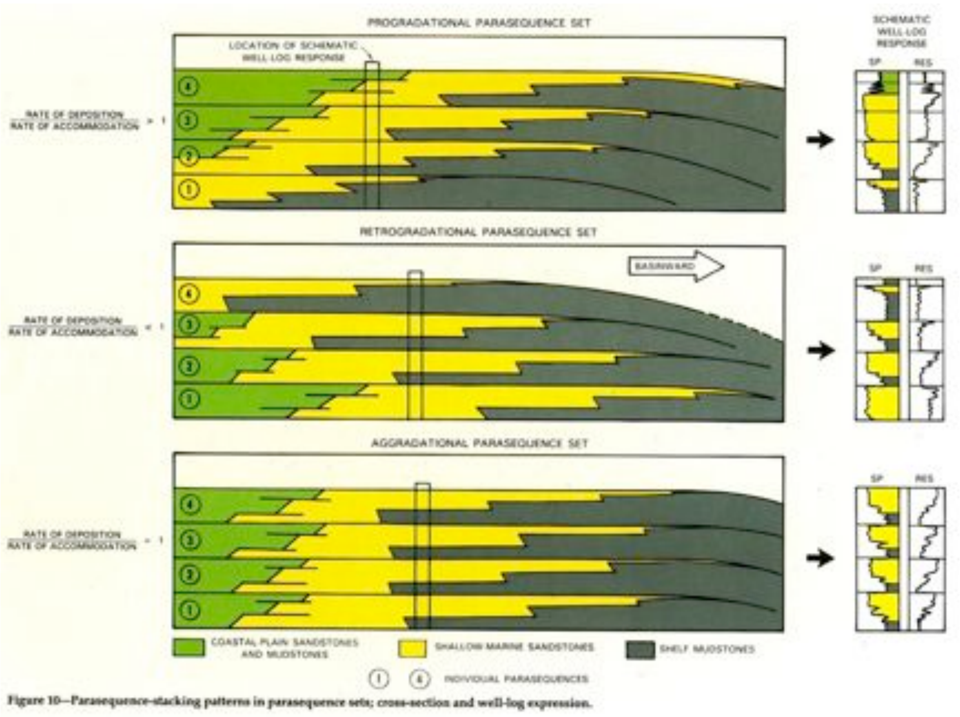

Figure 65 - A proposed scheme for different parasequence sets (Van Wagoner et al. 1990)

The thicknesses of a parasequence are primarily controlled by water depth, where it represents the rise in relative sea-level. Although, thickness analysis can only be applied under certain circumstances. For example, a parasequence set may exhibit a thinning upward trend due to basinward thinning, yet this feature is not related to decreasing rates of sea level rise (Emery and Myers 2008). The top of the Kobbe Formation, which is the flattened correlative surface in all three wells, is terminated by a major flooding event capping the thick sandstone packages below (Figure 56).

7. Is the Karentoppen Member a suitable analogue for the Kobbe Formation?

I propose that by comparing the outcrop section from fieldwork studies on Sørkapp and the cores from the Hammerfest Basin has improved a broader understanding of the sandbody geometry and lateral extensiveness of the Kobbe Formation in the Hammerfest Basin.

Correlating and interpreting three cores from the Goliat Field may give an impression of the sand body geometry and lateral continuity (Figure 56), though including an analogue through outcrop studies can create a more complete picture (Figure 66). The specific outcrops at Karentoppen are thought to be the only known proximal facies of Anisian-Ladinian sandstone on Svalbard. By detailed outcrop studies and core analysis, conceptual models and proposed depositional environments were made (Figure 56). By comparing these two studies, one can see that the vertical stacking pattern and depositional origin of the reservoir sandstone in the Goliat Field is quite similar to the outcrops at Karentoppen.

The lateral extensiveness of the reservoir section in the Goliat Field is shown by the correlation of depositional environments between the three wells (Figure 56). This large-scale sand body geometry is also seen from the outcrops at Karentoppen, where the interpreted amalagamated channel structures are visible for hundreds of meters (Figure 66). The highlighted blue colour on figure 66 are a few chosen channel structures visible within proposed distributary channels interpreted in FA3. The highlighted red structure is the laterally extensive sandstone body within FA5, which is characteristic of the Karentoppen Member and suggests that the outcrop seen at a distance is in fact also within this member.
The two transects between wells 7122/7-3, 7122/7-4S and 7122/7-5 are in the range of 2 km apart and display a more distal depositional environment than the studied outcrop. However, the structural similarities and sand body geometry of the studied outcrops are strikingly similar and are therefore considered a good analogue to the reservoir section in the Goliat Field.
More detailed and extensive studies on the outcrops surrounding Karentoppen would increase the understanding of the Karentoppen Member and sand body geometry. This

may be of use to better understand the size and dimension of other proposed reservoir sandstones with similar depositional origin as the Karentoppen Formation.

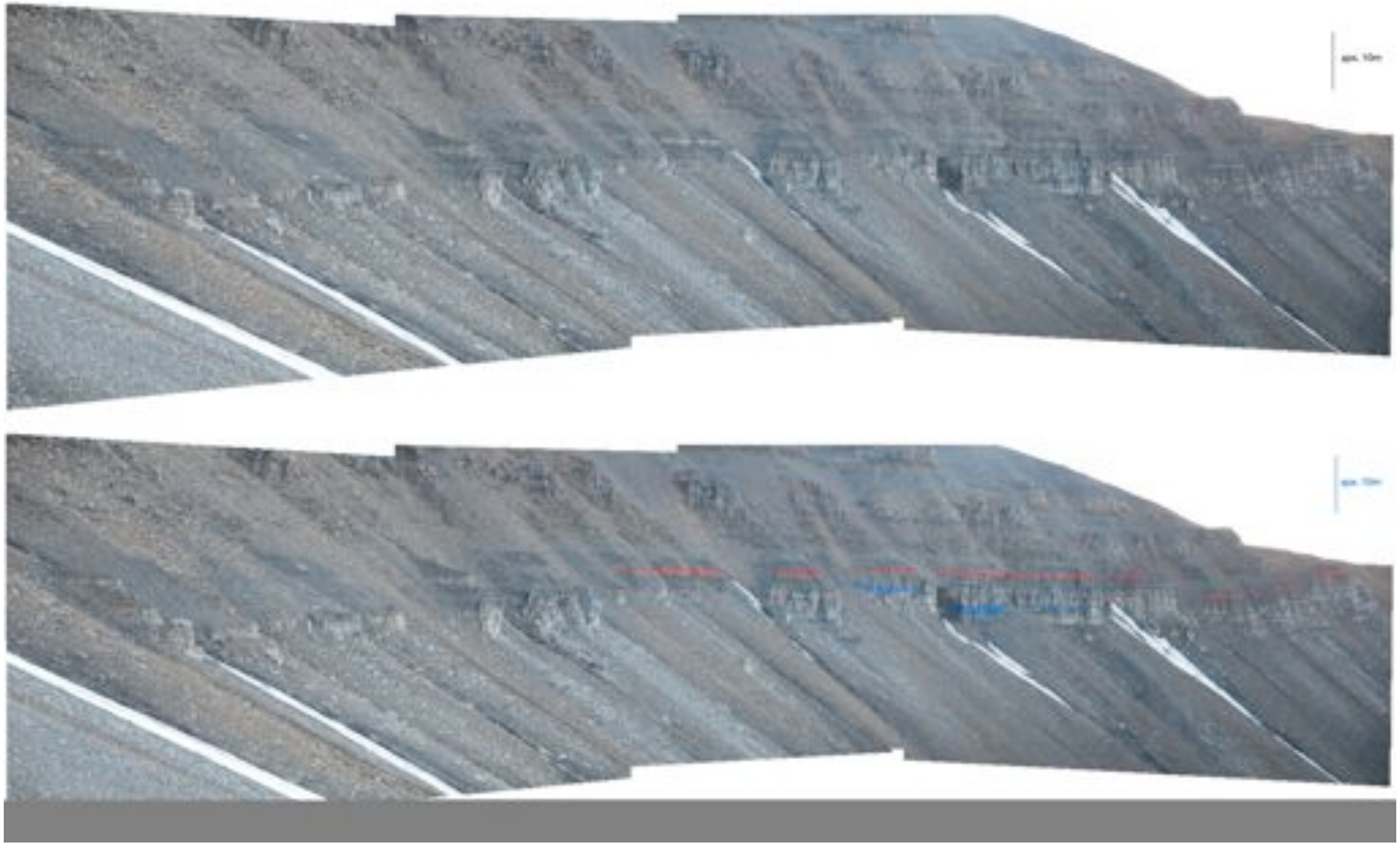

Figure 66 – Two identical photos, the lower one including a few possible channel structures (highlighted in colours), of the suggested Karentoppen Member outcrop approximately NW beyond the studied outcrop. Lateral scale is difficult to find, though it is the range of 300-500m wide.

8. Conclusion

The primary focus of the present study is to establish a refined sedimentological facies model of the Kobbe Formation in the Goliat Field. The task is solved by detailed sedimentological and sequence stratigraphical analyses of the Kobbe Formation and the Mid-Triassic Karentoppen Member on southwestern Spitsbergen, Svalbard (Figure 67). Three cores from the Goliat Field and outcrop studies on Svalbard are conducted to better define thicknesses, lateral continuity and vertical stacking patterns of the sandstone bodies. The Kobbe Formation is later compared with the relatively more distal facies development of the Karentoppen Formation.

The Karentoppen Member of the Bravaisberget Formation comprises of a shallow marine – delta front environment within an overall progradation east to southeast deltaic system (Figure 67). Both the Bravaisberget Formation and the Karentoppen Member have been thoroughly studied by many workers, and the outcrop area in this project has not been studied since Professor Atle Mørk described the Karentoppen Member in the 1980s. In order to summarize the project in the best way, a division in to three points is made;

1. The studied core sections of the Kobbe Formation and the Karentoppen Member are interpreted and sub-divided into facies associations based on interpreted depositional environments and lithological characteristics. The Karentoppen Member comprises of five facies associations grading from offshore transition (FA1), delta front environment (FA2), lower delta plain (FA3), shallow marine shelf sediments (FA4) and back into a proximal delta front environment (FA5).
2. The Kobbe Formation within the Goliat Field is divided into sets of facies associations based on the three individual wells interpreted (7122/7-3, 7122/7-4S, 7122/7-5). Well 7122/7-4S is defined as the most proximal environment of the three wells and is sub-divided into five facies associations. The core dominantly comprises of an estuarine environment with tidal-fluvial channels (FA1-FA5). Well 7122/7-3 comprises of six facies associations and is relatively more distal than well 7122/7-4S. The cores dominantly comprise of an estuarine environment with tidal-influenced fluvial channels and mouth bars (FA1-FA6). Well 7122/7-5 is interpreted as the most distal of the three wells and comprises of four facies associations. The core dominantly comprises of lower delta plain and shallow marine shelf sediments environments (FA1-FA4).

3. The sand body thickness and lateral continuity observed from the two study areas show similarities and the Karentoppen Member is suggested to be an analogue to the reservoir section in the Goliat Field. The reservoir section and the outcrop section show similar thicknesses and lateral extensiveness as well as similar depositional environments, though a slight difference in proximity. This is in concordance with previous studies, as well as the palaeogeographic setting of the outcrop is oriented towards the E-SE and shows a parallel palaeo-shoreline orientation based on palaeocurrent data.

Figure 67 - A conceptual model of the deltaic systems (clastic wedges) in Goliat (from Geir Dalen; Eni Norge pers. com) and Karentoppen (this study) superimposed on Anisian Paleogeography provided and modified by Riis et al 2008.

9. References

Albertson, M.L., Dai, Y.B., Jensen, R.A., and Hunter, R., (1950), Diffusion of submerged jets: American Society of Civil Engineers Transactions, v. 115, p. 639–697.

Aydin, A., and Johnson, A. M., (1983), Analysis of faulting in porous sandstones: Journal of Structural Geology, v. 5, no. 1, p. 19-31.

Axelsson, V., (1967), The Laitaure Delta: a study of deltaic morphology and processes: *Geografiska Annaler, Series A, Physical Geography*, v. 49, **p. 127.**

Bates, C.C., (1953), Rational theory of delta formation: American Association of Petroleum Geologists, Bulletin, v. 37, p. 2119–2162.

Baydin, S.S., (1970), Formation of modern delta branches on non-tidal rivers with large sediment discharge: Hydrology of Deltas, Volume 1: *International Association of Scientific Hydrology-UNESCO, Studies and Reports in Hydrology*, v. 9, **p. 113–120.**

Bhattacharya, J.P. and Walker, R.S. (1992) Deltas. In: Facies Models: Response to Sea-level Change (Eds R.S. Walker and N.P. James), *Geol. Assoc. Can*., **pp.157–177**

Birkenmajer, K. (1977), Triassic sedimentary formations of the Hornsund area, Spitsbergen: *Studia Geol. Polon,* 51, **pp. 7-74**

Bjørlykke, K. and P. Avseth (2010). Petroleum Geology, Springer Verlag.

Buchan, S. H., Challinor, A., Harland, W. B. and Parker, J. R. (1965), The Triassic stratigraphy of Svalbard: *Norsk Polarinst.* Skr. 135, **pp. 1-94**

Collinson, J. D., (1969), The sedimentology of the Grindslow Shales and the Kinderscout Grit: a deltaic complex in the Namurian of northern England: Journal of Sedimentary Petrology, v. 39, no. 1, p. 194-221.

Dalland, A. (1979). Structural geology and petroleum potential of Nordenskiöld Land, Svalbard. Norsk Petroleumsforening, Norwegian Sea Symposium, pp. 1-20.

Dallmann, W.K. (Ed.). (1999). Lithostratigraphic Lexicon of Svalbard. *Norwegian Polar Institute, Polar Environmental Centre*, **320pp**. Review and recommendations for nomenclature use. Upper Paleozoic to Quaterneary Bedrock.
Tromsø, Norway

Dalrymple, R., (2010b), Introduction to siliciclastic facies models: Facies models, v. 4, p. 59-72.

Dalrymple, R. W., and Zaitlin, B. A., (1994), High‐resolution sequence stratigraphy of a complex, incised valley succession, Cobequid Bay—Salmon River estuary, Bay of Fundy, Canada: Sedimentology, v. 41, no. 6, p. 1069-1091.

Dalrymple, R. W., Zaitlin, B. A., and Boyd, R., (1992), Estuarine facies models; conceptual basis and stratigraphic implications: Journal of Sedimentary Research, v. 62, no. 6, p. 1130-1146.

Davis, R. A., (2011), Principles of tidal sedimentology, Springer Verlag.

Dumas, S., Arnott, R., and Southard, J. B., (2005), Experiments on oscillatory-flow and combined-flow bed forms: implications for interpreting parts of the shallow-marine sedimentary record: Journal of Sedimentary Research, v. 75, no. 3, p. 501-513.

Doré, A.G., 1991. The structural foundation and evolution of Mesozoic seaways between Europe and the Arctic. Palaeogeography Palaeoclimatology Palaeoecology 87, 441-492.

Dypvik, H., Nagy, J., Eikeland, T.A., Backer-Owe, K., Andresen, A., Haremo, P., Bjærke, T., Johansen, H. & Elvhøi, A. (1991). The Janusfjellet Subgroup (Bathonian to Hauterivian) on central Spitsbergen: a revised lithostratigraphy. *Polar Research* V. 9, No. 2, pp. 1-43.

Eidvin, T., Jansen, E. & Riis, F. 1993. Chronology of tertiary fan deposits off the western Barents Sea; implications for the uplift and erosion history of the Barents Sea. Marine Geology, 112, 109–131.

Elliott, T. (1974). "Interdistributary bay sequences and their genesis." Sedimentology **21**(4): 611-622.

Embry. A., and E. Johannessen, (1992). T-R sequence stratigraphy, facies analysis and reservoir distribution in the uppermost Triassic-Lower Jurassic succession, western Sverdrup Basin. Arctic Canada, in T. Vorren et aI., eds., Arctic geology and petroleum potential: *Norwegian Petroleum Society Special Publication* 2. p. 121- 146

Faleide, J. I., Solheim, A., Fiedler, A., Hjelmestuen, B. O., Andersen, E. S. & Vanneste, K. (1996). Late Cenozoic evolution of the western Barent Sea – Svalbard continental margin.Global Planetary Change, 12, 53–74.

Faleide, J. I., Tsikalas, F., Breivik, A.J, Mjelde, R., Ritzmann, O., Engen, Ø., Wilson, J. & Eldholm, O. (2008). Structure and evolution of the continental margin off Norway and the Barents Sea. Episodes, 31, pp. 82-91.

Fossen, H., Schultz, R. A., Shipton, Z. K., and Mair, K., (2007), Deformation bands in sandstone: a review: Journal of the Geological Society, v. 164, no. 4, p. 755-769.

Fossum, B. J., Schmidt, W. J., Jenkins, D. A., Bogatsky, V. L. & Rap- poport, B. I. (2001). New frontiers for hydrocarbon production in the Timan – Pechora Basin, Russia. In: Downey, M. W., Threet, J. C. & Morgans, W. A. (eds) Petroleum Provinces of the Twenty-first Century. American Association of Petroleum Geologists, Tulsa, OK, Memoirs, 74, 259–279.

Gabrielsen R.H., Færseth R.R., Jensen L.N., Kalheim J.E. & Riis F. (1990). Structural elements of the Norwegian continental shelf, part 1, the Barents Sea region. Norwegian Petroleum Directorate Bulletin 6. Stavanger: Norwegian Petroleum Directorate.

Gingras, M. K., and MacEachern, J. A., (2011), Tidal Ichnology of Shallow-Water Clastic Settings: Principles of Tidal Sedimentology, p. 57.

Gjelberg, J.G. & Steel, R.J. (1981). An outline of Lower-Middle Carboniferous sedimentation on Svalbard: effects of climatic, tectonic and sea level changes in rift basin sequences. *Canadian Society of Petroleum Geologists,* V. 7, pp. 543-561.

Gjelberg, J.G. & Steel,R.J. (1995). Helvetiafjellet Formation (Barremian-Aptian), Spitsbergen, characteristic of a transgressive succession. In Steel et al. (ed) *Norwegian Petroleum Society*, Special Publication No. 5, pp. 571-593.

Gjelberg, J., Martinsen, O., Charnock, M., Møller, N., and Antonsen, P., (2005) The reservoir development of the Late Maastrichtian–Early Paleocene Ormen Lange gas field, Møre Basin, Mid-Norwegian Shelf, Volume 6, Geological Society of London, p. 1165-1184.

Gjelberg, H. K. (2010). "Facies Analysis and Sandbody Geometry of the Paleogene Battfjellet Formation, Central Western Nordenskiöld Land, Spitsbergen."

Glørstad-Clark, E., J. I. Faleide, et al. (2010). "Triassic seismic sequence stratigraphy and paleogeography of the western Barents Sea area." Marine and Petroleum Geology **27**(7): 1448-1475.

Gudlaugsson, S. T., Faleide, J. I., Johansen, S. E. & Breivik, A. J. (1998). Late Palaeozoic structural development of the South-westernBarents Sea. Marine and Petroleum Geology, 15, 73–102.

Harland,W.B. (1997). The geology of Svalbard, 17. *Memoirs of the Geological Society London*.

Helland-Hansen, W., and Gjelberg, J. G., (1994), Conceptual basis and variability in sequence stratigraphy: a different perspective: Sedimentary Geology, v. 92, no. 1-2, p. 31-52.

Helland-Hansen, W. & Martinesn, O.J. (1996). Shoreline Trajectories and Sequences: Description of Variable Depositional-Dip Scenarios. *Journal of Sedimentary Research*, V. 66, No. 4, pp. 670-688.

Helland-Hansen, W. (2010). Facies and stacking patterns of shelf-deltas within the Paleogene Battfjellet Formation, Nordenskiöld Land, Svalbard: implications for subsurface reservoir prediction. *Sedimentology*, V. 57, No. 1, pp. 190-208.

Henriksen, E., A. Ryseth, et al. (2011). "Tectonostratigraphy of the greater Barents Sea: implications for petroleum systems." Geological Society, London, Memoirs 35(1): 163-195.

Hill, P.R., Meulé, S. & Longuépée, H. (2003). Combined-Flow Processes and Sedimentary Structures on the Shoreface of the Wave-Dominated Grande-Riviére-De-La-Baleine Delta. *Journal of Sedimentary Reaserch*, V. 73, No. 2, pp. 217-226.

Krajewski, K. P., (2008), The Botneheia Formation (Middle Triassic) in Edgeøya and Barentsøya, Svalbard: lithostratigraphy, facies, phosphogenesis, paleoenvironment: Polish Polar Research, v. 29, no. 4, p. 319-364.

Krajewski, K. P., Karcz, P., Wozny, E., and Mørk, A., (2007), Type section of the Bravaisberget Formation (Middle Triassic) at Bravaisberget, western Nathorst Land, Spitsbergen, Svalbard: Polish Polar Research, v. 28, p. 79-122.

Krajewski K.P. (2000a). Phosphogenic facies and processes in the Triassic of Svalbard. *Studia Geologica Polonica* 116: **7–84**

Krajewski K.P. (2000b). Isotopic composition of apatite−bound sulphur in the Triassic phosphogenic facies of Svalbard. *Studia Geologica Polonica* 116: **85–109**

Krajewski K.P. (2000c). Diagenetic recrystallization and neoformation of apatite in the Triassic phosphogenic facies of Svalbard. *Studia Geologica Polonica* 116: **111–137**

Krajewski K.P. (2000d). Phosphorus concentration and organic carbon preservation in the Blank− nuten Member (Botneheia Formation, Middle Triassic) in Sassenfjorden, Spitsbergen. *Studia Geologica Polonica* 116: **139–173**

Krajewski K.P. (2000e). Phosphorus and organic carbon reservoirs in the Bravaisberget Formation (Middle Triassic) in Hornsund, Spitsbergen. *Studia Geologica Polonica* 116: **175–209**

Løseth, T. M., Ryseth, A. E., and Young, M., (2009), Sedimentology and sequence stratigraphy of the middle Jurassic Tarbert Formation, Oseberg South area (northern North Sea): Basin Research, v. 21, no. 5, p. 597-619.

Mørk, A., Knarud, R. & Worsley, D. (1982). Depositional and diagenetic environments of the Triassic and Lower Jurrasic succsession of Svalbard. In Arctic Geology and

Geophysics. Ed. By A. F. Embry and H. R. Balkwill. *Canadian Society of Petroleum Geologists*, Memoir V. 8, **pp. 371-398**

Mørk A., Embry A.F. and Weitschat W. (1989). Triassic transgressive–regressive cycles in the Sverdrup Basin, Svalbard, and the Barents Shelf. In: J.D. Collinson (ed.) Correlation in Hydrocarbon Exploration. Graham & Trotman, London: 113–130.

Mørk, A., Elvebakk, G. et al. (1999a). The type section of the Vikinghøgda formation: a new Lower Triassic unit in central and eastern Svalbard. Polar Research, 18, 51–82.

Mørk A. and Elvebakk G. (1999): Lithological description of subcropping Lower and Middle Triassic rocks from the Svalis Dome, Barents Sea. Polar Research 18: 83–104.

Nummedal, D., and Swift, D. J. P., (1987), Transgressive stratigraphy at sequence-bounding unconformities: some principles derived from Holocene and Cretaceous examples: Sea-Level Fluctuation and Coastal Evolution: SEPM, Special Publication, v. 41, p. 241-260.

Nøttvedt, A., Berglund, L. T., Rasmussen, E. & Steel, R. 1988. Some aspects of Tertiary tectonics and sedimentation along the western Barents Shelf. In: Morton, A. C. & Parsons, L. M. (eds) Early Ter- tiary Volcanism and the opening of the North Atlantic. Geological Society, London, Special Publications, 39, 421–425.

Olsen, H.A. (2008). Sedimentology and Paleogeography of the Battfjellet Fm, Southern Van Mijenfjorden, Svalbard. University of Bergen, Bergen.

Pattison, S. A. J., and Walker, R. G., (1994), Incision and filling of a lowstand valley: late Albian Viking Formation at Crystal, Alberta, Canada: Journal of Sedimentary Research-Section B-Stratigraphy and Global Studies, v. 64, no. 3, p. 365-379.

Reading, H.G. (1996). Sedimentary environments: processes, facies and stratigraphy (3 ed.): *Blackwell Publishing company*

Riis, F., Lundschien, B. A., Høy, T., Mørk, A., and Mørk, M. B. E., (2008), Evolution of the Triassic shelf in the northern Barents Sea region: Polar Research, v. 27, no. 3, p. 318-338.

Sokolov, V. N. and Pcelina, T. M. (1967). On the Lower and Middle Triassic of Sørkapp Land in Vestspitsbergen: *Doklady Akad.* SSSR 1967 176 (b), **pp. 1374-1377**

Richardsen, G., Vorren, T. O. & Tørudbakken, B. O. (1993). Cretaceous uplift and erosion in the southern Barents Sea: a discussion based on analysis of seismic interval velocities. Norwegian Journal of Geology, 73, 3–20.

Ryseth, A., & Augustson, J. H. et al. 2003. Cenozoic stratigraphy and evolution of the Sørvestsnaget Basin, southwest Barents Sea. Norwegian Journal of Geology, 83, 107–130.

Skarpeid, S.S. (2010). Facies Architecture and Paleogeography of the Battfjellet Formation, Rypefjellet, Spitsbergen. University of Bergen. 113pp.

Steel, R.J., & Worsley, D. (1984). Svalbard's post-Caledonian strata – an atlas of sedimentational patterns and paleogeographic evolution. *Norwegian Petroleum Society (Graham & Trotman)* (Petroleum Geology of the North European Margin), pp. 109-135.

Stemmerik, L., Elvebakk, G. & Worsley, D. 1999. Upper Palaeozoic carbonate reservoirs on the Norwegian Arctic Shelf: delineation of reservoir models with application to the Loppa high. Petroleum Geoscience, 5, 173–187.

Mitchum, R.M. Jr (1977) Seismic stratigraphy and global changes of sea level, part 1: glossary of terms used in seis- mic stratigraphy. In: Seismic Stratigraphy – Applications to Hydrocarbon Exploration (Ed. C.E. Payton), AAPG Mem., 26, 205–212.

Nøttvedt, A., Cecchi, M. et al. (1993a) Svalbard – Barents Sea correlation: a short review. In: Vorren, T. O., Bergsager, E., Dahl- Stamnes, Ø. A., Holter, E., Johansen, B., Lie, E. & Lund, T. B. (eds) Arctic Geology and Petroleum Potential. Elsevier, Amster-dam/Norwegian Petroleum Society, Trondheim, Special Publi- cations, 2, 363–375.

Nøttvedt, A., Livbjerg, F., Midbøe, P. S. & Rasmussen, E. 1993b. Hydrocarbon potential of the Central Spitsbergen Basin. In: Vorren, T. O., Bergsager, E. et al. (eds) Arctic Geology and Petroleum Potential. Elsevier, Amsterdam/Norwegian Petroleum Society, Trondheim, Special Publications, 2, 333–361.

Olariu, C. and Bhattacharya, J.P. (2006) Terminal distributary channels and delta front architecture of river-dominated deltas. *J. Sed. Res.*, 76, **212–233**

O'Leary, N., White, N. et al. (2004). Evolution of the Timan-Pechora and South Barents basins. Geological Magazine, 141, 141–160.

Overeem, I., Krooneneberg, S.B., Veldkamp, A., Groenesteijn, K., Rusakov, G.V., and Svitoch, A.A., (2003), Small-scale stratigraphy in a large ramp delta: recent and Holocene sedimentation in the Volga delta, *Caspian Sea: Sedimentary Geology*, v. 159, **pp. 133–157**

Pattison, S. A. J. and R. G. Walker (1994). "Incision and filling of a lowstand valley: late Albian Viking Formation at Crystal, Alberta, Canada." Journal of Sedimentary Research-Section B-Stratigraphy and Global Studies **64**(3): 365-379.

Pemberton, S.G., Frey, R.W., Ranger, M.J., and Maceachern, J.A., (1992), The conceptual framework of ichnology, in Pemberton, S.G., ed., Applications of Ichnology to Petroleum Exploration, *A Core Workshop: SEPM, Core Workshop* 17, **p. 1–32**

Van Wagoner, J.C., Mitchum, R.M., Campion, K.M. and Rahmanian, V.D. (1990) Siliciclastic Sequence Stratigraphy in Well Logs, Cores, and Outcrops: Concepts for High Resolution Correlation of Time and Facies. *AAPG Meth.* Explor. Ser., 7, 55

Vorren, T. O., Richardsen, G., Knutsen, S. M. & Henriksen, E. (1991). Cenozoic erosion and sedimentation in the western Barents Sea. Marine and Petroleum Geology, 8, 317–340.

Walker, R.G. (1978). Deep-Water Sandstone Facies and Ancient Submarine Fans: Models for Exploration for Stratigraphic Traps. *AAPG Bulletin,* 62.

Walker, R.G. & Plint, A.G. (1992) Wave- and storm-domi- nated shallow marine systems. In: Facies Models: Response to Sea Level Change (Ed. by R.G.Walker & N.P. James), Geol. Assoc., Canada, 219-238.

Worlsey, D., and Mørk, A. (1978). The Triassic stratigraphy of southern Spitsbergen: *Norsk Polarinst.* Årbok 1977, **pp.43-60**

Worsley D., Johansen R. & Kristensen S.E. 1988. The Mesozoic and Cenozoic succession of Tromsøflaket. In A. Dalland et al. (eds.): A lithostratigraphic scheme for the Mesozoic and Cenozoic succession offshore mid- and northern Norway. Norwegian Petroleum Directorate Bulletin 4, 42–65. Stavanger: Norwegian Petroleum Directorate.

Worsley, D. (2008). The post-Caledonian development of Svalbard and the western Barents Sea. *Polar Research, V.* 27, No. 3, pp. 298-317.

Van Heerden, I.L., (1983), Deltaic sedimentation in eastern Atchafalaya Bay, Louisiana: Center for Water Resources, *Louisiana State University: Baton Rouge*, **117 p**

Willis, B. J., (1997), Architecture of fluvial - dominated valley - fill deposits in the Cretaceous Fall River Formation: Sedimentology, v. 44, no. 4, p. 735-757.

10. Appendix

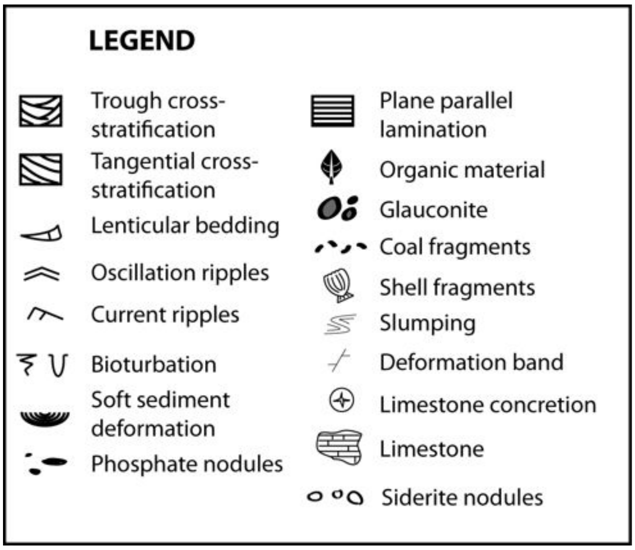

Figure 68 – Legend for the logs from both fieldwork and wells